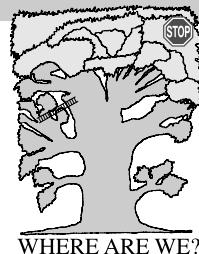


Chapter 14

INTERMOLECULAR MOTION OF ELECTRONS AND NUCLEI: CHEMICAL REACTIONS



Where are we?

We are already picking fruit in the crown of the TREE.

Example

Why do two substances react and another two do not? Why does increasing the temperature often start a reaction? Why does a reaction mixture change colour? As we know from Chapter 6, this tells us about some important electronic structure changes. On the other hand the products (as opposed to the reactants) tell us about profound changes in the positions of the nuclei that take place simultaneously. Something dramatic is going on. But what?

What is it all about

How atom A eliminates atom C from diatomic molecule BC? How can a chemical reaction be described as a molecular event? Where does the reaction barrier come from? Such questions will be discussed in this chapter.

The structure of the chapter is the following.

Hypersurface of the potential energy for nuclear motion (Δ)

p. 766

- Potential energy minima and saddle points
- Distinguished reaction coordinate (DRC)
- Steepest descent path (SDP)
- Our goal
- Chemical reaction dynamics (pioneers' approach)

AB INITIO APPROACH

p. 775

Accurate solutions for the reaction hypersurface (three atoms) (∇)

p. 775

- Coordinate system and Hamiltonian
- Solution to the Schrödinger equation
- Berry phase

APPROXIMATE METHODS

p. 781

Intrinsic Reaction Coordinate (IRC) or statics (Δ)

p. 781

Reaction path Hamiltonian method (∇)

p. 783

- Energy close to IRC
- Vibrationally adiabatic approximation
- Vibrationally non-adiabatic model
- Application of the reaction path Hamiltonian method to the reaction $\text{H}_2 + \text{OH} \rightarrow \text{H}_2\text{O} + \text{H}$

Acceptor–donor (AD) theory of chemical reactions (U♦)

p. 798

- Maps of the molecular electrostatic potential
- Where does the barrier come from?
- MO, AD and VB formalisms
- Reaction stages
- Contributions of the structures as the reaction proceeds
- Nucleophilic attack $\text{H}^- + \text{ethylene} \rightarrow \text{ethylene} + \text{H}^-$
- Electrophilic attack $\text{H}^+ + \text{H}_2 \rightarrow \text{H}_2 + \text{H}^+$
- Nucleophilic attack on the polarized chemical bond in the VB picture
- What is going on in chemist' flask?
- Role of symmetry
- Barrier means a cost of opening the closed-shells

Barrier for the electron transfer reaction (U§)

p. 828

- Diabatic and adiabatic potential
- Marcus theory

We are already acquainted with the toolbox for describing the electronic structure at any position of the nuclei. It is time now to look at possible *large* changes of the electronic structure at *large* changes of nuclear positions. The two motions: of the electrons and nuclei will be coupled together (especially in a small region of the configurational space).

Our plan consists of four parts:

- In the first part (after using the Born–Oppenheimer approximation, fundamental to this chapter), we assume that we have calculated the ground-state electronic energy, i.e. the potential energy for the nuclear motion. It will turn out that the hypersurface has a *characteristic “drain-pipe” shape, and the bottom in the central section, in many cases, exhibits a barrier*. Taking a three-atom example, we will show how the problem *could* be solved, if we *were capable* of calculating the quantum dynamics of the system accurately.
- In the second part we will concentrate on a specific representation of the system's energy that takes *explicitly* into account the above mentioned reaction drain-pipe (“*reaction path Hamiltonian*”). Then we will focus on describing how a chemical reaction proceeds. Just to be more specific, an example will be shown in detail.
- In the third part (acceptor–donor theory of chemical reactions) we will find the answer to the question, of *where the reaction barrier comes from and what happens to the electronic structure when the reaction proceeds*.
- The fourth part will pertain to the *reaction barrier height* in electron transfer (a subject closely related to the second and the third parts).

Why is this important?

Chemical reactions are at the heart of chemistry, making possible the achievement of its ultimate goals, which include synthesizing materials with desired properties. What happens

in the chemist's flask is a complex phenomenon¹ which consists of an astronomical number of elementary reactions of individual molecules. In order to control the reactions in the flask, it would be good to *first understand the rules which govern these elementary reaction acts*.

What is needed?

- Hartree–Fock method (Chapter 8, necessary).
- Conical intersection (Chapter 6, necessary).
- Normal modes (Chapter 7, necessary).
- Appendices M (recommended), E (recommended), Z (necessary), I (recommended), G (just mentioned).
- Elementary statistical thermodynamics or even phenomenological thermodynamics: entropy, free energy (necessary).

Classical works

Everything in chemistry began in the twenties of the twentieth century.

The first publications that considered conical intersection – a key concept for chemical reactions – were two articles from the Budapest schoolmates: Janos (John) von Neumann and Jenő Pál (Eugene) Wigner “Über merkwürdige diskrete Eigenwerte” published in *Physikalische Zeitschrift*, 30 (1929) 465 and “Über das Verhalten von Eigenwerten bei adiabatischen Prozessen” which also appeared in *Physikalische Zeitschrift*, 30 (1929) 467. ★ Then a paper “The Crossing of Potential Surfaces” by their younger schoolmate Edward Teller was published in the *Journal of Chemical Physics*, 41 (1937) 109. ★ A classical theory of the “reaction drain-pipe” with entrance and exit channels was first proposed by Henry Eyring, Harold Gershinowitz and Cheng E. Sun in “Potential Energy Surface for Linear H₃”, the *Journal of Chemical Physics*, 3 (1935) 786, and then by Joseph O. Hirschfelder, Henry Eyring and Bryan Topley in an article “Reactions Involving Hydrogen Molecules and Atoms” in *Journal of Chemical Physics*, 4 (1936) 170 and by Meredith G. Evans and Michael Polanyi in “Inertia and Driving Force of Chemical Reactions” which appeared in *Transactions of the Faraday Society*, 34 (1938) 11. ★ Hugh Christopher Longuet-Higgins, U. Öpik, Maurice H.L. Pryce and Robert A. Sack in a splendid paper “Studies of the Jahn–Teller Effect”, *Proceedings of the Royal Society of London*, A244 (1958) 1 noted for the first time, that the wave function changes its phase close to a conical intersection, which later on became known as the Berry phase. ★ The acceptor–donor description of chemical reactions was first proposed by Robert S.J. Mulliken in “Molecular Compounds and their Spectra”, *Journal of the American Chemical Society*, 74 (1952) 811. ★ The idea of the intrinsic reaction coordinate (IRC) was first given by Isaiah Shavitt in “The Tunnel Effect Corrections in the Rates of Reactions with Parabolic and Eckart Barriers”, Report WIS-AEC-23, Theoretical Chemistry Lab., University of Wisconsin (1959) as well as by Morton A. Eliason and Joseph O. Hirschfelder in the *Journal of the Chemical Physics*, 30 (1959) 1426 in an article “General Collision Theory Treatment for the Rate of Bimolecular, Gas Phase Reactions”. ★ The symmetry rules allowing some reactions and forbidding others were first proposed by Robert B. Woodward and Roald Hoffmann in two letters to the editor: “Stereochemistry of Electrocyclic Reactions” and “Selection Rules for Sigmatropic Reactions”, *Journal of American Chemical Society*, 87 (1965) 395, 2511 as well as by Kenichi Fukui and Hiroshi Fujimoto in an article published

¹See Chapter 15.

in the *Bulletin of the Chemical Society of Japan*, 41 (1968) 1989. ★ The concept of the steepest descent method was formulated by Kenichi Fukui in “*A Formulation of the Reaction Coordinate*”, which appeared in the *Journal of Physical Chemistry*, 74 (1970) 4161, although the idea seems to have a longer history. ★ Other classical papers include a seminal article by Sason S. Shaik “*What Happens to Molecules as They React? Valence Bond Approach to Reactivity*” in *Journal of the American Chemical Society*, 103 (1981) 3692. ★ The Hamiltonian path method was formulated by William H. Miller, Nicolas C. Handy and John E. Adams, in an article “*Reaction Path Hamiltonian for Polyatomic Molecules*” in the *Journal of the Chemical Physics*, 72 (1980) 99. ★ The first quantum dynamics simulation was performed by a PhD student George C. Schatz (under the supervision of Aron Kupperman) for the reaction $\text{H}_2 + \text{H} \rightarrow \text{H} + \text{H}_2$, reported in “*Role of Direct and Resonant Processes and of their Interferences in the Quantum Dynamics of the Collinear H + H₂ Exchange Reaction*”, in *Journal of Chemical Physics*, 59 (1973) 964. ★ John Polanyi, Dudley Herschbach and Yuan Lee proved that the lion’s share of the reaction energy is delivered through the rotational degrees of freedom of the products, e.g., J.D. Barnwell, J.G. Loeser, D.R. Herschbach, “*Angular Correlations in Chemical Reactions. Statistical Theory for Four-Vector Correlations*” published in the *Journal of Physical Chemistry*, 87 (1983) 2781. ★ Ahmed Zewail (Egypt/USA) developed an amazing experimental technique known as femtosecond spectroscopy, which for the first time allowed the study of the reacting molecules at different stages of an ongoing reaction (“*Femtochemistry – Ultrafast Dynamics of The Chemical Bond*”, vol. I and II, A.H. Zewail, World Scientific, New Jersey, Singapore (1994)). ★ Among others, Josef Michl, Lionel Salem, Donald G. Truhlar, Robert E. Wyatt, and W. Ronald Gentry contributed to the theory of chemical reactions.

John Charles Polanyi (born 1929), Canadian chemist of Hungarian origin, son of Michael Polanyi (one of the pioneers in the field of chemical reaction dynamics), professor at the University of Toronto. John was attracted to chemistry by Meredith G. Evans, who was a student of his father. Three scholars: John Polanyi, Yuan Lee and Dudley Herschbach shared the 1986 Nobel prize “for their contribu-



tions concerning the dynamics of chemical elementary processes”.

Yuan T. Lee is a native of Taiwan, called by his colleagues “a Mozart of physical chemistry”. He wrote that he was deeply impressed by a biography of Mme Curie and that her idealism decided his own path.



Dudley Herschbach writes in his CV, that he spent his childhood in a village close to San Jose, picking fruit, milking cows, etc. Thanks to his wonderful teacher he became interested in chemistry. He graduated from Harvard University (physical chemistry), where as he says, he has found “an exhilarating academic environment”. In 1959 he became professor at University of California at Berkeley. In 1967 the group was joined by Yuan Lee and constructed a “supermachine” for studying crossing molecular beams and the reactions in



them. One of the topics was the alkali metal atom – iodine collisions. These investigations were supported by John Polanyi, who studied the chemiluminescence in IR, i.e. the heat radiation of chemical reactions.

14.1 HYPERSURFACE OF THE POTENTIAL ENERGY FOR NUCLEAR MOTION

Theoretical chemistry is still in a stage which experts in the field characterized as “the primitive beginnings of chemical *ab initio* dynamics”.² The majority of the systems studied so far are *three-atomic* systems.³

The Born–Oppenheimer approximation works wonders, as it is possible to consider the (classical or quantum) dynamics of the *nuclei*, while the electrons disappear from the scene (their role became, after determining the potential energy for the motion of the nuclei, described in the electronic energy, the quantity corresponding to $E_0^0(\mathbf{R})$ from eq. (6.8) on p. 225).

Even with this approximation our job is not simple:

- The reactants as well as the products may be quite large systems and the many-dimensional ground-state potential energy hypersurface $E_0^0(\mathbf{R})$ may have a very complex shape, whereas we are most often interested in the small fragment of the hypersurface that pertains to a particular one of many possible chemical reactions.
- We have many such hypersurfaces $E_k^0(\mathbf{R})$, $k = 0, 1, 2, \dots$, each corresponding to an electronic state: $k = 0$ means the ground state, $k = 1, 2, \dots$ correspond to the excited states. There are processes which take place on a single hypersurface without changing the chemical bond pattern,⁴ but the very essence of chemical reaction is to change the bond pattern, and therefore excited states come into play.

It is quite easy to see where the fundamental difficulty is. Each of the hypersurfaces $E_k^0(\mathbf{R})$ for the motion of $N > 2$ nuclei depends on $3N - 6$ atomic coordinates (the number of translational and rotational degrees of freedom was subtracted).

Determining the hypersurface is not an easy matter:

- A high accuracy of 1 kcal/mol is required, which is (for a fixed configuration) very difficult to achieve for *ab initio* methods,⁵ and even more difficult for the semi-empirical or empirical methods.

²R.D. Levine and R.B. Bernstein, “*Molecular Reaction Dynamics and Chemical Reactivity*”, Oxford University Press, 1987.

³John Polanyi recalls that the reaction dynamics specialists used to write as the first equation on the blackboard $A + BC \rightarrow AB + C$, which made any audience burst out laughing. However, one of the outstanding specialists (Richard Zare) said about the simplest of such reactions (H_3) (*Chem. Engin. News*, June 4 (1990) 32): “*I am smiling, when somebody calls this reaction the simplest one. Experiments are extremely difficult, because one does not have atomic hydrogen in the stockroom, especially the high speed hydrogen atoms (only these react). Then, we have to detect the product, i.e. the hydrogen, which is a transparent gas. On top of that it is not sufficient to detect the product in a definite spot, but we have to know which quantum state it is in*”.

⁴Strictly speaking a change of conformation or formation of an intermolecular complex represents a chemical reaction. Chemists, however, reserve this notion for more profound changes of electronic structure.

⁵We have seen in Chapter 10, that the correlation energy is very difficult to calculate.

- The *number of points* on the hypersurface which have to be calculated is extremely large and increases exponentially with the system size.⁶
- There is no general methodology telling us what to do with the calculated points. There is a consensus that we should approximate the hypersurface by a smooth analytical function, but no general solution has yet been offered.⁷

14.1.1 POTENTIAL ENERGY MINIMA AND SADDLE POINTS

Let us denote $E_0^0(\mathbf{R}) \equiv V$. The most interesting points of the hypersurface V are its *critical points*, i.e. the points for which the gradient ∇V is equal to zero:

critical points

$$G_i = \frac{\partial V}{\partial X_i} = 0 \quad \text{for } i = 1, 2, \dots, 3N, \quad (14.1)$$

where X_i denote the Cartesian coordinates that describe the configurations of N nuclei. Since $-G_i$ represents the force acting along the axis X_i , therefore no forces act on the atoms in the configuration of a critical point.

There are several types of critical points. Each type can be identified after considering the *Hessian*, i.e. the matrix with elements

Hessian

$$V_{ij} = \frac{\partial^2 V}{\partial X_i \partial X_j} \quad (14.2)$$

calculated for the critical point. There are three types of critical points: maxima, minima and saddle points (cf. Chapter 7 and Fig. 7.11, as well as the Bader analysis, p. 573). The saddle points, as will be shown in a while, are of several classes depending on the signs of the Hessian eigenvalues. Six of the eigenvalues are equal to zero (rotations and translations of the total system, see p. 294), because this type of motion proceeds without any change of the potential energy V .

We will concentrate on the remaining $3N - 6$ eigenvalues:

- In the minimum the $3N - 6$ Hessian eigenvalues $\lambda_k \equiv \omega_k^2$ (ω is the angular momentum of the corresponding normal modes) are all positive,
- In the maximum – all are negative.
- For a saddle point of the n -th order, $n = 1, 2, \dots, 3N - 7$, the n eigenvalues are negative, the rest are positive. Thus, a first-order saddle point corresponds to all

⁶Indeed, if we assume that ten values for each coordinate axis is sufficient (and this looks like a rather poor representation), then for N atoms we have 10^{3N-6} quantum mechanical calculations of good quality to perform. This means that for $N = 3$ we may still pull it off, but for larger N everybody has to give up. For example, for the reaction $\text{HCl} + \text{NH}_3 \rightarrow \text{NH}_4\text{Cl}$ we would have to calculate 10^{12} points in the configurational space, while even a single point is a computational problem.

⁷Such an approximation is attractive for two reasons: first, we dispose of the (approximate) values of the potential energy for *all* points in the configuration space (not only those for which the calculations were performed), and second, the analytical formula may be differentiated and the derivatives give the forces acting on the atoms.

It is advisable to construct the above mentioned analytical functions following some theoretical arguments. These are supplied by intermolecular interaction theory (see Chapter 13).

but one the Hessian eigenvalues positive, i.e. one of the angular frequencies ω is therefore imaginary.

saddle

The eigenvalues were obtained by diagonalization of the Hessian. Such diagonalization corresponds to a rotation of the local coordinate system (cf. p. 297). Imagine a two-dimensional surface that at the minimum could be locally approximated by an ellipsoidal valley. The diagonalization means such a rotation of the coordinate system x, y that both axes of the ellipse coincide with the new axes x', y' (Chapter 7). On the other hand, if our surface locally resembled a cavalry saddle, diagonalization would lead to such a rotation of the coordinate system that one axis would be directed along the horse, and the other across.⁸

femtosecond
spectroscopy

IR and Raman spectroscopies providing the vibration frequencies and force constants tell us a lot about how the energy hypersurface close to minima, looks, both for the reactants and the products. On the other hand theory and recently also femtosecond spectroscopy,⁹ are the only source of information about the first order saddle points. However, the latter are extremely important for determining reaction rates since any saddle point is a kind of pivot point – it is as important for the reaction as the Rubicon was for Caesar.¹⁰

The simplest chemical reactions are those which do not require crossing any reaction barrier. For example, the reaction $\text{Na}^+ + \text{Cl}^- \rightarrow \text{NaCl}$ or other similar reactions (like recombination of radicals) that are not accompanied by bond breaking take place *without any barrier*.¹¹

After the barrierless reactions, there is a group of reactions in which the reactants and the products are separated by a single first-order saddle point (no intermediate products). *How do we describe such a reaction in a continuous way?*

14.1.2 DISTINGUISHED REACTION COORDINATE (DRC)

We often define a reaction path in the following way. First, we make

- a choice of a particular distance (s) between the reacting molecules (e.g., an interatomic distance, one of the atoms belongs to molecule A, the other to B);
- then we minimize the potential energy by optimization of all atomic positions, while keeping the s distance fixed;
- change s by small increments from its reactant value until the product value is obtained (for each s optimizing all other distances);

⁸A cavalry saddle represents a good example of the first order saddle of a two-dimensional surface.

⁹In this spectroscopy we hit a molecule with a laser pulse of a few femtoseconds. The pulse perturbs the system, and when relaxing it is probed by a series of new pulses, each giving a spectroscopic fingerprint of the system. A femtosecond is an incredibly short time, light is able to move only about $3 \cdot 10^{-5}$ cm. Ahmed Zewail, the discoverer of this spectroscopy received the Nobel prize 1999.

¹⁰In 49 B.C. Julius Caesar with his Roman legions crossed the Rubicon river (the border of his province of Gaul), and this initiated a civil war with the central power in Rome. His words, “*alea iacta est*” (the die is cast) became a symbol of a final and irreversible decision.

¹¹As a matter of fact, the formation of van der Waals complexes may also belong to this group. However in large systems, when precise docking of molecules take place, the final docking may occur with a steric barrier.

- this defines a path (DRC) in the configurational space, the progress along the path is measured by s .

A deficiency of the DRC is an arbitrary choice of the distance. The energy profile obtained (the potential energy vs s) depends on the choice. Often the DRC is reasonably close to the reactant geometry and becomes misleading when close to the product value (or *vice versa*). There is no guarantee that such a reaction path passes through the saddle point. On top of this other coordinates may undergo discontinuities, which feels a little catastrophic.

14.1.3 STEEPEST DESCENT PATH (SDP)

Because of the Boltzmann distribution the potential energy *minima* are most important, mainly low-energy ones.¹²

The saddle points of the first order are also important, because we may prove that any two minima may be connected by at least one saddle point¹³ which corresponds to the highest energy *point* on the lowest-energy *path* from one minimum to the other (pass). Thus, *the least energy-demanding path from the reactants to products goes via a saddle point of the first order*. This steepest descent path (SDP) is determined by the direction $-\nabla V$. First, we choose a first-order saddle point \mathbf{R}_0 , then diagonalize the Hessian matrix calculated at this point and the eigenvector \mathbf{L} corresponding to the single negative eigenvalue of the Hessian (cf. p. 297). Now, let us move *a little* from position \mathbf{R}_0 in the direction indicated by \mathbf{L} , and then let us follow vector $-\nabla V$ until it reduces to zero (then we are at the minimum). In this way we have traced half the SDP. The other half will be determined starting down from the other side of the saddle point and following the $-\mathbf{L}$ vector first.

In a moment we will note a certain disadvantage of the SDP, which causes us to prefer another definition of the reaction path (see p. 781).

14.1.4 OUR GOAL

We would like to present a theory of elementary chemical reactions within the Born–Oppenheimer approximation, i.e. which describes nuclear motion on the potential energy hypersurface.

We have the following alternatives:

1. To perform *molecular dynamics*¹⁴ on the hypersurface V (a point on the hypersurface represents the system under consideration).

¹²Putting aside some subtleties (e.g., does the minimum support a vibrational level), the minima correspond to stable structures, since a small deviation from the minimum position causes a gradient of the potential to become non-zero, and this means a force pushing the system back towards the minimum position.

¹³Several first-order saddle points to pass mean a multi-stage reaction that consists of several steps, each one representing a pass through a single first-order saddle point (elementary reaction).

¹⁴A classical approach. We have to assume that the bonds may break – this is a very non-typical molecular dynamics problem.

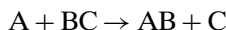
2. To solve the *time-independent Schrödinger equation* $\hat{H}\psi = E\psi$ for the motion of the nuclei with potential energy V .
3. To solve the *time-dependent Schrödinger equation* with the boundary condition for $\psi(x, t = 0)$ in the form of a wave packet.¹⁵ The wave packet may be directed into the entrance channel towards the reaction barrier (from various starting conditions). In the barrier range, the wave packet splits into a wave packet crossing the barrier and a wave packet reflected from the barrier (cf. p. 153).
4. To perform a semi-classical analysis that highlights the existence of the SDP, or a similar path, leading from the reactant to the product configuration.

Before going to more advanced approaches let us consider possibility 1.

14.1.5 CHEMICAL REACTION DYNAMICS (A PIONEERS' APPROACH)

The SDP does not represent the only possible reaction path. It is only the *least-energy expensive path* from reactants to products. In real systems, the point representing the system will attempt to get through the pass in many different ways. Many such attempts are unsuccessful (*non-reactive trajectories*). If the system leaves the entrance channel (*reactive trajectories*), it will not necessarily pass through the saddle point, because it may have some extra kinetic energy, which may allow it to go with a higher energy than that of the barrier. Everything depends on the starting position and velocity of the point running through the entrance channel.

In the simplest case of a three-atom reaction



the potential energy hypersurface represents a function of $3N - 6 = 3$ coordinates (the translations and rotations of the total system were separated). Therefore, even in such a simple case, it is difficult to draw this dependence. We may simplify the problem by considering only a limited set of geometries, e.g., the three atoms in a linear configuration. In such a case we have only two independent variables¹⁶ R_{AB}

¹⁵For example, a Gaussian function (in the nuclear coordinate space) moving from a position in this space with a starting velocity.

¹⁶After separating the centre-of-mass motion. The separation may be done in the following way. The kinetic energy operator has the form

$$\hat{T} = -\frac{\hbar^2}{2M_A} \frac{\partial^2}{\partial X_A^2} - \frac{\hbar^2}{2M_B} \frac{\partial^2}{\partial X_B^2} - \frac{\hbar^2}{2M_C} \frac{\partial^2}{\partial X_C^2}.$$

We introduce some new coordinates:

- the centre-of-mass coordinate $X_{CM} = (M_A X_A + M_B X_B + M_C X_C)/M$ with the total mass $M = M_A + M_B + M_C$,
- $R_{AB} = X_B - X_A$,
- $R_{BC} = X_C - X_B$.

and R_{BC} and the function $V(R_{AB}, R_{BC})$ may be visualized by a map quite similar to those used in geography. The map has a characteristic shape shown in Fig. 14.1.

- *Reaction map.* First of all we can see the characteristic “*drain-pipe*” shape of the potential energy V for the motion of the nuclei, i.e. the function $V(R_{AB}, R_{BC}) \rightarrow \infty$ for $R_{AB} \rightarrow 0$ or for $R_{BC} \rightarrow 0$, therefore we have a high energy wall along the axes. When R_{AB} and R_{BC} are both large we have a kind of plateau that goes gently downhill towards the bottom of the curved drain-pipe extending nearly parallel to the axes. The chemical reaction $A + BC \rightarrow AB + C$ means a motion close to the bottom of the “*drain-pipe*” from a point corresponding to a large R_{AB} , while R_{BC} has a value corresponding to the equilibrium BC length to a point, corresponding to a large R_{BC} and R_{AB} with a value corresponding to the length of the isolated molecule AB (arrows in Fig. 14.1).
- *Barrier.* A projection of the “*drain-pipe*” bottom on the $R_{AB} R_{BC}$ plane gives the SDP. Therefore, the SDP represents one of the important features of the “*landscape topography*”. Travel on the potential energy surface along the SDP

reaction
drain-pipe

reaction barrier

To write the kinetic energy operator in the new coordinates we start with relations

$$\begin{aligned}\frac{\partial}{\partial X_A} &= \frac{\partial R_{AB}}{\partial X_A} \frac{\partial}{\partial R_{AB}} + \frac{\partial X_{CM}}{\partial X_A} \frac{\partial}{\partial X_{CM}} = -\frac{\partial}{\partial R_{AB}} + \frac{M_A}{M} \frac{\partial}{\partial X_{CM}}, \\ \frac{\partial}{\partial X_B} &= \frac{\partial R_{AB}}{\partial X_B} \frac{\partial}{\partial R_{AB}} + \frac{\partial R_{BC}}{\partial X_B} \frac{\partial}{\partial R_{BC}} + \frac{\partial X_{CM}}{\partial X_B} \frac{\partial}{\partial X_{CM}} = \frac{\partial}{\partial R_{AB}} - \frac{\partial}{\partial R_{BC}} + \frac{M_B}{M} \frac{\partial}{\partial X_{CM}}, \\ \frac{\partial}{\partial X_C} &= \frac{\partial R_{BC}}{\partial X_C} \frac{\partial}{\partial R_{BC}} + \frac{\partial X_{CM}}{\partial X_C} \frac{\partial}{\partial X_{CM}} = \frac{\partial}{\partial R_{BC}} + \frac{M_C}{M} \frac{\partial}{\partial X_{CM}}.\end{aligned}$$

After squaring these operators and substituting them into \hat{T} we obtain, after a brief derivation,

$$\hat{T} = -\frac{\hbar^2}{2M} \frac{\partial^2}{\partial X_{CM}^2} - \frac{\hbar^2}{2\mu_{AB}} \frac{\partial^2}{\partial R_{AB}^2} - \frac{\hbar^2}{2\mu_{BC}} \frac{\partial^2}{\partial R_{BC}^2} + \hat{T}_{ABC},$$

where the reduced masses

$$\frac{1}{\mu_{AB}} = \frac{1}{M_A} + \frac{1}{M_B}, \quad \frac{1}{\mu_{BC}} = \frac{1}{M_B} + \frac{1}{M_C},$$

whereas \hat{T}_{ABC} stands for the mixed term

$$\hat{T}_{ABC} = -\frac{\hbar^2}{M_B} \frac{\partial^2}{\partial R_{AB} \partial R_{BC}}.$$

In this way we obtain the centre-of-mass motion separation (the first term). The next two terms represent the kinetic energy operators for the independent pairs AB and BC, while the last one is the mixed term \hat{T}_{ABC} , whose presence is understandable: atom B participates in two motions, those associated with: R_{AB} and R_{BC} . We may eventually get rid of \hat{T}_{ABC} after introducing a skew coordinate system with the R_{AB} and R_{BC} axes (the coordinates are determined by projections parallel to the axes). After a little derivation, we obtain the following condition for the angle θ between the two axes, which assures the mixed term:

$$\cos \theta_{\text{opt}} = \frac{2}{M_B} \frac{\mu_{AB} \mu_{BC}}{\mu_{AB} + \mu_{BC}}$$

vanish. If all the atoms have their masses equal, we obtain $\theta_{\text{opt}} = 60^\circ$.

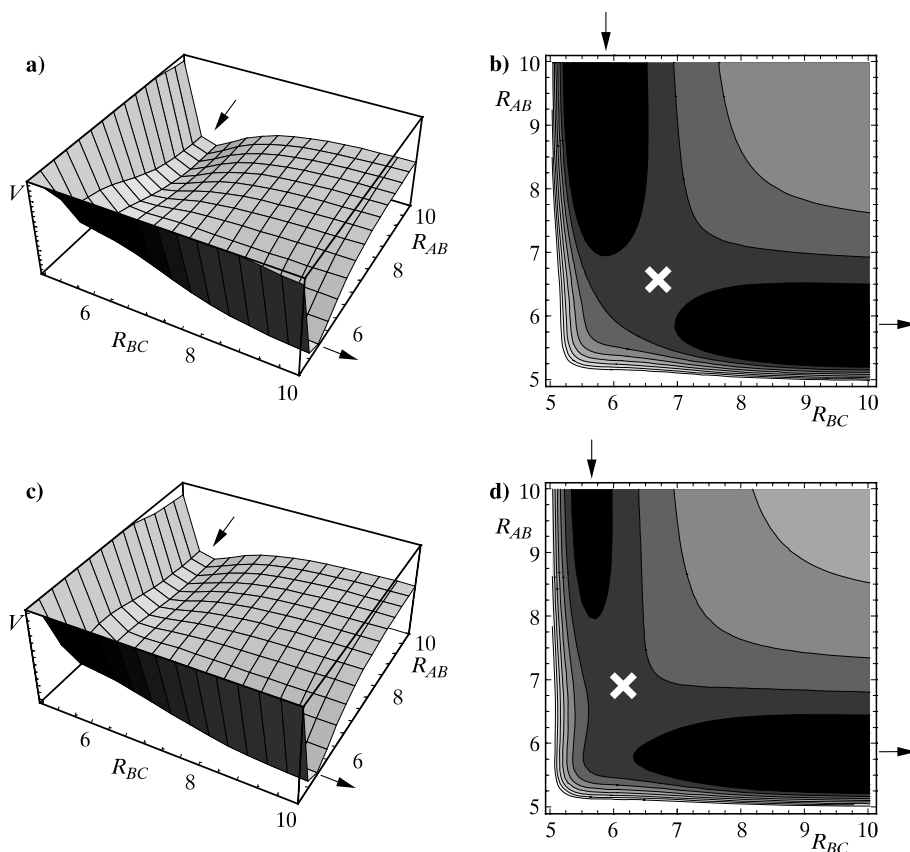


Fig. 14.1. The “drain-pipe” $A + BC \rightarrow AB + C$ (for a fictitious system). The surface of the potential energy for the motion of the nuclei is a function of distances R_{AB} and R_{BC} . On the left-hand side there is the view of the surface, while on the right-hand side the corresponding maps are shown. The barrier positions are given by the crosses on the right-hand figures. Figs. (a) and (b) show the symmetric entrance and exit channels with the separating barrier. Figs. (c) and (d) correspond to an exothermic reaction with the barrier in the entrance channel (“an early barrier”). Figs. (e) and (f) correspond to an endothermic reaction with the barrier in the exit channel (“a late barrier”). This endothermic reaction will not proceed spontaneously, because due to the equal width of the two channels, the reactant free energy is lower than the product free energy. Figs. (g) and (h) correspond to a spontaneous endothermic reaction, because due to the much wider exit channel (as compared to the entrance channel) the free energy is lower for the products. There is a van der Waals complex well in the entrance channel just before the barrier. There is no such well in the exit channel.

is not a flat trip, because the drain-pipe consists of two valleys: the reactant valley (*entrance channel*) and the product valley (*exit channel*) separated by a pass (*saddle point*), which causes the reaction barrier. The saddle point corresponds to the situation, in which the old chemical bond is already weakened (but still exists), while the new bond is just emerging. This explains (as has been shown by Henry Eyring, Michael Polanyi and Meredith Evans) why the energy required to go from the entrance to the exit barrier is much smaller than the dissociation

entrance and
exit channel

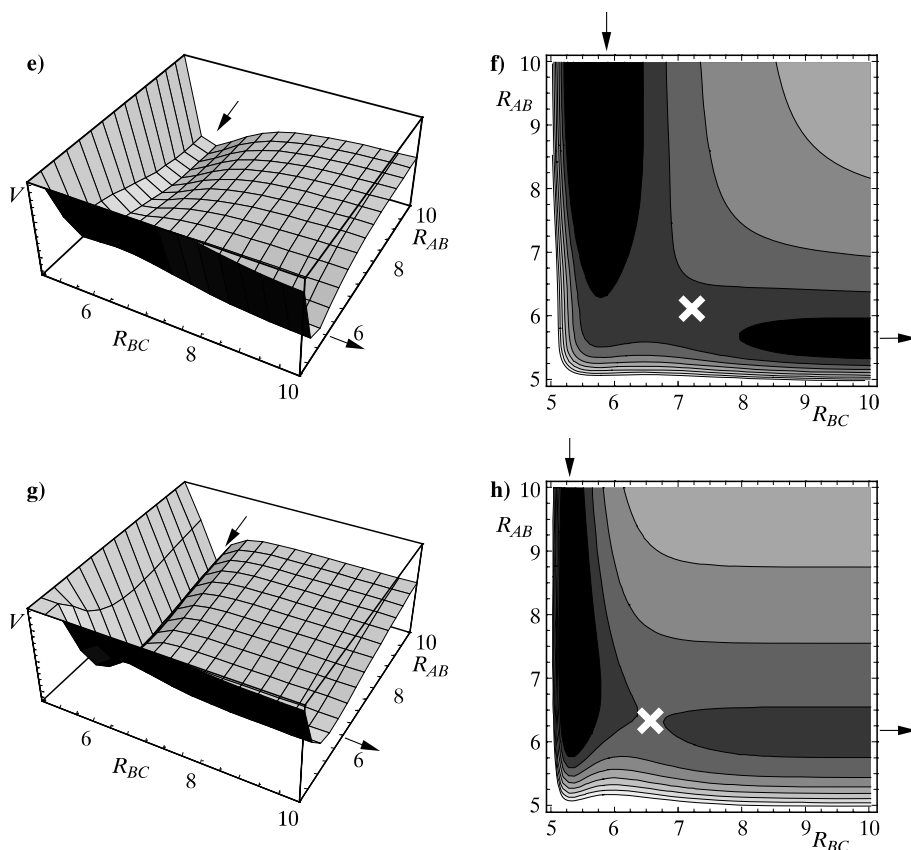


Fig. 14.1. Continued.

energy of BC , e.g., for the reaction $\text{H} + \text{H}_2 \rightarrow \text{H}_2 + \text{H}$ the activation energy (to overcome the reaction barrier) amounts only to about 10% of the hydrogen molecule binding energy. Simply, when the BC bond breaks, a new bond AB forms at the same time compensating for the energy cost needed to break the BC bond.

The barrier may have different positions in the reaction “drain-pipe”, e.g., it may be in the entrance channel (*early barrier*), Fig. 14.1.c,d, or in the exit channel (*late barrier*), Fig. 14.1.e,f, or, it may be inbetween (symmetric case, Fig. 14.1.a,b). The barrier position influences the course of the reaction.

early or late
barrier

When determining the SDP, kinetic energy was neglected, i.e. the motion of the point representing the system resembles a “crawling”. A chemical reaction does not, however, represent any crawling over the energy hypersurface, but rather a dynamics that begins in the entrance channel and ends in the exit channel, including motion “uphill” against the potential energy V . Overcoming the barrier thus is possible only, when the system has an excess of kinetic energy.

What will happen, if we have an early barrier? A possible reactive trajectory for such a case is shown in Fig. 14.2.a.

It is seen that the most effective way to pass the barrier is to set the point (representing the system) in fast motion along the entrance channel. This means that atom A has to have lots of kinetic energy when attacking the molecule BC . After passing the barrier the point slides downhill, entering the exit channel. Since, after sliding down, it has large kinetic energy, a *bobsleigh effect* takes place, i.e. the point climbs up the potential wall (as a result of the repulsion of atoms A and B) and then moves by making zigzags similar to a bobsleigh team. This zigzag means, of course, that strong oscillations of AB take place (and the C atom leaves the rest of the system). Thus,

bobsleigh effect

early location of a reaction barrier may result in a vibrationally excited product.

A different thing happens when the barrier is *late*. A possible reactive (i.e. successful) trajectory is shown in Fig. 14.2.b. For the point to overcome the barrier it has to have a large momentum along the BC axis, because otherwise it would climb up the potential energy wall in vain as the energy cost is too large. This may happen if the point moves along a zigzag-like way *in the entrance channel* (as shown in Fig. 14.2.b). This means that

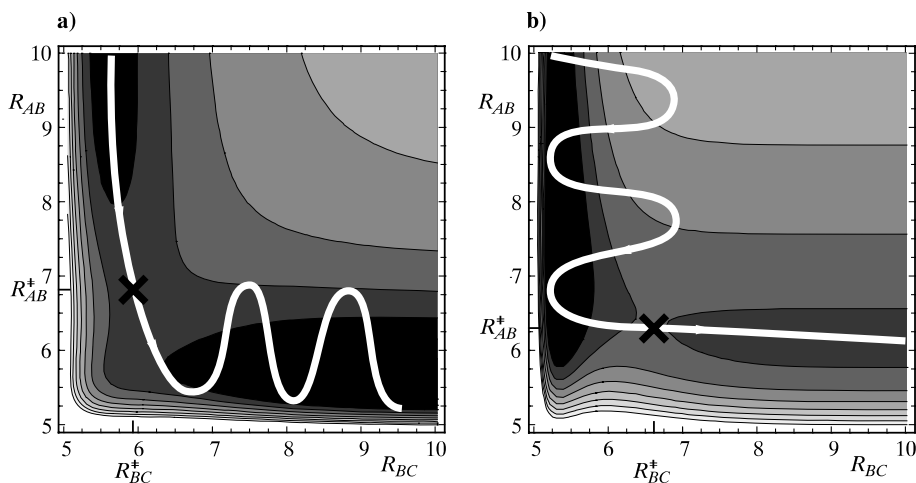


Fig. 14.2. A potential energy map for the collinear reaction $A + BC \rightarrow AB + C$ as a function of R_{AB} and R_{BC} . The distances R_{AB}^\ddagger and R_{BC}^\ddagger determine the saddle point position. Fig. (a) shows a reactive trajectory. If the point that represents the system runs sufficiently fast along the entrance channel towards the barrier, it will overcome the barrier by a “charge ahead”. Then, in the exit channel the point has to oscillate, which means product vibrations. Fig. (b) shows a reaction with a late barrier. In the entrance channel a promising reactive trajectory is shown as the wavy line. This means the system oscillates in the entrance channel in order to be able to attack the barrier directly after passing the corner area (bobsleigh effect).

to overcome a late barrier, the *vibrational excitation* of the reactant BC is effective,

because an increase in the kinetic energy of A will not produce much. Of course, the conditions for the reaction to occur matter less for high collision energies of the reactants. On the other hand, a too fast a collision may lead to unwanted reactions occurring, e.g., dissociation of the system into $A + B + C$. Thus there is an energy window for any given reaction.

AB INITIO APPROACH

14.2 ACCURATE SOLUTIONS FOR THE REACTION HYPERSURFACE (THREE ATOMS¹⁷)

14.2.1 COORDINATE SYSTEM AND HAMILTONIAN

This approach to the chemical reaction problem corresponds to point 2 on p. 770.

Jacobi coordinates

For three atoms of masses M_1, M_2, M_3 , with total mass $M = M_1 + M_2 + M_3$ we may introduce the Jacobi coordinates (see p. 279) in three different ways (Fig. 14.3.a).

Each of the coordinate systems (let us label them $k = 1, 2, 3$) highlights two atoms “close” to each other (i, j) and a third “distant” (k). Now, let us choose a pair of vectors $\mathbf{r}_k, \mathbf{R}_k$ for each of the choices of the Jacobi coordinates by the following procedure (\mathbf{X}_i represents the vector identifying nucleus i in a space-fixed coordinate system, SFCS, cf. Appendix I). First, let us define \mathbf{r}_k :

$$\mathbf{r}_k = \frac{1}{d_k}(\mathbf{X}_j - \mathbf{X}_i), \quad (14.3)$$

where the square of the *mass scaling parameter* equals

$$d_k^2 = \left(1 - \frac{M_k}{M}\right) \frac{M_k}{\mu}, \quad (14.4)$$

mass scaling
parameter

while μ represents the *reduced mass* (for three masses)

reduced mass

$$\mu = \sqrt{\frac{M_1 M_2 M_3}{M}}. \quad (14.5)$$

Now the second vector needed for the Jacobi coordinates is chosen as

$$\mathbf{R}_k = d_k \left[\mathbf{X}_k - \frac{M_i \mathbf{X}_i + M_j \mathbf{X}_j}{M_i + M_j} \right]. \quad (14.6)$$

¹⁷The method was generalized for an arbitrary number of atoms [D. Blume, C.H. Greene, “*Monte Carlo Hyperspherical Description of Helium Cluster Excited States*”, 2000].

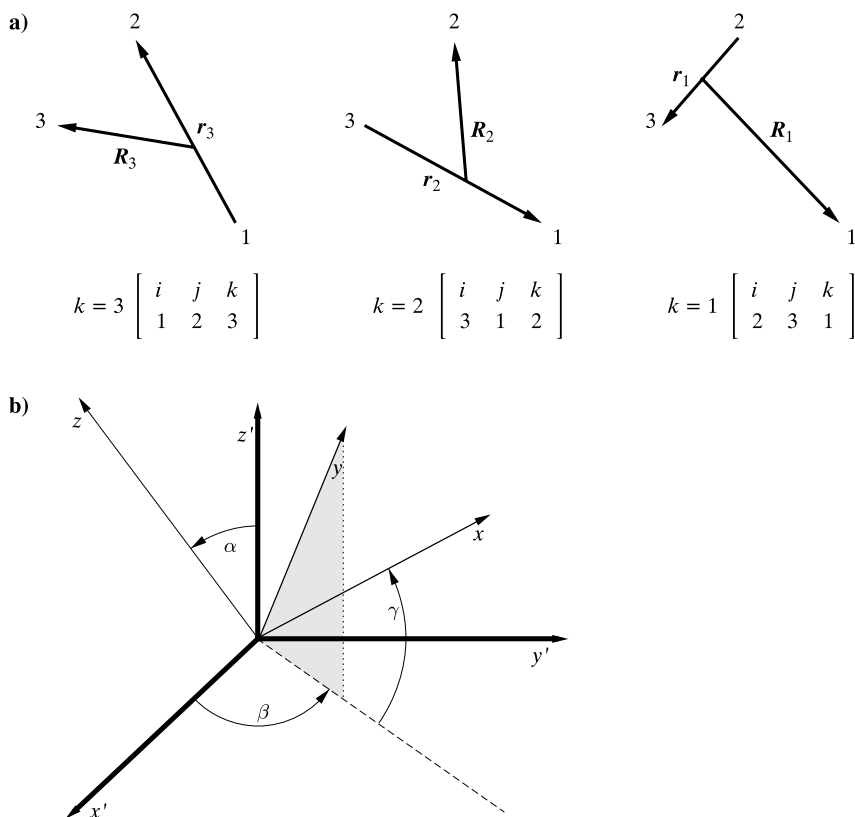


Fig. 14.3. (a) The three equivalent Jacobi coordinate systems. (b) The Euler angles show the mutual orientation of the two Cartesian coordinate systems. First, we project the y axis on the x', y' plane (the result is the dashed line). The first angle α is the angle between axes z' and z , the two other (β and γ) use the projection line described above. The relations among the coordinates are given by H. Eyring, J. Walter, G.E. Kimball, "*Quantum Chemistry*", John Wiley, New York, 1967.

The three Jacobi coordinate systems are related by the following formulae (cf. Fig. 14.3):

$$\begin{pmatrix} \mathbf{r}_i \\ \mathbf{R}_i \end{pmatrix} = \begin{pmatrix} \cos \beta_{ij} & \sin \beta_{ij} \\ -\sin \beta_{ij} & \cos \beta_{ij} \end{pmatrix} \begin{pmatrix} \mathbf{r}_j \\ \mathbf{R}_j \end{pmatrix}, \quad (14.7)$$

$$\begin{aligned} \tan \beta_{ij} &= -\frac{M_k}{\mu}, \\ \beta_{ij} &= -\beta_{ji}. \end{aligned} \quad (14.8)$$

The Jacobi coordinates will now be used to define what is called the (more convenient) hyperspherical democratic coordinates.

Democratic hyperspherical coordinates

When a chemical reaction proceeds, the role of the atoms changes and using the same Jacobi coordinate system all the time leads to technical problems. In order

not to favour any of the three atoms despite possible differences in their masses, we introduce *democratic hyperspherical coordinates*.

democratic
hyperspherical
coordinates

First, let us define the axis z of a Cartesian coordinate system, which is perpendicular to the molecular plane at the centre of mass, i.e. parallel to $\mathbf{A} = \frac{1}{2}\mathbf{r} \times \mathbf{R}$, where \mathbf{r} and \mathbf{R} are *any* (just democracy, the result is the same) of the vectors $\mathbf{r}_k, \mathbf{R}_k$. Note that by definition $|\mathbf{A}|$ represents the area of the triangle built of the atoms. Now, let us construct the axes x and y of the rotating with molecule coordinate system (RMCS, cf. p. 245) in the plane of the molecule taking care that:

- the Cartesian coordinate system is right-handed,
- the axes are oriented along the main axes of the moments of inertia,¹⁸ with $I_{yy} = \mu(r_y^2 + R_y^2) \geq I_{xx} = \mu(r_x^2 + R_x^2)$.

Finally, we introduce democratic hyperspherical coordinates equivalent to RMCS:

- the first coordinate measures the *size of the system*, or its “radius”:

$$\rho = \sqrt{R_k^2 + r_k^2}, \quad (14.9)$$

where ρ has no subscript, because the result is independent of k (to check this use eq. (14.7)),

- the second coordinate describes the system’s *shape*:

$$\cos \theta = \frac{2|\mathbf{A}|}{\rho^2} \equiv u. \quad (14.10)$$

Since $|\mathbf{A}|$ is the area of the triangle, $2|\mathbf{A}|$ means, therefore, the area of the corresponding parallelogram. The last area (in the nominator) is compared to the area of a square with side ρ (in the denominator; if u is small, the system is elongated like an ellipse with three atoms on its circumference)

- the third coordinate represents the angle ϕ_k for any of the atoms (in this way we determine, where the k -th atom is on the ellipse)

$$\cos \phi_k = \frac{2(\mathbf{R}_k \cdot \mathbf{r}_k)}{\rho^2 \sin \theta} \equiv \cos \phi. \quad (14.11)$$

As chosen, the hyperspherical democratic coordinates (which cover all possible atomic positions within the plane $z = 0$) have the following ranges: $0 \leq \rho < \infty$, $0 \leq \theta \leq \frac{\pi}{2}$, $0 \leq \phi \leq 4\pi$.

Hamiltonian in these coordinates

The hyperspherical democratic coordinates represent a useful alternative for RMCS from Appendix I (they themselves form another RMCS), and therefore

¹⁸These directions are determined by diagonalization of the inertia moment matrix (cf. Appendix K).

do not depend on the orientation with respect to the body-fixed coordinate system (BFCS). However, the molecule has somehow to “be informed” that it rotates (preserving the length and the direction of the total angular momentum), because a centrifugal force acts on its parts and the Hamiltonian expressed in BFCS (cf. Appendix I) has to contain information about this rotation.

The exact kinetic energy expression for a polyatomic molecule in a space fixed coordinate system (SFCS, cf. Appendix I) has been derived in Chapter 6 (eq. (6.34)). After separation of the centre-of-mass motion, the Hamiltonian is equal to $\hat{H} = \hat{T} + V$, where V represents the electronic energy playing the role of the potential energy for the motion of the nuclei (an analogue of $E_0^0(R)$ from eq. (6.8), we assume the Born–Oppenheimer approximation). In the democratic hyperspherical coordinates we obtain¹⁹

$$\hat{H} = -\frac{\hbar^2}{2\mu\rho^5} \frac{\partial}{\partial\rho} \rho^5 \frac{\partial}{\partial\rho} + \hat{\mathcal{H}} + \hat{\mathcal{C}} + V(\rho, \theta, \phi), \quad (14.12)$$

with

$$\hat{\mathcal{H}} = \frac{\hbar^2}{2\mu\rho^2} \left[-\frac{4}{u} \frac{\partial}{\partial u} u(1-u^2) \frac{\partial}{\partial u} - \frac{1}{1-u^2} \left(4 \frac{\partial^2}{\partial\phi^2} - \hat{J}_z^2 \right) \right], \quad (14.13)$$

$$\hat{\mathcal{C}} = \frac{\hbar^2}{2\mu\rho^2} \left[\frac{1}{1-u^2} 4i\hat{J}_z u \frac{\partial}{\partial\phi} + \frac{2}{u^2} \left[\hat{J}_x^2 + \hat{J}_y^2 + \sqrt{1-u^2} (\hat{J}_x^2 - \hat{J}_y^2) \right] \right], \quad (14.14)$$

where the first part, and the term with $\frac{\partial^2}{\partial\phi^2}$ in $\hat{\mathcal{H}}$, represent what are called deformation terms, the term with \hat{J}_z^2 and the terms in $\hat{\mathcal{C}}$ describe the rotation of the system.

14.2.2 SOLUTION TO THE SCHRÖDINGER EQUATION

Soon we will need some basis functions that depend on the angles θ and ϕ , preferentially each of them somehow adapted to the problem we are solving. These basis functions will be generated as the eigenfunctions of $\hat{\mathcal{H}}$ obtained at a fixed value $\rho = \rho_p$:

$$\hat{\mathcal{H}}(\rho_p) \Phi_{k\Omega}(\theta, \phi; \rho_p) = \varepsilon_{k\Omega}(\rho_p) \Phi_{k\Omega}(\theta, \phi; \rho_p), \quad (14.15)$$

where, because of two variables θ, ϕ we have two quantum numbers k and Ω (numbering the solutions of the equations).

The total wave function that also takes into account rotational degrees of freedom (θ, ϕ) is constructed as (the quantum number $J = 0, 1, 2, \dots$ determines the length of the angular momentum of the system, while the quantum number $M = -J, -J+1, \dots, 0, \dots, J$ gives the z component of the angular momentum)

¹⁹J.G. Frey, B.J. Howard, *Chem. Phys.* 99 (1985) 415.

a linear combination of the basis functions $U_{k\Omega} = D_{\Omega}^{JM}(\alpha, \beta, \gamma)\Phi_{k\Omega}(\theta, \phi; \rho_p)$:

$$\psi^{JM} = \rho^{-\frac{5}{2}} \sum_{k\Omega} F_{k\Omega}^J(\rho; \rho_p) U_{k\Omega}(\alpha, \beta, \gamma, \theta, \phi; \rho_p), \quad (14.16)$$

where α, β, γ are the three Euler angles (Fig. 14.3.b) that define the orientation of the molecule with respect to the distant stars, $D_{\Omega}^{JM}(\alpha, \beta, \gamma)$ represent the eigenfunctions of the symmetric top,²⁰ $\Phi_{k\Omega}$ are the solutions to eq. (14.15), while $F_{k\Omega}^J(\rho; \rho_p)$ stand for the ρ -dependent expansion coefficients, i.e. functions of ρ (centred at point ρ_p). Thanks to $D_{\Omega}^{JM}(\alpha, \beta, \gamma)$ the function ψ^{JM} is the eigenfunction of the operators \hat{J}^2 and \hat{J}_z .

In what is known as the *close coupling method* the function from eq. (14.16) is inserted into the Schrödinger equation $\hat{H}\psi^{JM} = E_J\psi^{JM}$. Then, the resulting equation is multiplied by a function $U_{k'\Omega'} = D_{\Omega'}^{JM}(\alpha, \beta, \gamma)\Phi_{k'\Omega'}(\theta, \phi; \rho_p)$ and integrated over angles $\alpha, \beta, \gamma, \theta, \phi$, which means taking into account all possible orientations of the molecule in space (α, β, γ) and all possible shapes of the molecule (θ, ϕ) which are allowed for a given size ρ . We obtain a set of linear equations for the unknowns $F_{k\Omega}^J(\rho; \rho_p)$:

close coupling
method

$$\rho^{-\frac{5}{2}} \sum_{k\Omega} F_{k\Omega}^J(\rho; \rho_p) \langle U_{k'\Omega'} | (\hat{H} - E_J) U_{k\Omega} \rangle_{\omega} = 0. \quad (14.17)$$

The summation extends over some assumed set of k, Ω (the number of k, Ω pairs is equal to the number of equations). The symbol $\omega \equiv (\alpha, \beta, \gamma, \theta, \phi)$ means integration over the angles. The system of equations is solved numerically.

If, when solving the equations, we apply the boundary conditions suitable for a discrete spectrum (vanishing for $\rho = \infty$), we obtain the stationary states of the three-atomic molecule. We are interested in chemical reactions, in which one of the atoms comes to a diatomic molecule, and after a while another atom flies out leaving (after reaction) the remaining diatomic molecule. Therefore, we have to apply suitable boundary conditions. As a matter of fact we are not interested in details of the collision, we are positively interested in what comes to our detector from the spot where the reaction takes place. What may happen at a certain energy E to a given reactant state (i.e. what the product state is; such a reaction is called “*state-to-state*”) is determined by the corresponding *cross section*²¹ $\sigma(E)$. The cross section can be calculated from what is called the *S* matrix, whose elements are constructed from the coefficients $F_{k\Omega}^J(\rho; \rho_p)$ found from eqs. (14.17). The *S* matrix plays a role of an energy dependent dispatcher: such a reactant state changes to such a product state with such and such probability.

state-to-state
reaction

cross section

We calculate the *reaction rate* k assuming all possible energies E of the system (satisfying the Boltzmann distribution) and taking into account that fast products

reaction rate
constant

²⁰D.M. Brink, G.R. Satchler, “*Angular Momentum*”, Clarendon Press, Oxford, 1975.

²¹After summing up the experimental results over all the angles, this is ready to be compared with the result of the above mentioned integration over angles.

arrive more often at the detector when counting per unit time

$$k = \text{const} \int dE E \sigma(E) \exp\left(-\frac{E}{k_B T}\right), \quad (14.18)$$

where k_B is the Boltzmann constant.

The calculated reaction rate constant k may be compared with the result of the corresponding “state-to-state” experiment.

14.2.3 BERRY PHASE

When considering accurate quantum dynamics calculations (point 3 on p. 770) we encounter the problem of what is called Berry phase.

In Chapter 6 wave function (6.19) corresponding to the adiabatic approximation was assumed. In this approximation the electronic wave function depends parametrically on the positions of the nuclei. Let us imagine we take one (or more) of the nuclei on an excursion. We set off, go slowly (in order to allow the electrons to adjust), the wave function deforms, and then, we are back home and put the nucleus exactly in place. Did the wave function come back exactly too? Not necessarily. By definition (cf. Chapter 2) a class Q function has to be a unique function of coordinates. This, however, does not pertain to a parameter. What certainly came back is the probability density $\psi_k(\mathbf{r}; \mathbf{R})^* \psi_k(\mathbf{r}; \mathbf{R})$, because it decides that we cannot distinguish the starting and the final situations. *The wave function itself might undergo a phase change, i.e. the starting function is equal to $\psi_k(\mathbf{r}; \mathbf{R}_0)$, while the final function is $\psi_k(\mathbf{r}; \mathbf{R}_0) \exp(i\phi)$ and $\phi \neq 0$.* This phase shift is called the Berry phase.²² Did it happen or not? Sometimes we can tell.

Let us consider a quantum dynamics description of a chemical reaction according to point 3 from p. 770. For example, let us imagine a molecule BC fixed in space, with atom B directed to us. Now, atom A, represented by a wave packet, rushes towards atom B. We may imagine that the atom A approaches the molecule and makes a bond with the atom B (atom C leaves the diatomic molecule) or atom A may first approach atom C, then turn back and make a bond with atom B (as before). The two possibilities correspond to two waves, which finally meet and interfere. If the phases of the two waves differed, we would see this in the results of the interference. The scientific community was surprised that some details of the reaction $\text{H} + \text{H}_2 \rightarrow \text{H}_2 + \text{H}$ at higher energies are impossible to explain without taking the Berry phase²³ into account. One of the waves described above made a turn around the conical intersection point (because it had to by-pass the equilateral triangle configuration, cf. Chapter 6). As it was shown in the work of Longuet-Higgins *et al.* mentioned above, this is precisely the reason why the function acquires a phase shift. We have shown in Chapter 6 (p. 264) that such a trip

²²The discoverers of this effect were H.C. Longuet-Higgins, U. Öpik, M.H.L. Pryce and R.A. Sack, *Proc. Roy. Soc. London, A* 244 (1958) 1. The problem of this geometric phase diffused into the consciousness of physicists much later after an article by M.V. Berry, *Proc. Roy. Soc. London A* 392 (1984) 45.

²³Y.-S.M. Wu, A. Kupperman, *Chem. Phys. Letters* 201 (1993) 178.

around a conical intersection point results in changing the phase of the function by π .

The phase appears, when the system makes a “trip” in configurational space. We may make the problem of the Berry phase more familiar by taking an example from everyday life. Let us take a 3D space. Please put your arm down against your body with the thumb directed forward. During the operations described below, please do not move the thumb with respect to the arm. Now stretch your arm horizontally sideways, rotate it to your front and then put down along your body. Note that now your thumb is not directed towards your front anymore, but towards your body. When your arm has come back, the thumb had made a rotation of 90° .

Your thumb corresponds to $\psi_k(\mathbf{r}; \mathbf{R})$, i.e. a vector in the Hilbert space, which is coupled with a slowly varying neighbourhood (\mathbf{R} corresponds to the hand positions). When the neighbourhood returns, the vector may have been rotated in the Hilbert space [i.e. multiplied by a phase $\exp(i\phi)$].

APPROXIMATE METHODS

14.3 INTRINSIC REACTION COORDINATE (IRC) OR STATICS

This section addresses point 4 of our plan from p. 770.

On p. 770 two reaction coordinates were proposed: DRC and SDP. Use of the first of them may lead to some serious difficulties (like energy discontinuities). The second reaction coordinate will undergo in a moment a useful modification and will be replaced by the so called *intrinsic reaction coordinate* (IRC).

What the IRC is?

Let us use the Cartesian coordinate system once more with $3N$ coordinates for the N nuclei: X_i , $i = 1, \dots, 3N$, where X_1, X_2, X_3 denote the x, y, z coordinates of atom 1 of mass M_1 , etc. The i -th coordinate is therefore associated with mass M_i of the corresponding atom. The classical Newtonian equation of motion for an atom of mass M_i and coordinate X_i is:²⁴

$$M_i \ddot{X}_i = -\frac{\partial V}{\partial X_i} \quad \text{for } i = 1, \dots, 3N. \quad (14.19)$$

Let us introduce what are called *mass-weighted coordinates* (or, more precisely, weighted by the square root of mass)

mass-weighted
coordinates

$$x_i = \sqrt{M_i} X_i. \quad (14.20)$$

In such a case we have

$$\sqrt{M_i} \sqrt{M_i} \ddot{X}_i = -\frac{\partial V}{\partial x_i} \frac{\partial x_i}{\partial X_i} = \sqrt{M_i} \left(-\frac{\partial V}{\partial x_i} \right) \quad (14.21)$$

²⁴Mass \times acceleration equals force; a dot over the symbol means a time derivative.

or

$$\ddot{x}_i = -\frac{\partial V}{\partial x_i} \equiv -g_i, \quad (14.22)$$

where g_i stands for the i -th component of the gradient of potential energy V calculated in mass-weighted coordinates. This equation can easily be integrated and we obtain

$$\dot{x}_i = -g_i t + v_{0,i} \quad (14.23)$$

or, for a small time increment dt and initial speed $v_{0,i} = 0$ (for the definition of the IRC as a path characteristic for potential energy V we want to neglect the influence of the kinetic energy) we obtain

$$\frac{dx_i}{-g_i} = t \, dt = \text{independent of } i. \quad (14.24)$$

Thus,

in the coordinates weighted by the square roots of the masses, a displacement of atom number i is proportional to the potential gradient (and does not depend on the atom mass).

If mass-weighted coordinates were not introduced, a displacement of the point representing the system on the potential energy map *would not follow the direction of the negative gradient or the steepest descent* (on a geographic map such a motion would look natural, because slow rivers flow this way). Indeed, the formula analogous to (14.24) would have the form: $\frac{dX_i}{-G_i} = \frac{t}{M_i} dt$, and therefore, during a single watch tick dt , light atoms would travel long distances while heavy atoms short distances.

Thus, after introducing mass-weighted coordinates, we may forget about masses, in particular about the atomic and the total mass, or equivalently, we may treat these as unit masses. The atomic displacements in this space will be measured in units of $\sqrt{\text{mass} \times \text{length}}$, usually in: $\sqrt{u}a_0$, where $12u = {}^{12}\text{C}$ atomic mass, $u = 1822.887m$ (m is the electron mass), and sometimes also in units of \sqrt{u} Å.

Eq. (14.24) takes into account our assumption about the zero initial speed of the atom in any of the integration steps (also called “*trajectory-in-molasses*”), because otherwise we would have an additional term in dx_i : the initial velocity times time. Broadly speaking, when the watch ticks,

the system, represented by a point in $3N$ -dimensional space, crawls over the potential energy hypersurface along the negative gradient of the hypersurface (in mass weighted coordinates). When the system starts from a saddle point of the first order, a small deviation of the position makes the system slide down on one or the other side of the saddle. The trajectory of the nuclei during such a motion is called the *intrinsic reaction coordinate* or IRC.

The point that represents the system slides down with infinitesimal speed along the IRC.

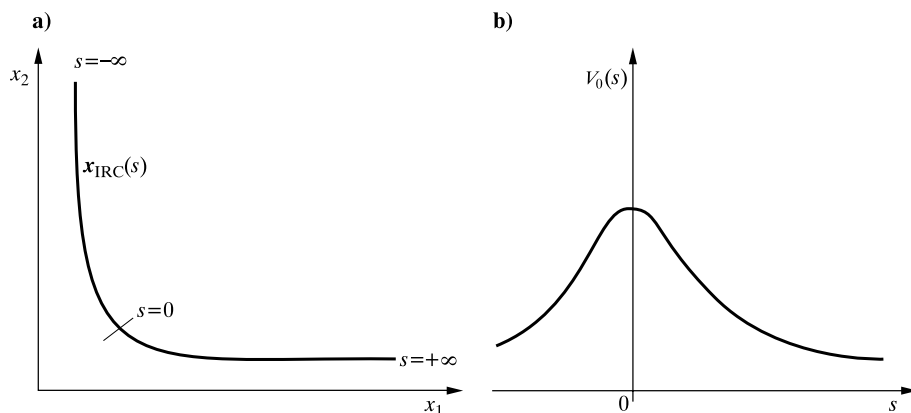


Fig. 14.4. A schematic representation of the IRC: (a) curve $x_{\text{IRC}}(s)$ and (b) energy profile when moving along the IRC [i.e. curve $V_0(x_{\text{IRC}}(s))$] in the case of two mass-weighted coordinates x_1, x_2 .

Measuring the travel along the IRC

In the space of the mass-weighted coordinates, trajectory IRC represents a certain curve x_{IRC} that depends on a parameter s : $x_{\text{IRC}}(s)$.

The parameter s measures the length along the reaction path IRC

(e.g., in $\sqrt{u}a_0$ or $\sqrt{u} \text{ \AA}$). Let us take two close points on the IRC and construct the vector: $\xi(s) = x_{\text{IRC}}(s + ds) - x_{\text{IRC}}(s)$, then

$$(ds)^2 = \sum_i [\xi_i(s)]^2. \quad (14.25)$$

We assume that $s = 0$ corresponds to the saddle point, $s = -\infty$ to the reactants, and $s = \infty$ to the products (Fig. 14.4).

For each point on the IRC, i.e. on the curve $x_{\text{IRC}}(s)$ we may read the mass-weighted coordinates, and use them to calculate the coordinates of each atom. Therefore, each point on the IRC corresponds to a certain structure of the system.

14.4 REACTION PATH HAMILTONIAN METHOD

14.4.1 ENERGY CLOSE TO IRC

A hypersurface of the potential energy represents an expensive product. We have first to calculate the potential energy for a grid of points. If we assume that ten points per coordinate is a sufficient number, then we have to perform 10^{3N-6}

advanced quantum mechanical calculations, for $N = 10$ atoms this gives $\dots 10^{24}$ calculations, which is an unreasonable task. Now you see why specialists so much prefer three-atomic systems.

Are all the points necessary? For example, if we assume low energies, the system will in practice, stay close to the IRC. Why, therefore, worry about other points? This idea was exploited by Miller, Handy and Adams.²⁵ They decided to introduce the coordinates that are natural for the problem of motion in the reaction “drain-pipe”. The approach corresponds to point 4 from p. 770.

The authors derived the

REACTION PATH HAMILTONIAN:

an approximate expression for the energy of the reacting system in the form, that stresses the existence of the IRC and of deviations from it.

This formula (*Hamilton function of the reaction path*) has the following form:

$$H(s, p_s, \{Q_k, P_k\}) = T(s, p_s, \{Q_k, P_k\}) + V(s, \{Q_k\}), \quad (14.26)$$

where T is the kinetic energy, V stands for the potential energy, s denotes the reaction coordinate along the IRC, $p_s = \frac{ds}{dt}$ represents the momentum coupled with s (mass = 1), $\{Q_k\}$, $k = 1, 2, \dots, 3N - 7$, stand for other coordinates orthogonal to the reaction path $\mathbf{r}_{\text{IRC}}(s)$ (this is why Q_k will depend on s) and the momenta $\{P_k\}$ conjugated with them.

We obtain the coordinates Q_k in the following way. At point s on the reaction path we diagonalize the Hessian, i.e. the matrix of the second derivatives of the potential energy and consider all the resulting normal modes ($\omega_k(s)$ are the corresponding frequencies; cf. Chapter 7) *other* than that, which corresponds to the reaction coordinate s (the later corresponds to the “imaginary”²⁶ frequency ω_k). The diagonalization also gives the normal vectors $L_k(s)$, each having a direction in the $(3N - 6)$ -dimensional configurational space (the mass-weighted coordinate system). *The coordinate $Q_k \in (-\infty, +\infty)$ measures the displacement along the direction of $L_k(s)$.* The coordinates s and $\{Q_k\}$ are called the *natural coordinates*. To stress that Q_k is related to $L_k(s)$, we will write it as $Q_k(s)$.

The potential energy, close to the IRC, can be approximated (*harmonic approximation*) by

$$V(s, \{Q_k\}) \cong V_0(s) + \frac{1}{2} \sum_{k=1}^{3N-7} \omega_k(s)^2 Q_k(s)^2, \quad (14.27)$$

where the term $V_0(s)$ represents the potential energy that corresponds to the bottom of the reaction “drain-pipe” at a point s along the IRC, while the second term tells us what will happen to the potential energy if we displace the point (i.e. the

²⁵W.H. Miller, N.C. Handy, J.E. Adams, *J. Chem. Phys.* 72 (1980) 99.

²⁶For large $|s|$ the corresponding ω^2 is close to zero. When $|s|$ decreases (we approach the saddle point), ω^2 becomes negative (i.e. ω is imaginary). For simplicity we will call this the “imaginary frequency” for any s .

system) perpendicular to $\mathbf{x}_{\text{IRC}}(s)$ along all the normal oscillator coordinates. In the *harmonic approximation* for the oscillator k , the energy goes up by half the force constant \times the square of the normal coordinate Q_k^2 . The force constant is equal to ω_k^2 , because the mass is equal to 1.

The kinetic energy turns out to be more complicated

$$T(s, p_s, \{Q_k, P_k\}) = \frac{1}{2} \frac{[p_s - \sum_{k=1}^{3N-7} \sum_{k'=1}^{3N-7} B_{kk'} Q_{k'} P_k]^2}{[1 + \sum_{k=1}^{3N-7} B_{ks} Q_k]^2} + \sum_{k=1}^{3N-7} \frac{P_k^2}{2}. \quad (14.28)$$

The last term is recognized as the vibrational kinetic energy for the oscillations perpendicular to the reaction path (recall that the mass is treated as equal to 1). If in the first term we insert $B_{kk'} = 0$ and $B_{ks} = 0$, the term would be equal to $\frac{1}{2} p_s^2$ and, therefore, would describe the kinetic energy of a point moving as if the reaction coordinate were a straight line.

CORIOLIS AND CURVATURE COUPLINGS:

$B_{kk'}$ are called the *Coriolis coupling constants*. They couple the normal modes perpendicular to the IRC.

The B_{ks} are called the *curvature coupling constants*, because they would be equal zero if the IRC was a straight line. They couple the translational motion along the reaction coordinate with the vibrational modes orthogonal to it. All the above coupling constants B depend on s .

Coriolis
coupling
constant

curvature
coupling
constant

Therefore, in the reaction path Hamiltonian we have the following quantities that characterize the reaction “drain-pipe”:

- The reaction coordinate s that measures the progress of the reaction along the “drain-pipe”.
- The value $V_0(s) \equiv V_0(\mathbf{x}_{\text{IRC}}(s))$ represents the energy that corresponds to the bottom of the “drain-pipe”²⁷ at the reaction coordinate s .
- The width of the “drain-pipe” is characterized by $\{\omega_k(s)\}$.²⁸
- The curvature of the “drain-pipe” is hidden in constants B , their definition will be given later in this chapter. Coefficient $B_{kk'}(s)$ tells us how normal modes k and k' are coupled together, while $B_{ks}(s)$ is responsible for a similar coupling between reaction path $\mathbf{x}_{\text{IRC}}(s)$ and vibration k perpendicular to it.

14.4.2 VIBRATIONALLY ADIABATIC APPROXIMATION

Most often when moving along the bottom of the “drain-pipe”, potential energy $V_0(s)$ only changes moderately when compared to the potential energy changes

²⁷I.e. the classical potential energy corresponding to the point of the IRC given by s (this gives an idea of how the potential energy changes when walking along the IRC).

²⁸A small ω corresponds to a wide valley, when measured along a given normal mode coordinate (“soft” vibration), a large ω means a narrow valley (“hard” vibration).

the molecule undergoes when oscillating perpendicularly²⁹ to $\mathbf{x}_{\text{IRC}}(s)$. Simply, the valley bottom profile results from the fact that the molecule hardly holds together when moving along the reaction coordinate s , *a chemical bond breaks*, while *other bonds remain strong* and it is not so easy to stretch their strings. This suggests that there is *slow* motion along s and *fast* oscillatory motion along the coordinates Q_k .

Since we are mostly interested in the slow motion along s , we may average over the fast motion.

The philosophy behind the idea is that while the system moves slowly along s , it undergoes a large number of oscillations along Q_k . After such vibrational averaging the only information that remains about the oscillations are the vibrational quantum levels for each of the oscillators (the levels will depend on s).

VIBRATIONALLY ADIABATIC APPROXIMATION:

The fast vibrational motions will be treated quantum mechanically and their total energy will enter the potential energy for the classical motion along s .

This approximation parallels the adiabatic approximation made in Chapter 6, where the fast motion of electrons was separated from the slow motion of the nuclei. There the total electronic energy became the potential energy for the motion of nuclei, here the total vibrational energy (the energy of the corresponding harmonic oscillators in their quantum states) becomes the potential energy for the slow motion along s . This concept is called the *vibrationally adiabatic approximation*.

In this approximation, to determine the stage of the reaction we give two *classical* quantities: *where* the system is on the reaction path (s), and *how fast* the system moves along the reaction path (p_s). Also we need the *quantum states* of the oscillators vibrating perpendicularly to the reaction path (vibrational quantum number $v_k = 0, 1, 2, \dots$ for each of the oscillators). Therefore, the potential energy for the (slow) motion along the reaction coordinate s is:³⁰

$$\begin{aligned} V_{\text{adiab}}(s; v_1, v_2, \dots, v_{3N-7}) \\ = V_0(s) + \sum_{k=1}^{3N-7} \left(v_k + \frac{1}{2} \right) \hbar [\omega_k(s) - \omega_k(-\infty)], \end{aligned} \quad (14.29)$$

where we have chosen an additive constant in the potential as equal to the vibrational energy of the reactants (with minus sign): $-\sum_{k=1}^{3N-7} (v_k + \frac{1}{2}) \hbar \omega_k(-\infty)$. Note that even though $v_k = 0$ for each of the oscillators, there is a non-zero vibrational correction to the classical potential energy $V_0(s)$, because the zero-vibrational energy changes if s changes.

²⁹I.e. when moving along the coordinates Q_k , $k = 1, 2, \dots, 3N - 7$.

³⁰Even if (according to the vibrationally adiabatic approximation) the vibrational quantum numbers were kept constant during the reaction, their energies as depending on s through ω would change.

The vibrationally adiabatic potential V_{adiab} was created for a given set of vibrational quantum numbers v_k , fixed during the reaction process. Therefore, it is impossible to exchange energy between the vibrational modes (we assume therefore the Coriolis coupling constants $B_{kk'} = 0$), as well as between the vibrational modes and the reaction path (we assume the curvature coupling constants $B_{ks} = 0$). This would mean a change of v_k 's.

From eq. (14.29) we may draw the following conclusion.

When during the reaction the frequency of a normal mode decreases dramatically (which corresponds to breaking of a chemical bond), the square bracket becomes negative. This means that an excitation of the bond before the reaction decreases the (vibrationally adiabatic) reaction barrier and the reaction rate will increase.

As a matter of fact, this is a quite obvious: a vibrational excitation that engages the chemical bond to be broken already weakens the bond before the reaction.

Why do chemical reactions proceed?

Exothermic reactions. When the reactants (products) have a kinetic energy higher than the barrier and the corresponding momentum p_s is large enough, with a high probability the barrier will be overcome (cf. p. 155). Even if the energy is lower than the barrier there is still a non-zero probability of passing to the other side because of the tunnelling effect. In both cases (passing over and under the barrier) it is easier when the kinetic energy is large.

The barrier *height* is usually different for the reaction reactants \rightarrow products and for the products \rightarrow reactants (Fig. 14.1). If the barrier height is smaller for the reactants, this *may* result in an excess of the product concentration over the reactant concentration.³¹ Since the reactants have higher energy than the products, the potential energy excess will change into the kinetic energy³² of the products (which is observed as a temperature increase – the reaction is exothermic). This may happen if the system has the possibility to pump the potential (i.e. electronic) energy excess into the translational and rotational degrees of freedom or to a “third body or bodies” (through collisions, e.g., with the solvent molecules) or has the possibility to emit light quanta. *If the system has no such possibilities the reaction will not take place.*

Endothermic reactions. The barrier height does not always decide.

Besides the barrier height the *widths* of the entrance and exit channels also count.

³¹Because a lower barrier is easier to overcome.

³²Most often rotational energy.

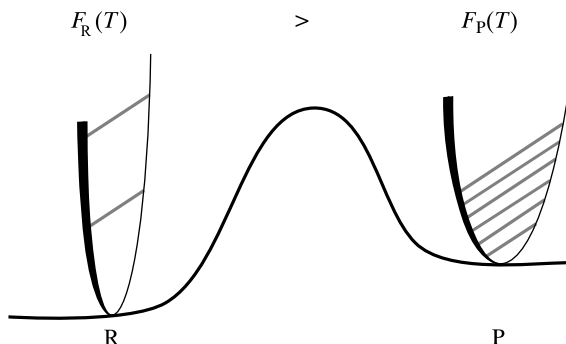


Fig. 14.5. Why do some endothermic reactions proceed spontaneously? The figure shows the energy profile as a function of s , i.e. along the intrinsic reaction coordinate (IRC). As we can see, the reactants have lower energy than the products. Yet it is not V that decides the reaction to proceed, but the free energy $F = E - TS$, where T is the temperature and S the entropy. The free energy depends on the density of the vibrational states of the reactants and products. The more numerous the low-energy vibrational levels the larger the entropy and the lower the free energy, if $T > 0$. As we can see, the reactant vibrational levels are scarce, while on the product side they are densely distributed. When the energy gain related to the entropy overcomes the potential energy loss, then the (endothermic) reaction will proceed spontaneously.

For the time being let us take an example with $V_0(-\infty) = V_0(\infty)$, i.e. the barrier calculated from IRC is *the same* in both directions. Imagine a narrow entrance channel, i.e. large force constants for the oscillators, and a wide exit channel, i.e. low force constants.

The vibrational energies in the entrance channel are high, while in the exit channel they are low. This results in $V_{\text{adiab}}(-\infty; v_1, v_2, \dots, v_{3N-7}) > V_{\text{adiab}}(\infty; v_1, v_2, \dots, v_{3N-7})$, i.e. the barrier for the reaction reactants \rightarrow products is low, while for the reaction products \rightarrow reactants it is high. The products will form more often than the reactants.

On top of that if the entrance channel is narrow, while the exit channel is wide, the density of the vibrational states will be small in the entrance channel and large in the exit channel (Figs. 14.1.g,h and 14.5). Therefore, for $T > 0$ there will be a lot of possibilities to occupy the low-energy vibrational levels for the products, while only a few possibilities for the reactants. This means a high entropy of the products and a small entropy of the reactants, i.e. the products will be more stabilized by the entropy than the reactants.³³ Once again we can see, that

while the energy in the endothermic reaction *increases*, the decisive factor is the free energy which *decreases*. The reactants \rightarrow products reaction occurs “uphill” in potential energy, but “downhill” in free energy.

Kinetic and thermodynamic pictures

- In a macroscopic reaction carried out in a chemist’s flask we have a statistical ensemble of the systems that are in different microscopic stages of the reaction.

³³It pertains to the term $-TS$ in the free energy.

- The ensemble may be modelled by a reaction “drain-pipe” (we assume the barrier) with a lot of points, each representing one of the reacting systems.
- When the macroscopic reaction begins (e.g., we mix two reactants) a huge number of points appear in the entrance channel, i.e. we have the reactants only. As the reactant molecules assemble or dissociate the points appear or disappear.
- If the barrier were high (no tunnelling) and temperature $T = 0$, all the reactants would be in their zero-vibrational states³⁴ and in their ground rotational states. This state would be stable even when the product valley corresponded to a lower energy (this would be a metastable state).
- Raising the temperature causes some of the ensemble elements in the entrance channel to acquire energy comparable to the barrier height. Those elements might have a chance to pass the barrier either by tunnelling (for energy smaller than the barrier) or by going over the barrier. Not all of the elements with sufficient energies would pass the barrier, only those with reactive trajectories.
- After passing the barrier the energy is conserved, but changes into the translational, vibrational and rotational energy of products or may be transferred to a “third body” (e.g., the solvent molecules) or changed into electromagnetic radiation.
- The probability of the reactive trajectories might be calculated in a way similar to that described in Chapter 4 (tunnelling³⁵), with additional taking into account the initial vibrational and rotational states of the reactants as well as averaging over the energy level populations.
- The products would have also a chance to pass the barrier back to the reactant side, but at the beginning the number of the elements passing the barrier in the reactant-to-product direction would be larger (non-equilibrium state).
- However the higher the product concentration, the more often the products transform into the reactants. As an outcome we arrive at the *thermodynamic equilibrium state*, in which the average numbers of the elements passing the barrier per unit time in either direction are equal.
- If the barrier is high and the energies considered low, then the stationary states of the system could be divided into those (of energy $E_{i,R}$), which have high amplitudes in the entrance channel (the reactant states) and those (of energy $E_{i,P}$) with high amplitudes in the exit channel (product states). In such a case we may calculate the partition function for the reactants:

$$Z_R(T) = \sum_i g_i \exp\left(-\frac{E_{i,R} - E_{0,R}}{k_B T}\right)$$

and for the products

$$Z_P(T) = \sum_i g_i \exp\left(-\frac{E_{i,P} - E_{0,R}}{k_B T}\right) = \sum_i g_i \exp\left(-\frac{E_{i,P} - E_{0,P} - \Delta E}{k_B T}\right),$$

³⁴Please note, that even in this case ($T = 0$) the energy of these states would not only depend on the bottom of the valley, $V_0(s)$, but also on the valley's width through $\omega_k(s)$, according to eq. (14.29).

³⁵See also H. Eyring, J. Walter, G.E. Kimball, “*Quantum Chemistry*”, John Wiley, New York, 1967.

where g_i stands for the degeneracy of the i -th energy level and the difference of the ground-state levels is $\Delta E = E_{0,R} - E_{0,P}$.

- Having the partition functions, we may calculate (at a given temperature, volume and a fixed number of particles³⁶) the free or Helmholtz energy (F) corresponding to the entrance and to the exit channels (in thermodynamic equilibrium)

$$F_R(T) = -k_B T \frac{\partial}{\partial T} \ln Z_R(T), \quad (14.30)$$

$$F_P(T) = -k_B T \frac{\partial}{\partial T} \ln Z_P(T). \quad (14.31)$$

- The reaction goes in such a direction as to attain the minimum of free energy F .
- The higher the density of states in a given channel (this corresponds to higher entropy) the lower F . The density of the vibrational states is higher for wider channels (see Fig. 14.5).

14.4.3 VIBRATIONALLY NON-ADIABATIC MODEL

Coriolis coupling

The vibrationally adiabatic approximation is hardly justified, because the reaction channel is curved. This means that motion along s couples with some vibrational modes, and also the vibrational modes couple among themselves. We have therefore to use the non-adiabatic theory and this means we need coupling coefficients B . The Miller–Handy–Adams reaction path Hamiltonian theory gives the following expression for the $B_{kk'}$:

$$B_{kk'}(s) = \frac{\partial \mathbf{L}_k(s)}{\partial s} \cdot \mathbf{L}_{k'}(s), \quad (14.32)$$

where \mathbf{L}_k , $k = 1, 2, \dots, 3N - 7$, represent the orthonormal eigenvectors ($3N$ -dimensional, cf. Chapter 7, p. 297) of the normal modes Q_k of frequency ω_k (Fig. 14.6).

If the derivative in the above formula is multiplied by an increment of the reaction path Δs , we obtain $\frac{\partial \mathbf{L}_k(s)}{\partial s} \Delta s$ which represents a change of normal mode vector \mathbf{L}_k when the system moved along the IRC by the increment Δs . This change might be similar to normal mode eigenvector $\mathbf{L}_{k'}$. This means that $B_{kk'}$ measures how much eigenvector $\mathbf{L}_{k'}(s)$ resembles the *change* of eigenvector $\mathbf{L}_k(s)$ (when the system moves along the reaction path).³⁷ Coupling coefficient $B_{kk'}$ is usually

³⁶Similar considerations may be performed for a constant pressure (instead of volume). The quantity that then attains the minimum at the equilibrium state is the Gibbs potential G .

³⁷From differentiating the orthonormality condition $\mathbf{L}_k(s) \cdot \mathbf{L}_{k'}(s) = \delta_{kk'}$ we obtain

$$\begin{aligned} \frac{\partial}{\partial s} [\mathbf{L}_k(s) \cdot \mathbf{L}_{k'}(s)] &= \left[\frac{\partial \mathbf{L}_k(s)}{\partial s} \cdot \mathbf{L}_{k'}(s) + \mathbf{L}_k(s) \cdot \frac{\partial \mathbf{L}_{k'}(s)}{\partial s} \right] \\ &= \left[\frac{\partial \mathbf{L}_k(s)}{\partial s} \cdot \mathbf{L}_{k'}(s) + \frac{\partial \mathbf{L}_{k'}(s)}{\partial s} \cdot \mathbf{L}_k(s) \right] \\ &= B_{kk'} + B_{k'k} = 0. \end{aligned}$$

Hence, $B_{kk'} = -B_{k'k}$.

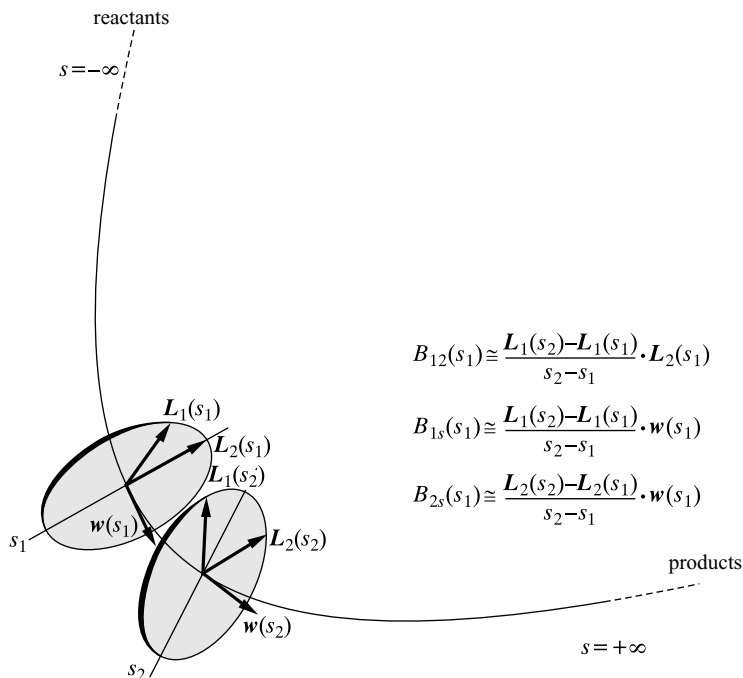


Fig. 14.6. Calculation of the Coriolis coupling coefficient (B_{12}) and the curvature coefficients (B_{1s} and B_{2s}) related to the normal modes 1 and 2 and reaction coordinate s . Diagonalization of the two Hessians calculated at points $s = s_1$ and $s = s_2$ gives two corresponding normal mode eigenvectors $L_1(s_1)$ and $L_2(s_1)$ as well as $L_1(s_2)$ and $L_2(s_2)$. At both points s_1 and s_2 we also calculate the vectors $\mathbf{w}(s_1)$ and $\mathbf{w}(s_2)$ that are tangent to the IRC. The calculated vectors inserted into the formulae give the approximations to B_{1s} , B_{2s} and B_{12} .

especially large close to those values of s , for which $\omega_k \cong \omega_{k'}$, i.e. for the crossing points of the vibrational frequency (or energy) curves $\omega_k(s)$. These are the points where we may expect an important energy flow from one normal mode to another, because the energy quanta match ($\hbar\omega_k(s) \cong \hbar\omega_{k'}(s)$). Coriolis coupling means that the directions of L_k and $L_{k'}$ change, when the reaction proceeds and this resembles a rotation in the configurational space about the IRC.

Curvature couplings

Curvature coupling constant B_{ks} links the motion along the reaction valley with the normal modes orthogonal to the IRC (Fig. 14.6):

$$B_{ks}(s) = \frac{\partial L_k(s)}{\partial s} \cdot \mathbf{w}(s), \quad (14.33)$$

where $\mathbf{w}(s)$ represents the unit vector tangent to the intrinsic reaction path $\mathbf{x}_{\text{IRC}}(s)$ at point s . Coefficient $B_{ks}(s)$ therefore represents a measure of how the *change* in the normal mode eigenvector $L_k(s)$ resembles a motion along the IRC. Large

$B_{ks}(s)$ makes energy flow from the normal mode to the reaction path (or *vice versa*) much easier.

DONATING MODES:

The modes with large $B_{ks}(s)$ in the *entrance* channel are called the *donating modes*, because an excitation of such modes makes possible an energy transfer to the reaction coordinate degree of freedom (an increase of the kinetic energy along the reaction path). This will make the reaction rate increase.

donating modes

In the vibrationally adiabatic approximation, coefficients B_{ks} are equal to zero. This means that in such an approximation an exothermic reaction would transform the net reaction energy (defined as the difference between the energy of the reactants and the products) into the kinetic energy of translational motion of products, because the energy of the system in the entrance channel could not be changed into the vibrational energy of the products (including the “vibrations” of a rotational character). However, as was shown by John Polanyi and Dudley Herschbach, the reactions do not go this way – a majority of the reaction energy goes into the rotational degrees of freedom (excited states of some modes). The rotations are hidden in the vibrations at $s = 0$ which are similar to the internal rotations and in the limit of $s \rightarrow +\infty$ transform into product rotations. Next, the excited products emit infrared quanta in the process of infrared fluorescence (the chemist’s test tube gets hot). This means that in order to have a realistic description of reaction we have to abandon the vibrationally adiabatic approximation.

14.4.4 APPLICATION OF THE REACTION PATH HAMILTONIAN METHOD TO THE REACTION $\text{H}_2 + \text{OH} \rightarrow \text{H}_2\text{O} + \text{H}$

The reaction represents one of a few polyatomic systems for which precise calculations were performed.³⁸ It may be instructive to see how a practical implementation of the reaction path Hamiltonian method looks.

Potential energy hypersurface

The *ab initio* configuration interaction calculations (Chapter 10) of the potential energy hypersurface for the system under study were performed by Walsh and Dunning³⁹ within the Born–Oppenheimer (“clamped nuclei”) approximation described in Chapter 6. The electronic energy obtained as a function of the nuclear configuration plays the role of the potential energy for the motion of the nuclei. The calculation gave the electronic energy for a relatively scarce set of configu-

³⁸G.C.J. Schatz, *J. Chem. Phys.* 74 (1981) 113; D.G. Truhlar, A.D. Isaacson, *J. Chem. Phys.* 77 (1982) 3516; A.D. Isaacson, D.G. Truhlar, *J. Chem. Phys.* 76 (1982) 380 and above all the paper by Thom Dunning Jr. and Elfi Kraka in “*Advances in Molecular Electronic Structure Theory: The Calculation and Characterization of Molecular Potential Energy Surfaces*”, ed. T.H. Dunning, Jr., JAI Press, Inc., Greenwich, CN (1989) 1.

³⁹S.P. Walsh, T.H. Dunning, Jr., *J. Chem. Phys.* 72 (1980) 1303.

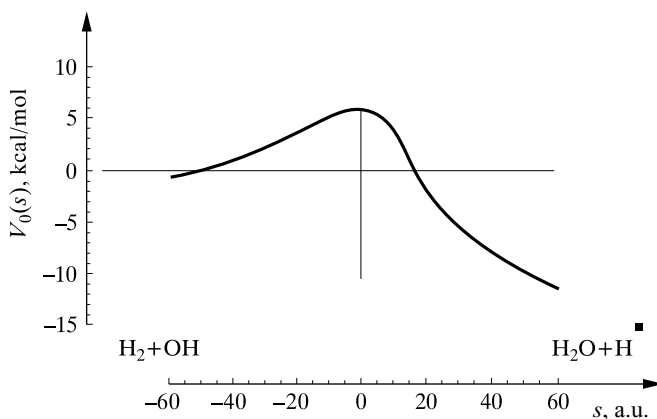


Fig. 14.7. The reaction $\text{H}_2 + \text{OH} \rightarrow \text{H}_2\text{O} + \text{H}$ energy profile $V_0(s)$ for $-\infty \leq s \leq \infty$. The value of the reaction coordinate $s = -\infty$ corresponds to the reactants, while $s = \infty$ corresponds to the products. It turns out that the product energy is lower than the energy of the reactants (i.e. the reaction is exothermic). The barrier height in the entrance channel calculated as the difference of the top of the barrier and the lowest point of the entrance channel amounts to 6.2 kcal/mol. According to T. Dunning, Jr. and E. Kraka, from “*Advances in Molecular Electronic Structure Theory*”, ed. T. Dunning, Jr., JAI Press, Greenwich, CN (1989), courtesy of the authors.

rations of the nuclei, but then the numerical results were fitted by an analytical function.⁴⁰ The IRC energy profile is shown in Fig. 14.7.

It is seen from Fig. 14.7 that the barrier height for the reactants is equal to about 6.2 kcal/mol, while the reaction energy calculated as the difference of the products minus the energy of the reactants is equal to about -15.2 kcal/mol (an exothermic reaction). What happens to the atoms when the system moves along the reaction path? This is shown in Fig. 14.8.

The saddle point configuration of the nuclei when compared to those corresponding to the reactants and to products tells us whether the barrier is early or late. The difference of the OH distances for the saddle point and for the product (H_2O) amounts to 0.26 \AA , which represents $\frac{0.26}{0.97} = 27\%$, while the HH distance difference for the saddle point and of the reactant (H_2) is equal to 0.11 \AA , which corresponds to $\frac{0.11}{0.74} = 15\%$. In conclusion, the saddle point resembles the reactants more than the products, i.e. the barrier is *early*.

Normal mode analysis

Let us see what the normal mode analysis gives when performed for some selected points along the IRC. The calculated frequencies are shown in Fig. 14.9 as wave numbers $\bar{\nu} = \omega/(2\pi c)$.

As we can see, before the reaction takes place we have two normal mode frequencies ω_{HH} and ω_{OH} . When the two reacting subsystems approach one another

⁴⁰G.C. Schatz, H. Elgersma, *Chem. Phys. Letters* 73 (1980) 21.

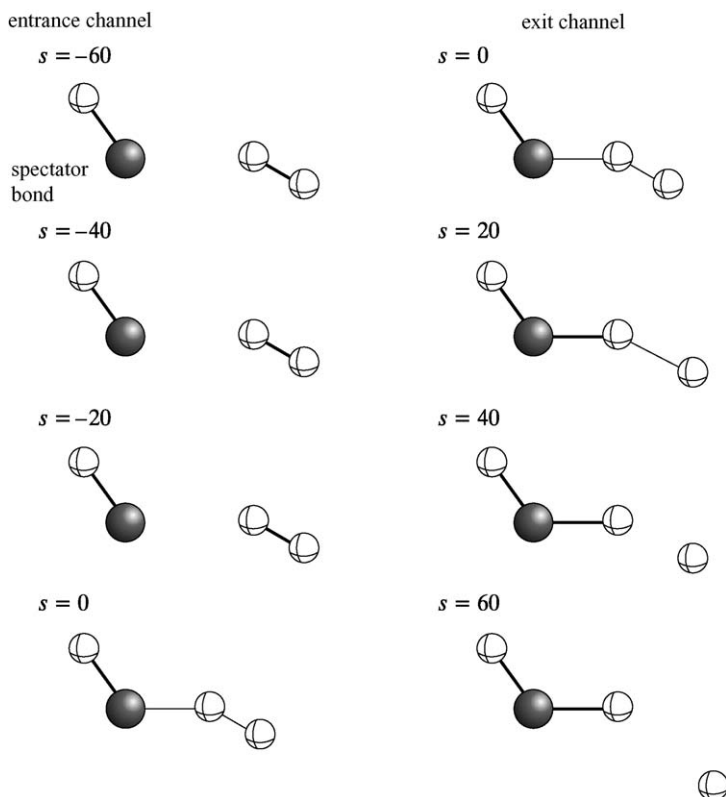


Fig. 14.8. The optimum atomic positions in the reacting system $\text{H}_2 + \text{OH} \rightarrow \text{H}_2\text{O} + \text{H}$ as functions of the reaction coordinate s . According to T. Dunning, Jr. and E. Kraka, from *Advances in Molecular Electronic Structure Theory*, ed. T. Dunning, Jr., JAI Press, Greenwich, CN (1989), courtesy of the authors.

we have to treat them as an entity. The corresponding number of vibrations is $3N - 6 = 3 \times 4 - 6 = 6$ normal modes. Two of them have frequencies close to those of HH and OH, three others have frequencies close to zero and correspond to the vibrational and rotational motions of the loosely bound reactants,⁴¹ the last “vibrational mode” is connected with a motion along the reaction path and has an imaginary frequency. Such a frequency means that the corresponding curvature of the potential energy is negative.⁴² For example, at the saddle point, when moving along the reaction path, we have a potential energy maximum instead of minimum as would be for a regular oscillator. Fig. 14.9 shows five (real) frequencies. The frequency ω_{HH} drops down close to the saddle point. This is precisely the bond to be broken. Interestingly, the frequency minimum is

⁴¹van der Waals interactions, see Chapter 13.

⁴²Note that $\omega = \sqrt{k/m}$, where the force constant k stands for the second derivative of the potential energy, i.e. its curvature.

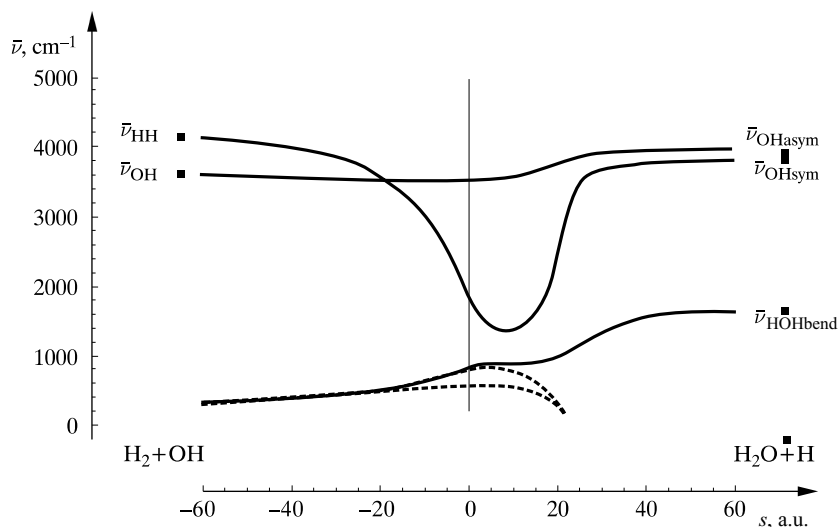


Fig. 14.9. The reaction $\text{H}_2 + \text{OH} \rightarrow \text{H}_2\text{O} + \text{H}$. The vibrational frequencies (in wave numbers $\bar{\nu} = \omega/(2\pi c)$) for the normal modes along the coordinate s . Only the real wave numbers are given (the “vibration” along s is imaginary and not given). According to T. Dunning, Jr. and E. Kraka, from “*Advances in Molecular Electronic Structure Theory*”, ed. T. Dunning, Jr., JAI Press, Greenwich, CN (1989), courtesy of the authors.

attained at 9 a.u. beyond the saddle point. Afterwards the frequency increases fast and when the reaction is completed it turns out to be the OH symmetric stretching frequency of the water molecule. Knowing only this, we can tell what has happened: the HH bond was broken and a new OH bond was formed. At the end of the reaction path we have, in addition, the antisymmetric stretching mode of the H_2O ($\bar{\nu}_{\text{OHasy}}$), which evolved from the starting value of ω_{OH} while changing only a little (this reflects that one OH bond exists all the time and in fact represents a “spectator” to the reaction) as well as the HOH bending mode ($\bar{\nu}_{\text{HOHbend}}$), which appeared as a result of the strengthening of an intermolecular interaction in $\text{H}_2 + \text{OH}$ when the reaction proceeded. The calculations have shown that this vibration corresponds to the *symmetric* stretching mode⁴³ of the H_2O ($\bar{\nu}_{\text{OHsym}}$). The two other modes at the beginning of the reaction have almost negligible frequencies, and after an occasional increasing of their frequencies near the saddle point end up with zero frequencies for large s . Of course, at the end we have to have $3 \times 3 - 6 = 3$ vibrational modes of the H_2O and so we do.

spectator bond

⁴³At first sight this looks like contradicting chemical intuition since the antisymmetric mode is apparently compatible to the reaction path (one hydrogen atom being far away while the other is close to the oxygen atom). However, everything is all right. The SCF LCAO MO calculations for the water molecule within a medium size basis set give the OH bond length equal to 0.95 Å, whereas the OH radical bond length is equal to 1.01 Å. This means that when the hydrogen atom approaches the OH radical (making the water molecule), the hydrogen atom of the radical has to get *closer* to the oxygen atom. The resulting motion of both hydrogen atoms is similar to the symmetric (not antisymmetric) mode.

Example 1. *Vibrationally adiabatic approximation*

Let us consider several versions of the reaction that differ by assuming various vibrational states of the reactants.⁴⁴ Using eq. (14.29), for each set of the vibrational quantum numbers we obtain the vibrationally adiabatic potential V_{adiab} as a function of s (Fig. 14.10).

The adiabatic potentials obtained are instructive. It turns out that:

- The adiabatic potential corresponding to the vibrational ground state ($v_{\text{OH}}, v_{\text{HH}} = (0, 0)$) gives lower barrier height than the classical potential $V_0(s)$ (5.9 kcal/mol vs 6.1). The reason for this is the lower zero-vibration energy for the saddle point configuration than for the reactants.⁴⁵
- The adiabatic potential for the vibrational ground state has its maximum at $s = -5$ a.u., not at the saddle point $s = 0$.
- Excitation of the OH stretching vibration does not significantly change the energy profile, in particular the barrier is lowered by only about 0.3 kcal/mol. Thus, the OH is definitely a spectator bond.
- This contrasts with what happens when the H_2 molecule is excited. In such a case the barrier is lowered by as much as about 3 kcal/mol. This suggests that the HH stretching vibration is a “donating mode”.

donating mode

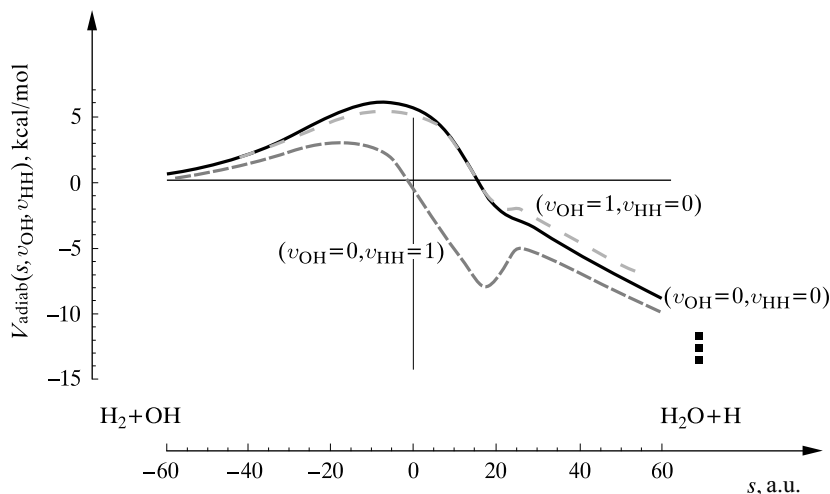


Fig. 14.10. The reaction $\text{H}_2 + \text{OH} \rightarrow \text{H}_2\text{O} + \text{H}$ (within the vibrationally adiabatic approximation). Three sets of the vibrational numbers $(v_{\text{OH}}, v_{\text{HH}}) = (0, 0), (1, 0), (0, 1)$ were chosen. Note, that the height and position of the barrier depend on the vibrational quantum numbers assumed. An excitation of H_2 considerably decreases the barrier height. The small squares on the right show the limiting values. According to T. Dunning, Jr. and E. Kraka, from “*Advances in Molecular Electronic Structure Theory*”, ed. T. Dunning, Jr., JAI Press, Greenwich, CN (1989), courtesy of the authors.

⁴⁴We need the frequencies of the modes which are orthogonal to the reaction path.

⁴⁵This stands to reason, because when the Rubicon is crossed, all the bonds are weakened with respect to the reactants.

Example 2. Non-adiabatic theory

Now let us consider the vibrationally non-adiabatic procedure. To do this we have to include the coupling constants B . This is done in the following way. Moving along the reaction coordinate s we perform the normal mode analysis resulting in the vibrational eigenvectors $L_k(s)$. This enables us to calculate how these vectors change and to determine the derivatives $\partial L_k / \partial s$. Now we may calculate the corresponding dot products (see eqs. (14.32) and (14.33)) and obtain the coupling constants $B_{kk'}(s)$ and $B_{ks}(s)$ at each selected point s . A role of the coupling constants B in the reaction rate can be determined after dynamic studies assuming various starting conditions (the theory behind this approach will not be presented in this book). Yet some important information may be extracted just by inspecting functions $B(s)$. The functions $B_{ks}(s)$ are shown in Fig. 14.11.

As we can see:

- In the entrance channel the value of $B_{\text{OH},s}$ is close to zero, therefore, there is practically no coupling between the OH stretching vibrations and the reaction path and hence there will be practically no energy flow between those degrees of freedom. This might be expected from a weak dependence of ω_{OH} as a function of s . Once more we see that the OH bond plays only the role of a reaction spectator.
- This is not the case for $B_{\text{HH},s}$. This quantity attains maximum just before the saddle point (let us recall that the barrier is early). The energy may, therefore, flow from the vibrational mode of H_2 to the reaction path (and *vice versa*) and a

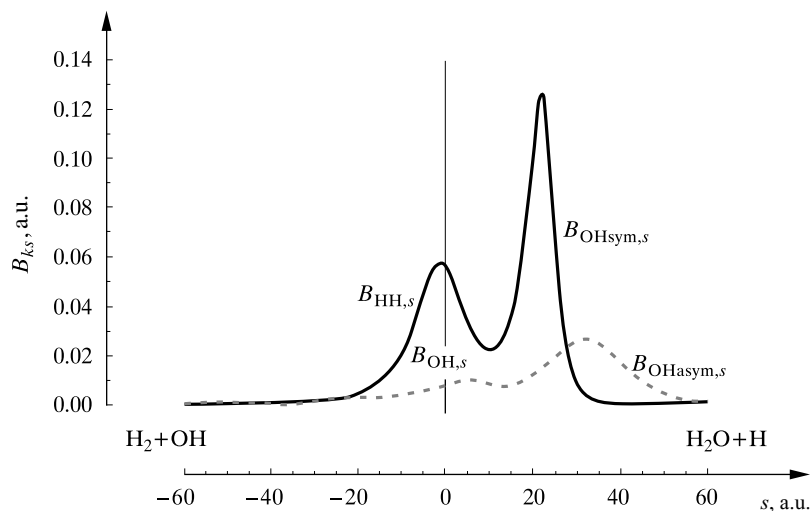


Fig. 14.11. The reaction $\text{H}_2 + \text{OH} \rightarrow \text{H}_2\text{O} + \text{H}$. The curvature coupling constants $B_{ks}(s)$ as functions of s . The $B_{ks}(s)$ characterize the coupling of the k -th normal mode with the reaction coordinate s . According to T. Dunning, Jr. and E. Kraka, from “*Advances in Molecular Electronic Structure Theory*”, ed. T. Dunning, Jr., JAI Press, Greenwich, CN (1989), courtesy of the authors.

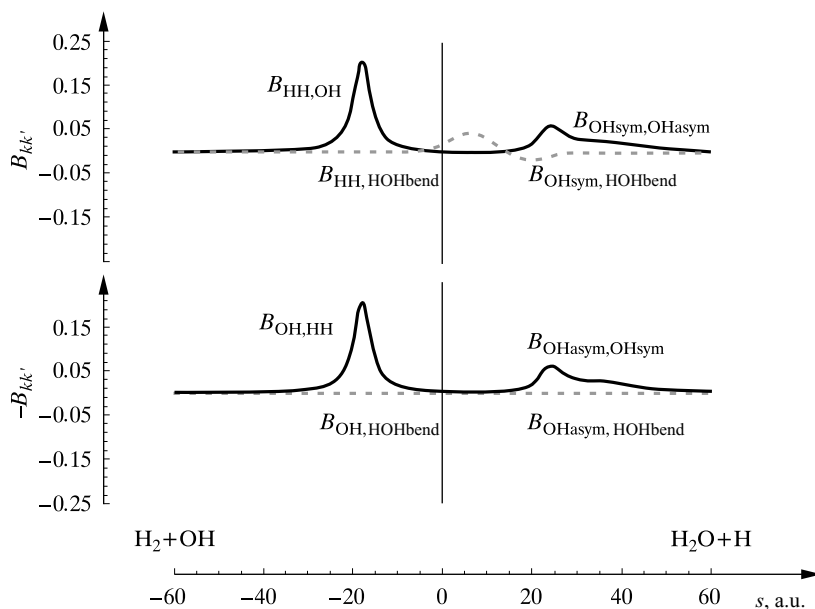


Fig. 14.12. The reaction $\text{H}_2 + \text{OH} \rightarrow \text{H}_2\text{O} + \text{H}$. The Coriolis coupling constants $B_{kk'}(s)$ as functions of s . A high value of $B_{kk'}(s)$ means that close to reaction coordinate s the changes of the k -th normal mode eigenvector resemble eigenvector k' . According to T. Dunning, Jr. and E. Kraka, from “*Advances in Molecular Electronic Structure Theory*”, ed. T. Dunning, Jr., JAI Press, Greenwich, CN (1989), courtesy of the authors.

vibrational excitation of H_2 may have an important impact on the reaction rate (recall please the lowering of the adiabatic barrier when this mode is excited).

The Coriolis coupling constants $B_{kk'}$ as functions of s are plotted in Fig. 14.12 (only for the OH and HH stretching and HOH bending modes).

The first part of Fig. 14.12 pertains to the HH vibrational mode, the second to the OH vibrational mode. As we can see:

- the maximum coupling for the HH and OH modes occurs long before the saddle point (close to $s = -18$ a.u.) enabling the system to exchange energy between the two vibrational modes;
- in the exit channel we have quite significant couplings between the symmetric and antisymmetric OH modes and the HOH bending mode.

14.5 ACCEPTOR–DONOR (AD) THEORY OF CHEMICAL REACTIONS

14.5.1 MAPS OF THE MOLECULAR ELECTROSTATIC POTENTIAL

Chemical reaction dynamics is possible only for very simple systems. Chemists, however, have most often to do with medium-size or large molecules. Would it be

possible to tell anything about the barriers for chemical reactions in such systems? Most of chemical reactions start from a situation when the molecules are far away, but already interact. The main contribution is the electrostatic interaction energy, which is of long-range character (Chapter 13). Electrostatic interaction depends strongly on the mutual orientation of the two molecules (*steric effect*). Therefore, the orientations are biased towards the privileged ones (energetically favourable). There is quite a lot of experimental data suggesting that privileged orientations lead, at smaller distances, to low reaction barriers. There is no guarantee of this, but it often happens for electrophilic and nucleophilic reactions, because the attacking molecule prefers those parts of the partner that correspond to high electron density (for electrophilic attack) or to low electron density (for nucleophilic attack).

steric effect

electrophilic attack

We may use an electrostatic probe (e.g., a unit positive charge) to detect, which parts of the molecule “like” the approaching charge (energy lowering), and which do not (energy increasing).

The electrostatic interaction energy of the point-like probe in position \mathbf{r} with molecule A is described by the formula (the definition of the electrostatic potential produced by molecule A, see Fig. 14.13.a):

nucleophilic attack

$$V_A(\mathbf{r}) = + \sum_a \frac{Z_a}{|\mathbf{r}_a - \mathbf{r}|} - \int \frac{\rho_A(\mathbf{r}')}{|\mathbf{r}' - \mathbf{r}|} d^3\mathbf{r}', \quad (14.34)$$

where the first term describes the interaction of the probe with the nuclei denoted by index a , and the second means the interaction of the probe with the electron density distribution of the molecule A denoted by ρ_A (according to Chapter 11).⁴⁶

In the Hartree–Fock or Kohn–Sham approximation (Chapter 11, p. 570; we assume the n_i -tuple occupation of the molecular orbital $\varphi_{A,i}$, $n_i = 0, 1, 2$)

$$\rho_A(\mathbf{r}) = \sum_i n_i |\varphi_{A,i}(\mathbf{r})|^2. \quad (14.35)$$

In order to obtain $V_A(\mathbf{r})$ at point \mathbf{r} it is sufficient to calculate the distances of the point from any of the nuclei (trivial) as well as the one-electron integrals, which appear after inserting into (14.34) $\rho_A(\mathbf{r}') = 2 \sum_i |\varphi_{A,i}(\mathbf{r}')|^2$. Within the LCAO MO approximation the electron density distribution ρ_A represents the sum of products of two atomic orbitals (in general centred at two different points). As a result the task reduces to calculating typical one-electron three-centre integrals of the nuclear attraction type (cf. Chapter 8 and Appendix P), because the third centre corresponds to the point \mathbf{r} (Fig. 14.13). There is no computational problem with this for contemporary quantum chemistry.

⁴⁶By the way, to calculate the electrostatic interaction energy of the molecules A and B we have to take (instead of a probe) the nuclei of the molecule B and sum of the corresponding contributions, and then to do the same with the electronic cloud of B. This corresponds to the following formula: $E_{\text{elst}} = \sum_b Z_b V_A(\mathbf{r}_b) - \int d^3\mathbf{r} \rho_B(\mathbf{r}) V_A(\mathbf{r})$, where b goes over the nuclei of B, and ρ_B represents its electronic cloud.

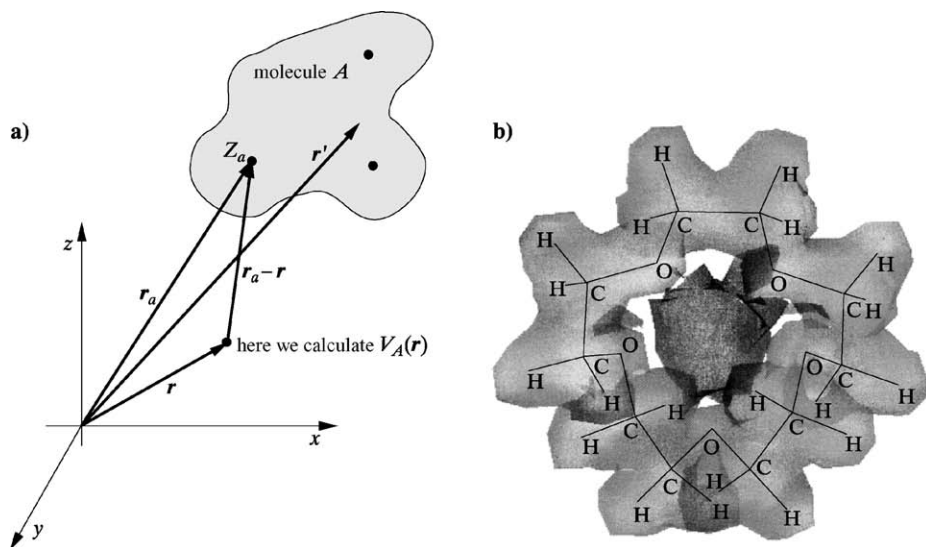


Fig. 14.13. Interaction of the positive unit charge (probe) with molecule A. Fig. (a) shows the coordinate system and the vectors used in eq. (14.34). Fig. (b) shows the equipotential surfaces $|V_A(\mathbf{r})|$ for the crown ether molecule. The light shadowed surface corresponds to $V_A(\mathbf{r}) > 0$, and the darker one to $V_A(\mathbf{r}) < 0$ (in more expensive books this is shown by using different colours). It is seen that the crown ether cavity corresponds to the negative potential, i.e. it would attract strongly cations.

In order to represent $V_A(\mathbf{r})$ graphically we usually choose to show an equipotential surface corresponding to a given absolute value of the potential, while additionally indicating its sign (Fig. 14.13.b). The sign tells us which parts of the molecule are preferred for the probe-like object to attack and which not. In this way we obtain basic information about the reactivity of different parts of the molecule.⁴⁷

ESP charges

Who attacks whom?

In chemistry a probe will not be a point charge, but rather a neutral molecule or an ion. Nevertheless our new tool (electrostatic potential) will still be useful:

- If the probe represents a cation, it will attack those parts of the molecule A which are electron-rich (electrophilic reaction).
- If the probe represents an anion, it will attack the electron-deficient parts (nucleophilic reaction).
- If the probe represents a molecule (B), its electrostatic potential V_B is the most interesting. Those AB configurations that correspond to the contacts of the associated sections of V_A and V_B with the opposite signs are the most (electrostatically) stable.

The site of the molecular probe (B) which attacks an electron-rich site of A itself has to be of electron-deficient character (and *vice versa*). Therefore, from

⁴⁷ Having the potential calculated according to (14.34) we may ask about the set of atomic charges that reproduce it. Such charges are known as ESP (ElectroStatic Potential).

the point of view of the attacked molecule (A), everything looks “upside down”: an electrophilic reaction becomes nucleophilic and *vice versa*. When two objects exhibit an affinity to each other, who attacks whom represents a delicate and ambiguous problem and let it be that way. Therefore where does such nomenclature in chemistry come from? Well, it comes from the concept of didactics.

The problem considered is related to the Umpolung problem from p. 703. A change of sign or an exchange of charges on the interacting molecules (both operations may have only a limited meaning in chemistry) should not influence the key features of some reaction mechanisms involving intermediate ionic species.

We may ask whether there is any difference between a reaction taking place in a vacuum and the same reaction proceeding in the electric field resulting from the neighbouring point charges. Why might this be of interest? Well, many important chemical reactions proceed in the presence of catalysts, e.g., in the active centre of enzymes. To proceed, many chemical reactions require a chemist to heat the flask to very high temperatures, while in enzymes the same reaction proceeds in mild conditions. For example, in order to synthesize ammonia from atmospheric nitrogen chemists use the hellish conditions of an electric arc. However a similar reaction takes place in lupin roots. The enzymes are proteins, which Nature took care to make of a self-assembling character with a nearly unique, final conformation,⁴⁸ assuring active centre formation. Only in this *native* conformation does the active centre work as a catalyst: the reactant is recognized (cf. p. 750), and then docked in the reaction cavity, a particular bond is broken, the products are released and the enzyme comes back to the initial state. Well, why does the bond break? The majority of amino acids in an enzyme play an important yet passive role: just to allow a few important amino acids to make the reaction cavity as well as the reaction site. The role of the reaction cavity is to assure the reactant is properly oriented in space with respect to those amino acids that form the reaction site. The role of the latter is to create a specific electric field at the reactant position. Such a field lowers the reaction barrier, thus making it easier. Andrzej Sokalski,⁴⁹ reversing the problem, asked a very simple question: for a given reaction *how should the field-producing charges look in order to lower (most-effectively) the reaction barrier?* This is what we will need first when planning artificial enzymes for the reactions desired.

native
conformation

reaction cavity

As we have seen, for computational reasons we are able to take into account only reactions involving a *few* nuclei. However, chemists are interested in the reactivity of *much* larger molecules. We would like to know what particular features of the electronic structure make a chemical reaction proceed. This is the type of question that will be answered in the acceptor–donor theory.⁵⁰

Molecules attract each other at long distances

Let us assume that two molecules approach each other, say, because of their chaotic thermic motion. When the molecules are still far away, they already un-

⁴⁸Among myriads of other conformations, cf. Chapter 7.

⁴⁹W.A. Sokalski, *J. Mol. Catalysis* 30 (1985) 395.

⁵⁰More details about the acceptor–donor theory may be found in excellent paper by S. Shaik, *J. Am. Chem. Soc.* 103 (1981) 3692. The results reported in Tables 14.2–14.6 also originate from this paper.

dergo tiny changes due to the electric field produced by their partner (Chapters 12 and 13). The very fact that each of the molecules having permanent multipole moments is now immersed in a non-homogeneous electric field, means the multipole moments interact with the field and the resulting electrostatic interaction energy.

The electric field also distorts the partner's electronic cloud, and as a consequence of the Hellmann–Feynman theorem (Chapter 12) this creates a distortion of the nuclear framework. Thus, the multipole moments of a distorted molecule are a little changed (“induced moments”) with respect to the permanent ones. If we take the induced moment interaction with the field into account, then apart from the electrostatic interaction energy we obtain the induction energy contribution.⁵¹

Besides this, each of the molecules feels electric field fluctuations coming from motion of the electrons in the partner and adjusts to that motion. This leads to the dispersion interaction (Chapter 13).

Even at long intermolecular distances the dominating electrostatic interaction orients the molecules to make them attract each other. The induction and dispersion energies are always attractive. Therefore, in such a case all important energy contributions mean *attraction*.

They are already close...

What happens when the molecules are closer? Besides the effects just described a new one appears – the valence repulsion coming from the electron clouds overlap. Such an interaction vanishes exponentially with intermolecular distance. This is why we were able to neglect this interaction at longer distances.

steric factor

Two molecules, even simple ones, may undergo different reactions depending not only on their collision energy, but also on their mutual orientation with respect to one another (*steric factor*). The steric factor often assures selectivity, since only molecules of a certain shape (that fit together) may get their active centres close enough (cf. Chapter 13).

van der Waals
complex

Suppose that two molecules under consideration collide with a proper orientation in space.⁵² What will happen next? As we will see later, it depends on the molecules involved. Very often at the beginning there will be an energetic barrier to overcome. When the barrier is too high compared with the collision energy, then a *van der Waals* complex is usually formed, otherwise the barrier is overcome and the chemical reaction occurs. On the other hand for some reactants no reaction barrier exists.

⁵¹If one or both molecules do not have any non-zero permanent multipole moments, their electrostatic interaction energy is zero. If at least one of them has a non-zero permanent moment (and the partner has electrons), then there is a non-zero induction energy contribution.

⁵²A desired reaction to occur.

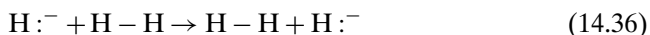
14.5.2 WHERE DOES THE BARRIER COME FROM?

The barrier always results from the intersection of diabatic potential energy hypersurfaces. We may think of diabatic states as preserving the electronic state (e.g., the system of chemical bonds): I and II, respectively.

Sometimes it is said that the barrier results from an avoided crossing (cf. Chapter 6) of two diabatic hypersurfaces that belong to the same irreducible representation of the symmetry group of the Hamiltonian (in short: “of the same symmetry”). This, however, cannot be taken literally, because, as we know from Chapter 6, the non-crossing rule is valid for diatomics only. The solution to this dilemma is the conical intersection described in Chapter 6 (cf. Fig. 6.15).⁵³ Instead of diabatic we have two adiabatic hypersurfaces (“upper” and “lower”⁵⁴), each consisting of the diabatic part I and the diabatic part II. A thermic reaction takes place as a rule on the lower hypersurface and corresponds to crossing the border between I and II.

14.5.3 MO, AD AND VB FORMALISMS

Let us take an example of a simple substitution reaction:



and consider the acceptor–donor formalism (AD). The formalism may be treated as intermediate between the configuration interaction (CI) and the valence bond (VB) formalisms. Any of the three formalisms is equivalent to the two others, provided they differ only by a linear transformation of many-electron basis functions.

In the CI formalism the Slater determinants are built of the molecular spinorbitals

In the VB formalism the Slater determinants are built of the atomic spinorbitals

In the AD formalism the Slater determinants are built of the acceptor and donor spinorbitals

MO picture → AD picture

Molecular orbitals for the total system $\varphi_1, \varphi_2, \varphi_3$ in a minimal basis set may be expressed (Fig. 14.14) using the molecular orbital of the donor (n , in our case the $1s$ atomic orbital of H^-) and the acceptor molecular orbitals (bonding χ and antibonding χ^*):

$$\begin{aligned} \varphi_1 &= a_1 n + b_1 \chi - c_1 \chi^*, \\ \varphi_2 &= a_2 n - b_2 \chi - c_2 \chi^*, \\ \varphi_3 &= -a_3 n + b_3 \chi - c_3 \chi^*, \end{aligned} \quad (14.37)$$

⁵³The term “conical” stems from a *linear* (or “conical-like”) dependence of the two adiabatic energy hypersurfaces on the distance from the conical intersection point.

⁵⁴On the energy scale.

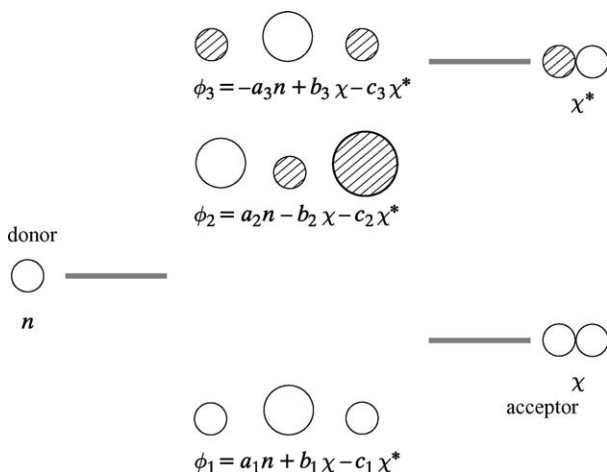


Fig. 14.14. A schematic representation of the molecular orbitals and their energies: of the donor (n representing the hydrogen atom 1s orbital), of the acceptor (bonding χ and antibonding χ^* of the hydrogen molecule) as well as of the total system H₃ in a linear configuration (centre of the figure). The lowest-energy molecular orbital of H₃ does not have any node, the higher has one while the highest has two nodes. In all cases we use the approximation that the molecular orbitals are built of the three 1s hydrogen atomic orbitals.

where $a_i, b_i, c_i > 0$, for $i = 1, 2, 3$. This convention comes from the fact that ϕ_1 is of the lowest energy and therefore exhibits no node, ϕ_2 has to play the role of the orbital second in energy scale and therefore has a single node, while ϕ_3 is the highest in energy and therefore has two nodes.⁵⁵

Any N -electron Slater determinant Ψ composed of the molecular spinorbitals $\{\phi_i\}$, $i = 1, 2, \dots$ (cf. eq. (M.1) on p. 986) may be written as a linear combination of the Slater determinants Ψ_i^{AD} composed of the spinorbitals u_i , $i = 1, 2, \dots$, of the *acceptor and donor*⁵⁶ (AD picture)

$$\Psi_k^{\text{MO}} = \sum_i C_k(i) \Psi_i^{\text{AD}}. \quad (14.38)$$

A similar expansion can also be written for the *atomic* spinorbitals (VB picture) instead of the donors and acceptors (AD picture).

⁵⁵Positive a, b, c make possible the node structure described above.

⁵⁶We start from the Slater determinant built of N molecular spinorbitals. Any of these is a linear combination of the spinorbitals of the donor and acceptor. We insert these combinations into the Slater determinant and expand the determinant according to the first row (Laplace expansion, see Appendix A on p. 889). As a result we obtain a linear combination of the Slater determinants all having the *donor or acceptor* spinorbitals in the first row. For each of the Slater determinants we repeat the procedure, but focusing on the second row, then the third row, etc. We end up with a linear combination of the Slater determinants that contain *only* the donor or acceptor spinorbitals. We concentrate on one of them, which contains some particular donor and acceptor orbitals. We are interested in the coefficient $C_k(i)$ that multiplies this Slater determinant.

In a moment we will be interested in some of the coefficients $C_k(i)$. For example, the expansion for the ground-state Slater determinant (in the MO picture)

$$\Psi_0 = N_0 |\varphi_1 \bar{\varphi}_1 \varphi_2 \bar{\varphi}_2| \quad (14.39)$$

gives

$$\Psi_0 = C_0(\text{DA})\Psi_{\text{DA}} + C_0(\text{D}^+\text{A}^-)\Psi_{\text{D}^+\text{A}^-} + \cdots, \quad (14.40)$$

where $\bar{\varphi}_i$ denotes the spinorbital with spin function β , and φ_i – the spinorbital with spin function α , N_0 stands for the normalization coefficient, while Ψ_{DA} , $\Psi_{\text{D}^+\text{A}^-}$ represent the normalized Slater determinants with the following electronic configurations, in $\Psi_{\text{DA}} : n^2 \chi^2$, in $\Psi_{\text{D}^+\text{A}^-} : n^1 \chi^2 (\chi^*)^1$, etc.

We are first interested in the coefficient $C_0(\text{DA})$. As shown by Fukui, Fujimoto and Hoffmann (cf. Appendix Z, p. 1058)⁵⁷

$$C_0(\text{DA}) \approx \langle \Psi_{\text{DA}} | \Psi_0 \rangle = \begin{vmatrix} a_1 & b_1 \\ a_2 & -b_2 \end{vmatrix}^2 = (a_1 b_2 + a_2 b_1)^2, \quad (14.41)$$

where in the determinant, the coefficients of the donor and acceptor orbitals appear in those molecular orbitals φ_i of the total system that are occupied in ground-state Slater determinant Ψ_0 (the coefficients of n and χ in φ_1 are a_1 and b_1 , respectively, while those in φ_2 are a_2 and $-b_2$, respectively, see eqs. (14.37)).

Roald Hoffmann, American chemist, born 1937 in Złoczów (then Poland) to a Jewish family, professor at Cornell University in Ithaca, USA. Hoffmann discovered the symmetry rules that pertain to some reactions of organic compounds. In 1981 he shared the Nobel Prize with Kenichi Fukui “for their theories, developed independently, concerning the course of chemical reactions”. Roald Hoffmann is also a poet and playwright. His poetry is influenced by chemistry, in which, as he wrote, was inspired by Marie Curie.

His CV reads like a film script. When in 1941 the Germans entered Złoczów, the four year old Roald was taken with his mother to a labour camp. One of the Jewish detainees betrayed a camp conspiracy network to the Germans. They massacred the camp, but Roald and his mother had earlier been smuggled out of the camp by his father and hidden in a Ukrainian teacher's house. Soon after, his father was killed. The Red Army pushed the Germans out in 1944 and Roald and his mother went via Przemyśl to Cracow. In 1949 they fi-



nally reached America. Roald Hoffmann graduated from Stuyvesant High School, Columbia University and Harvard University. In Harvard Roald met the excellent chemist Professor Robert Burns Woodward (syntheses of chlorophyll, quinine, strychnine, cholesterol, penicillin structure, vitamins), a Nobel Prize winner in 1965. Woodward alerted Hoffmann to a mysterious behaviour of polyenes in substitution reactions. Roald Hoffmann clarified the problem using the symmetry properties of the molecular orbitals (now known as the Woodward–Hoffmann symmetry rules, cf. p. 825).

⁵⁷ We assume that the orbitals n , χ and χ^* are orthogonal (approximation).

Kenichi Fukui (1918–1998), Japanese chemist, professor at the Kyoto University. One of the first scholars who stressed the importance of the IRC, and introduced what is called the frontier orbitals (mainly HOMO and LUMO), which govern practically all chemical processes. Fukui received the Nobel Prize in chemistry in 1981.



Now instead of Ψ_0 let us take two doubly excited configurations of the total system:⁵⁸

$$\Psi_{2d} = N_2 |\varphi_1 \bar{\varphi}_1 \varphi_3 \bar{\varphi}_3| \quad (14.42)$$

and

$$\Psi_{3d} = N_3 |\varphi_2 \bar{\varphi}_2 \varphi_3 \bar{\varphi}_3|, \quad (14.43)$$

where N_i stand for the normalization coefficients. Let us ask about the coefficients that *they* produce for the DA configuration (let us call these coefficients $C_2(\text{DA})$ for Ψ_{2d} and $C_3(\text{DA})$ for Ψ_{3d}), i.e.

$$\Psi_{2d} = C_2(\text{DA})\Psi_{\text{DA}} + C_2(\text{D}^+\text{A}^-)\Psi_{\text{D}^+\text{A}^-} + \cdots, \quad (14.44)$$

$$\Psi_{3d} = C_3(\text{DA})\Psi_{\text{DA}} + C_3(\text{D}^+\text{A}^-)\Psi_{\text{D}^+\text{A}^-} + \cdots. \quad (14.45)$$

According to the result described above (see p. 1058) we obtain:

$$C_2(\text{DA}) = \begin{vmatrix} a_1 & b_1 \\ -a_3 & b_3 \end{vmatrix}^2 = (a_1 b_3 + a_3 b_1)^2, \quad (14.46)$$

$$C_3(\text{DA}) = \begin{vmatrix} a_2 & -b_2 \\ -a_3 & b_3 \end{vmatrix}^2 = (a_2 b_3 - a_3 b_2)^2. \quad (14.47)$$

Such formulae enable us to calculate the contributions of the particular donor-acceptor resonance structures (e.g., DA, D^+A^- , etc., cf. p. 520) in the Slater determinants built of the molecular orbitals (14.37) of the total system. If one of these structures prevailed at a given stage of the reaction, this would represent important information about what has happened in the course of the reaction.

Please recall that at every reaction stage the main object of interest will be the ground-state of the system. The ground-state will be dominated⁵⁹ by various resonance structures. As usual the resonance structures are associated with the corresponding chemical structural formulae with the proper chemical bond pattern. *If at a reaction stage a particular structure dominated, then we would say that the system is characterized by the corresponding chemical bond pattern.*

14.5.4 REACTION STAGES

We would like to know the a , b , c values at *various reaction stages*, because we could then calculate the coefficients C_0 , C_2 and C_3 for the DA as well as for other donor-acceptor structures (e.g., D^+A^- , see below) and deduce what really happens during the reaction.

⁵⁸We will need this information later to estimate the configuration interaction role in calculating the CI ground state.

⁵⁹I.e. these structures will correspond to the highest expansion coefficients.

Reactant stage (R)

The simplest situation is at the starting point. When H^- is far away from H-H , then of course (Fig. 14.14) $\varphi_1 = \chi$, $\varphi_2 = n$, $\varphi_3 = -\chi^*$. Hence, we have $b_1 = a_2 = c_3 = 1$, while the other a , b , $c = 0$, therefore:

i	a_i	b_i	c_i
1	0	1	0
2	1	0	0
3	0	0	1

Using formulae (14.41), (14.46) and (14.47) (the superscript R recalls that the results correspond to reactants):

$$C_0^R(\text{DA}) = (0 \cdot 1 + 1 \cdot 1)^2 = 1, \quad (14.48)$$

$$C_2^R(\text{DA}) = 0, \quad (14.49)$$

$$C_3^R(\text{DA}) = (1 \cdot 0 - 0 \cdot 0)^2 = 0. \quad (14.50)$$

When the reaction begins, the reactants are correctly described as a Slater determinant with doubly occupied n and χ orbitals, which corresponds to the DA structure.

This is, of course, what we expected to obtain for the electronic configuration of the non-interacting reactants.

Intermediate stage (I)

What happens at the intermediate stage (I)?

It will be useful to express the atomic orbitals $1s_a$, $1s_b$, $1s_c$ through orbitals n , χ , χ^* (they span the same space). From Chapter 8, p. 371, we obtain

$$1s_a = n, \quad (14.51)$$

$$1s_b = \frac{1}{\sqrt{2}}(\chi - \chi^*), \quad (14.52)$$

$$1s_c = \frac{1}{\sqrt{2}}(\chi + \chi^*), \quad (14.53)$$

where we have assumed that the overlap integrals between different atomic orbitals are equal to zero.

The intermediate stage corresponds to the situation in which the hydrogen atom in the middle (b) is at the same distance from a as from c , and therefore the two atoms are equivalent. This implies that the nodeless, one-node and two-node orbitals have the following form (where \bigcirc stands for the $1s$ orbital and \bullet for the $-1s$

orbital)

$$\begin{aligned}
 \varphi_1 &= \bigcirc \bigcirc \bigcirc = \frac{1}{\sqrt{3}}(1s_a + 1s_b + 1s_c), \\
 \varphi_2 &= \bigcirc \cdot \bullet = \frac{1}{\sqrt{2}}(1s_a - 1s_c), \\
 \varphi_3 &= \bullet \bigcirc \bullet = \frac{1}{\sqrt{3}}(-1s_a + 1s_b - 1s_c).
 \end{aligned}
 \tag{14.54}$$

Inserting formulae (14.52) we obtain:

$$\begin{aligned}
 \varphi_1 &= \frac{1}{\sqrt{3}}\left(n + \sqrt{2}\chi + 0 \cdot \chi^*\right), \\
 \varphi_2 &= \frac{1}{\sqrt{2}}\left(n - \frac{1}{\sqrt{2}}(\chi + \chi^*)\right), \\
 \varphi_3 &= \frac{1}{\sqrt{3}}\left(-n + 0 \cdot \chi - \sqrt{2}\chi^*\right),
 \end{aligned}
 \tag{14.55}$$

	a_i	b_i	c_i
$i = 1$	$\frac{1}{\sqrt{3}}$	$\sqrt{\frac{2}{3}}$	0
$i = 2$	$\frac{1}{\sqrt{2}}$	$\frac{1}{2}$	$\frac{1}{2}$
$i = 3$	$\frac{1}{\sqrt{3}}$	0	$\sqrt{\frac{2}{3}}$

(14.56)

From eq. (14.41) we have

$$C_0^I(\text{DA}) = \left(\frac{1}{\sqrt{3}}\frac{1}{2} + \frac{1}{\sqrt{2}}\sqrt{\frac{2}{3}}\right)^2 = \frac{3}{4} = 0.75, \tag{14.57}$$

$$C_2^I(\text{DA}) = \left(\frac{1}{\sqrt{3}} \cdot 0 + \sqrt{\frac{2}{3}}\frac{1}{\sqrt{3}}\right)^2 = \frac{2}{9} = 0.22, \tag{14.58}$$

$$C_3^I(\text{DA}) = \left(\frac{1}{\sqrt{2}} \cdot 0 - \frac{1}{2}\frac{1}{\sqrt{3}}\right)^2 = \frac{1}{12} = 0.08. \tag{14.59}$$

The first of these three numbers is the most important. Something happens to the electronic ground-state of the system. At the starting point, the ground-state wave function had a DA contribution equal to $C_0^R(\text{DA}) = 1$, while now this contribution has decreased to $C_0^I(\text{DA}) = 0.75$. Let us see what will happen next.

Product stage (P)

How does the reaction end up?

Let us see how molecular orbitals φ corresponding to the products are expressed by n , χ and χ^* (they were defined for the starting point). At the end we have the molecule H–H (made of the middle and left hydrogen atoms) and the outgoing ion H^- (made of the right hydrogen atom).

Therefore the lowest-energy orbital at the end of the reaction has the form

$$\varphi_1 = \frac{1}{\sqrt{2}}(1s_a + 1s_b) = \frac{1}{\sqrt{2}}n + \frac{1}{2}\chi - \frac{1}{2}\chi^*, \quad (14.60)$$

which corresponds to $a_1 = \frac{1}{\sqrt{2}}$, $b_1 = \frac{1}{2}$, $c_1 = \frac{1}{2}$.

Since the φ_2 orbital is identified with $1s_c$, we obtain from eqs. (14.52): $a_2 = 0$, $b_2 = c_2 = \frac{1}{\sqrt{2}}$ (never mind that all the coefficients are multiplied by -1) and finally as φ_3 we obtain the antibonding orbital

$$\varphi_3 = \frac{1}{\sqrt{2}}(1s_a - 1s_b) = \frac{1}{\sqrt{2}}n - \frac{1}{2}\chi + \frac{1}{2}\chi^*, \quad (14.61)$$

i.e. $a_3 = \frac{1}{\sqrt{2}}$, $b_3 = \frac{1}{2}$, $c_3 = \frac{1}{2}$ (the sign is reversed as well). This leads to

i	a_i	b_i	c_i
1	$\frac{1}{\sqrt{2}}$	$\frac{1}{2}$	$\frac{1}{2}$
2	0	$\frac{1}{\sqrt{2}}$	$\frac{1}{\sqrt{2}}$
3	$\frac{1}{\sqrt{2}}$	$\frac{1}{2}$	$\frac{1}{2}$

(14.62)

Having a_i , b_i , c_i for the end of reaction, we may easily calculate $C_0^P(\text{DA})$ of eq. (14.41) as well as $C_2^P(\text{DA})$ and $C_3^P(\text{DA})$ from eqs. (14.46) and (14.47), respectively, for the reaction products

$$C_0^P(\text{DA}) = \left(\frac{1}{\sqrt{2}} \cdot \frac{1}{\sqrt{2}} + 0 \cdot \frac{1}{2} \right)^2 = \frac{1}{4}, \quad (14.63)$$

$$C_2^P(\text{DA}) = \left(\frac{1}{\sqrt{2}} \cdot \frac{1}{2} + \frac{1}{\sqrt{2}} \cdot \frac{1}{2} \right)^2 = \frac{1}{2}, \quad (14.64)$$

$$C_3^P(\text{DA}) = \left(0 \cdot \frac{1}{2} - \frac{1}{\sqrt{2}} \cdot \frac{1}{\sqrt{2}} \right)^2 = \frac{1}{4}. \quad (14.65)$$

Now we can reflect for a while. It is seen that during the reaction some important changes occur, namely

when the reaction begins, the system is 100% described by the structure DA, while after the reaction it resembles this structure only by 25%.

Role of the configuration interaction

We may object that our conclusions look quite naive. Indeed, there is something to worry about. We have assumed that, independent of the reaction stage, the ground-state wave function represents a single Slater determinant Ψ_0 , whereas we should rather use a configuration interaction expansion. In such an expansion, besides the dominant contribution of Ψ_0 , double excitations would be the most important (p. 560), which in our simple approximation of the three φ orbitals means a leading role for Ψ_{2d} and Ψ_{3d} :

$$\Psi_{CI} = \Psi_0 + \kappa_1 \Psi_{2d} + \kappa_2 \Psi_{3d} + \dots$$

The two configurations would be multiplied by some *small* coefficients (because all the time we deal with the electronic ground-state dominated by Ψ_0). It will be shown that the κ coefficients in the CI expansion $\Psi = \Psi_0 + \kappa_1 \Psi_{2d} + \kappa_2 \Psi_{3d}$ are *negative*. This will serve us to make a more detailed analysis (than that performed so far) of the role of the DA structure at the beginning and end of the reaction.

The coefficients κ_1 and κ_2 may be estimated using perturbation theory with Ψ_0 as unperturbed wave function. The first-order correction to the wave function is given by formula (5.25) on p. 208, where we may safely insert the total Hamiltonian \hat{H} instead of the operator⁶⁰ $\hat{H}^{(1)}$ (this frees us from saying what $\hat{H}^{(1)}$ looks like). Then we obtain

$$\kappa_1 \cong \frac{\langle \varphi_2 \bar{\varphi}_2 | \varphi_3 \bar{\varphi}_3 \rangle}{E_0 - E_{2d}} < 0, \quad (14.66)$$

$$\kappa_2 \cong \frac{\langle \varphi_1 \bar{\varphi}_1 | \varphi_3 \bar{\varphi}_3 \rangle}{E_0 - E_{3d}} < 0, \quad (14.67)$$

because from the Slater–Condon rules (Appendix M) we have $\langle \Psi_0 | \hat{H} \Psi_{2d} \rangle = \langle \varphi_2 \bar{\varphi}_2 | \varphi_3 \bar{\varphi}_3 \rangle - \langle \varphi_2 \bar{\varphi}_2 | \bar{\varphi}_3 \varphi_3 \rangle = \langle \varphi_2 \bar{\varphi}_2 | \varphi_3 \bar{\varphi}_3 \rangle - 0 = \langle \varphi_2 \bar{\varphi}_2 | \varphi_3 \bar{\varphi}_3 \rangle$ and, similarly, $\langle \Psi_0 | \hat{H} \Psi_{3d} \rangle = \langle \varphi_1 \bar{\varphi}_1 | \varphi_3 \bar{\varphi}_3 \rangle$, where E_0, E_{2d}, E_{3d} represent the energies of the corresponding states. The integrals $\langle \varphi_2 \bar{\varphi}_2 | \varphi_3 \bar{\varphi}_3 \rangle$ and $\langle \varphi_1 \bar{\varphi}_1 | \varphi_3 \bar{\varphi}_3 \rangle$ are Coulombic repulsions of a certain electron density distribution with *the same* charge distribution, *therefore*, $\langle \varphi_2 \bar{\varphi}_2 | \varphi_3 \bar{\varphi}_3 \rangle > 0$ and $\langle \varphi_1 \bar{\varphi}_1 | \varphi_3 \bar{\varphi}_3 \rangle > 0$.

Thus, the contribution of the DA structure to the ground-state CI function results mainly from its contribution to the single Slater determinant Ψ_0 [coefficient $C_0(\text{DA})$], but is modified by a small correction $\kappa_1 C_2(\text{DA}) + \kappa_2 C_3(\text{DA})$, where $\kappa < 0$.

What are the values of $C_2(\text{DA})$ and $C_3(\text{DA})$ at the beginning and at the end of the reaction? At the beginning our calculations gave: $C_2^R(\text{DA}) = 0$ and $C_3^R(\text{DA}) = 0$. Note that $C_0^R(\text{DA}) = 1$. Thus the electronic ground-state at the start of the reaction mainly represents the DA structure.

And what about the end of the reaction? We have calculated that $C_2^P(\text{DA}) = \frac{1}{2} > 0$ and $C_3^P(\text{DA}) = \frac{1}{4} > 0$. This means that at the end of the reaction the coefficient corresponding to the DA structure will be *certainly smaller* than $C_0^P(\text{DA}) =$

⁶⁰Because the unperturbed wave function Ψ_0 is an eigenfunction of the $\hat{H}^{(0)}$ Hamiltonian and is orthogonal to any of the expansion functions.

0.25, the value obtained for the single determinant approximation for the ground-state wave function.

Thus, taking the CI expansion into account *makes our conclusion* based on the single Slater determinant even *sharper*.

When the reaction starts, the wave function means the DA structure, while when it ends, this contribution is very strongly reduced.

14.5.5 CONTRIBUTIONS OF THE STRUCTURES AS REACTION PROCEEDS

What therefore represents the ground-state wave function at the end of the reaction? To answer this question let us consider first all possible occupations of the three energy levels (corresponding to n , χ , χ^*) by four electrons. As before we assume for the orbital energy levels: $\varepsilon_\chi < \varepsilon_n < \varepsilon_{\chi^*}$. The number of such singlet-type occupations is equal to six, Table 14.1 and Fig. 14.15.

Now, let us ask what is the contribution of each of these structures⁶¹ in Ψ_0 , Ψ_{2d} and Ψ_{3d} in the three stages of the reaction. This question is especially important for Ψ_0 , because this Slater determinant is dominant for the ground-state wave function. The corresponding contributions in Ψ_{2d} and Ψ_{3d} are less important, because these configurations enter the ground-state CI wave function multiplied by the tiny coefficients κ . We have already calculated these contributions for the DA structure. The contributions of all the structures are given⁶² in Table 14.2.

First, let us focus on which structures contribute to Ψ_0 (because this determines the main contribution to the ground-state wave function) at the three stages of the reaction. As has been determined,

at point R we have only the contribution of the DA structure.

Table 14.1. All possible singlet-type occupations of the orbitals: n , χ and χ^* by four electrons

ground state	DA	$(n)^2(\chi)^2$
singly excited state	D^+A^-	$(n)^1(\chi)^2(\chi^*)^1$
singly excited state	DA^*	$(n)^2(\chi)^1(\chi^*)^1$
doubly excited state	D^+A^{*-}	$(n)^1(\chi)^1(\chi^*)^2$
doubly excited state	$D^{+2}A^{-2}$	$(\chi)^2(\chi^*)^2$
doubly excited state	DA^{**}	$(n)^2(\chi^*)^2$

⁶¹We have already calculated some of these contributions.

⁶²Our calculations gave $C_0^I(\text{DA}) = 0.75$, $C_2^I(\text{DA}) = 0.22$, $C_3^I(\text{DA}) = 0.08$. In Table 14.2 these quantities are equal: 0.729, 0.250, 0.020. The only reason for the discrepancy may be the non-zero overlap integrals, which were neglected in our calculations and were taken into account in those given in Table 14.2.

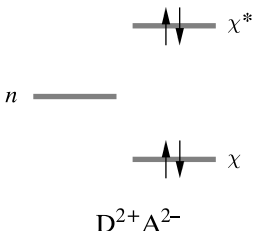
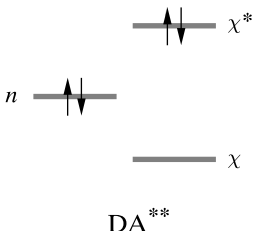
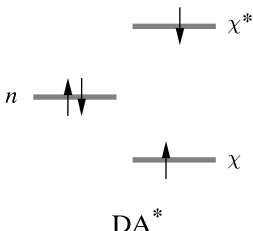
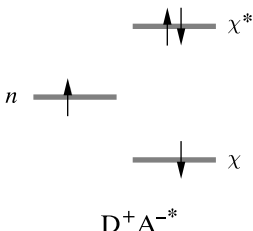
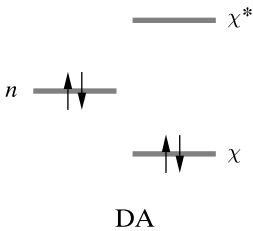
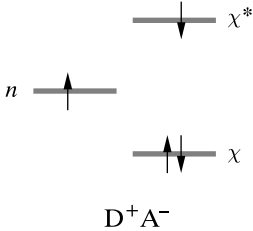
 <p>n</p> <p>χ^*</p> <p>χ</p> <p>$D^{2+}A^{2-}$</p>	 <p>n</p> <p>χ^*</p> <p>χ</p> <p>DA^{**}</p>
 <p>n</p> <p>χ^*</p> <p>χ</p> <p>DA^*</p>	 <p>n</p> <p>χ^*</p> <p>χ</p> <p>D^+A^{-*}</p>
 <p>n</p> <p>χ^*</p> <p>χ</p> <p>DA</p>	 <p>n</p> <p>χ^*</p> <p>χ</p> <p>D^+A^-</p>

Fig. 14.15. The complete set of the six singlet wave functions (“structures”), that arise from occupation of the donor orbital n and of the two acceptor orbitals (χ and χ^*).

However, as we can see (main contributions in bold in Table 14.2),

when the reaction advances along the reaction path to point I, the contribution of DA decreases to 0.729, other structures come into play with the dominant D^+A^- (the coefficient equal to -0.604).

At point P there are three dominant structures: D^+A^- , D^+A^{-*} and $D^{+2}A^{-2}$.

Now we may think of going beyond the single determinant approximation by performing the CI. In the R stage the DA structure dominates as before, but has some small admixtures of DA^{**} (because of Ψ_{3d}) and $D^{+2}A^{-2}$ (because of Ψ_{2d}), while at the product stage the contribution of the DA structure almost vanishes. Instead, some important contributions of the excited states appear, mainly of the

Table 14.2. The contribution of the six donor–acceptor structures in the three Slater determinants Ψ_0 , Ψ_{2d} and Ψ_{3d} built of molecular orbitals at the three reaction stages: reactant (R), intermediate (I) and product (P) [S. Shaik, *J. Am. Chem. Soc.* 103 (1981) 3692. Adapted with permission from the American Chemical Society. Courtesy of the author.]

Structure	MO determinant		R	I	P
DA	Ψ_0	$C_0(\text{DA})$	1	0.729	0.250
	Ψ_{2d}	$C_2(\text{DA})$	0	0.250	0.500
	Ψ_{3d}	$C_3(\text{DA})$	0	0.020	0.250
D^+A^-	Ψ_0	$C_0(\text{D}^+\text{A}^-)$	0	−0.604	−0.500
	Ψ_{2d}	$C_2(\text{D}^+\text{A}^-)$	0	0.500	0.000
	Ψ_{3d}	$C_3(\text{D}^+\text{A}^-)$	0	0.103	0.500
DA^*	Ψ_0	$C_0(\text{DA}^*)$	0	0.177	0.354
	Ψ_{2d}	$C_2(\text{DA}^*)$	0	0.354	−0.707
	Ψ_{3d}	$C_3(\text{DA}^*)$	0	0.177	0.354
D^+A^{-*}	Ψ_0	$C_0(\text{D}^+\text{A}^{-*})$	0	0.103	0.500
	Ψ_{2d}	$C_2(\text{D}^+\text{A}^{-*})$	0	0.500	0.000
	Ψ_{3d}	$C_3(\text{D}^+\text{A}^{-*})$	0	−0.604	−0.500
DA^{**}	Ψ_0	$C_0(\text{DA}^{**})$	0	0.021	0.250
	Ψ_{2d}	$C_2(\text{DA}^{**})$	0	0.250	0.500
	Ψ_{3d}	$C_3(\text{DA}^{**})$	1	0.729	0.250
$\text{D}^{+2}\text{A}^{-2}$	Ψ_0	$C_0(\text{D}^{+2}\text{A}^{-2})$	0	0.250	0.500
	Ψ_{2d}	$C_2(\text{D}^{+2}\text{A}^{-2})$	1	0.500	0.000
	Ψ_{3d}	$C_3(\text{D}^{+2}\text{A}^{-2})$	0	0.250	0.500

D^+A^- , D^+A^{-*} and $\text{D}^{+2}\text{A}^{-2}$ structures, but also other structures of smaller importance.

The value of the qualitative conclusions comes from the fact that they do not depend on the approximation used, e.g., on the atomic basis set, neglecting the overlap integrals, etc.

For example, the contributions of the six structures in Ψ_0 calculated using the Gaussian atomic basis set STO-3G and within the extended Hückel method are given in Table 14.3 (main contributions in bold). Despite the fact that even the geometries used for the R, I, P stages are slightly different, the qualitative results are the same. It is rewarding to learn things that do not depend on detail.

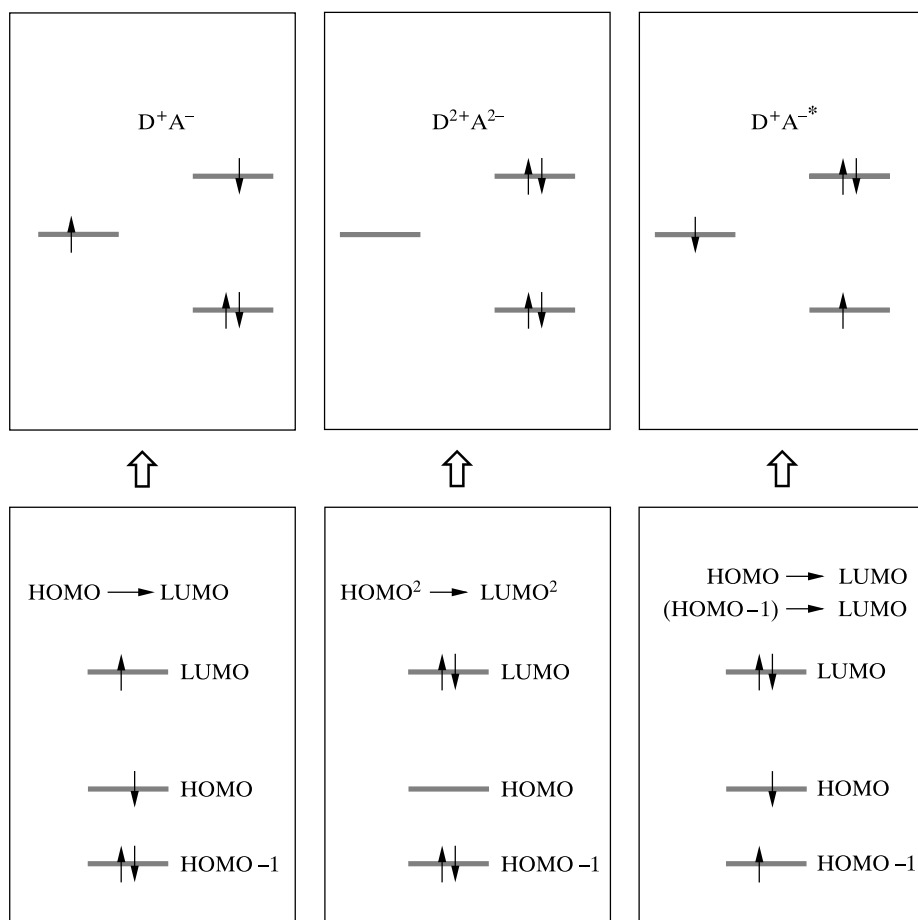
Where do the final structures D^+A^- , D^+A^{-*} and $\text{D}^{+2}\text{A}^{-2}$ come from?

As seen from Table 14.2, the main contributions at the end of the reaction come from the D^+A^- , D^+A^{-*} and $\text{D}^{+2}\text{A}^{-2}$ structures. What do they correspond to *when the reaction starts*? From Table 14.2 it follows that the $\text{D}^{+2}\text{A}^{-2}$ structure simply represents Slater determinant Ψ_{2d} (Fig. 14.16). But where do the D^+A^- and D^+A^{-*} structures come from? There are no such contributions either in Ψ_0 , or in Ψ_{2d} or in Ψ_{3d} . It turns out however that a similar analysis applied to the

Table 14.3. Contributions of the six donor–acceptor structures in the Ψ_0 Slater determinant at three different stages (R, I, P) of the reaction [S. Shaik, *J. Am. Chem. Soc.* 103 (1981) 3692. Adapted with permission from the American Chemical Society. Courtesy of the author.]

Structure	STO-3G			Extended Hückel		
	R	I	P	R	I	P
DA	1.000	0.620	0.122	1.000	0.669	0.130
D^+A^-	0.000	−0.410	−0.304	−0.012	−0.492	−0.316
DA^*	0.000	0.203	0.177	0.000	0.137	0.179
D^+A^{-*}	0.000	0.125	0.300	0.000	0.072	0.298
DA^{**}	0.000	0.117	0.302	0.000	0.176	0.301
$D^{+2}A^{-2}$	0.000	0.035	0.120	0.000	0.014	0.166

Most important acceptor–donor structures at P



These structures correspond to the following MO configurations at R

Fig. 14.16. What final structures are represented at the starting point?

normalized configuration⁶³ $N|\varphi_1\bar{\varphi}_1\varphi_2\bar{\varphi}_3|$ at stage R gives *exclusively* the D^+A^- structure, while applied to the $N|\varphi_1\bar{\varphi}_2\varphi_3\bar{\varphi}_3|$ determinant, it gives *exclusively* the D^+A^{-*} structure (Fig. 14.16). So we have traced them back. The first of these configurations corresponds to a single-electron excitation from HOMO to LUMO – this is, therefore, the lowest excited state of the reactants. Our picture is clarified:

the reaction starts from DA, at the intermediate stage (transition state) we have a large contribution of the first excited state that at the starting point was the D^+A^- structure related to the excitation of an electron from HOMO to LUMO.

The states DA and D^+A^- undergo the “quasi-avoided crossing” in the sense described on p. 262. This means that at a certain geometry, the roles played by HOMO and LUMO interchange, i.e. what was HOMO becomes LUMO and *vice versa*.⁶⁴

Donor and acceptor orbital populations at stages R, I, P

Linear combinations of orbitals n , χ and χ^* construct the molecular orbitals of the system in full analogy with the LCAO expansion of the molecular orbitals. Therefore we may perform a similar population analysis as that described in Appendix S, p. 1015. The analysis will tell us where the four key electrons of the system are (more precisely how many of them occupy n , χ and χ^*), and since the population analysis may be performed at different stages of the reaction, we may obtain information as to what happens to the electrons when the reaction proceeds. The object to analyze is the wave function Ψ . We will report the population analysis results for its dominant component, namely Ψ_0 . The results of the population analysis are reported in Table 14.4. The content of this table confirms our previous conclusions.

Table 14.4. Electronic population of the donor and acceptor orbitals at different reaction stages (R, I, P) [S. Shaik, *J. Am. Chem. Soc.* 103 (1981) 3692. Adapted with permission from the American Chemical Society. Courtesy of the author.]

Orbital	Population		
	R	I	P
n	2.000	1.513	1.000
χ	2.000	1.950	1.520
χ^*	0.000	0.537	1.479

⁶³ N stands for the normalization coefficient.

⁶⁴The two configurations differ by a single spinorbital and the resonance integral $\langle DA|\hat{H}|D^+A^- \rangle$ when reduced using the Slater–Condon rules is dominated by the one-electron integral involving HOMO (or n) and the LUMO (or χ^*). Such an integral is of the order of the overlap integral between these orbitals. The energy gap between the two states is equal to twice the absolute value of the resonance integral (the reason is similar to the bonding-antibonding orbital separation in the hydrogen molecule).

- The starting point (R) has occupation: $(n)^2(\chi)^2$, and that is fine, because we are dealing with the DA structure.
- The intermediate stage represents a mixture of two structures mainly (with almost equal contributions): $(n)^2(\chi)^2$, i.e. DA and $(n)^1(\chi)^2(\chi^*)^1$, i.e. D^+A^- . Therefore we may expect that the population of χ is close to 2, of n is about 1.5, while of χ^* is about 0.5. This is indeed the case.
- The final stage (P) is a mixture of the D^+A^- structure, which corresponds to the occupation $(n)^1(\chi)^2(\chi^*)^1$, of the structure D^+A^{-*} corresponding to $(n)^1(\chi)^1(\chi^*)^2$ and the structure $D^{+2}A^{-2}$ with occupation $(n)^0(\chi)^2(\chi^*)^2$. Equal contributions of these structures should therefore give the occupations of n , χ , χ^* equal to $\frac{2}{3}$, $\frac{5}{3}$ and $\frac{5}{3}$, respectively. The population analysis gives similar numbers, see Table 14.4, last column.

14.5.6 NUCLEOPHILIC ATTACK $H^- + \text{ETHYLENE} \rightarrow \text{ETHYLENE} + H^-$

Maybe the acceptor–donor theory described above pertains only to the $H^- + H-H$ reaction? Fortunately enough, its applicability goes far beyond. Let us consider a nucleophilic attack of the H^- ion on the ethylene molecule (Fig. 14.17), perpendicular to the ethylene plane towards the position of one of the carbon atoms. The arriving ion binds to the carbon atom forming the CH bond, while another proton with two electrons (i.e. H^- ion) leaves the system. Such a reaction looks like it is of academic interest only (except some isotopic molecules are involved, e.g., when one of the protons is replaced by a deuteron), but comprehension comes from the simplest examples possible, when the least number of things change.

The LCAO MO calculations for the ethylene molecule give the following result. The HOMO orbital is of the π bonding character, while the LUMO represents the antibonding π^* orbital (both are linear combinations of mainly carbon $2p_z$ atomic orbitals, z being the axis perpendicular to the ethylene plane). On the energy scale the H^- $1s$ orbital goes between the π and π^* energies, similarly as happened with the χ and χ^* orbitals in the $H^- + H-H$ reaction. The virtual orbitals (let us call them $2\chi^*$, $3\chi^*$, $4\chi^*$) are far away up in the energy scale, while the occupied σ -type orbitals are far down in the energy scale. Thus, the H^- $n = 1s$ orbital energy is close to that of χ and χ^* , while other orbitals are well separated from them.

This energy level scheme allows for many possible excitations, far more numerous than considered before. *Despite this*, because of the effective mixing of only those donor and acceptor orbitals that are of comparable energies, *the key partners are, as before, n , χ and χ^** . The role of the other orbitals is only marginal: their admixtures will only slightly deform the shape of the main actors of the drama n , χ and χ^* known as the *frontier orbitals*. The coefficients at various acceptor–donor structures in the expansion of Ψ_0 are shown in Table 14.5. The calculations were performed using the extended Hückel method⁶⁵ at three stages of the reaction (R, in which the H^- ion is at a distance of 3 Å from the attacked carbon atom; I, with a

frontier orbitals

⁶⁵Introduced to chemistry by Roald Hoffmann. He often says that he cultivates chemistry with an old, primitive tool, which because of this ensures access to the wealth of the complete Mendeleev periodic table.

Fig. 14.17. Nucleophilic substitution of ethylene by H^- . The figure aims to demonstrate that, despite considering a more complex system than the $\text{H}^- + \text{H}_2 \rightarrow \text{H}_2 + \text{H}^-$ reaction discussed so far, the machinery behind the scene works in the same way. The attack of H^- goes perpendicularly to the ethylene plane, onto one of the carbon atoms. The figure shows the (orbital) energy levels of the donor (H^- , left hand side) and of the acceptor (ethylene, right hand side). Similarly as for $\text{H}^- + \text{H}_2$ the orbital energy of the donor orbital n is between the acceptor orbital energies χ and χ^* corresponding to the bonding π and antibonding π^* orbitals. Other molecular orbitals of the ethylene (occupied and virtual: $2\chi^*$, $3\chi^*$, ...) play a marginal role, due to high energetic separation from the energy level of n .

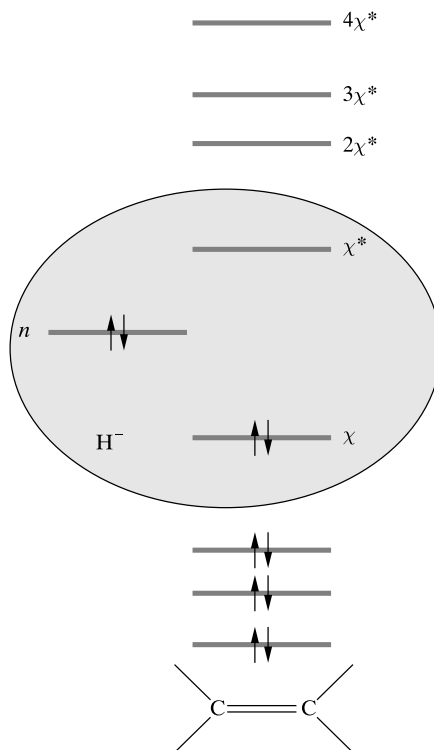


Table 14.5. Expansion coefficients at the acceptor–donor structures in the ground-state wave function at various stages of the reaction: reactant (R), intermediate (I) and product (P) [S. Shaik, *J. Am. Chem. Soc.* 103 (1981) 3692. Adapted with permission from the American Chemical Society. Courtesy of the author.]

Structure	Coefficients		
	R	I	P
DA	1.000	0.432	0.140
$\text{D}^+\text{A}^-(n \rightarrow \pi^*)$	0.080	0.454	0.380
$\text{DA}^*(\pi \rightarrow \pi^*)$	-0.110	-0.272	-0.191
$\text{D}^+\text{A}^-(n \rightarrow \pi^*, \pi \rightarrow \pi^*)$	-0.006	-0.126	-0.278
$\text{D}^+\text{A}^-(n \rightarrow 2\sigma^*)$	$<10^{-4}$	0.006	0.004
$\text{D}^+\text{A}^-(n \rightarrow 3\sigma^*)$	$<10^{-4}$	-0.070	-0.040

distance 1.5 Å and P, with a distance equal to 1.08 Å; in all cases the planar geometry of the ethylene was preserved). It is seen that, despite the fact that a more complex method was used, the emerging picture is quite similar: at the beginning the DA structure prevails, at the intermediate stage we have a “hybrid” of the DA and D^+A^- structures, while at the end we have a major role for the D^+A^- and D^+A^{*-} structures. We can see also that even if some higher excitations were taken into account (to the orbitals $2\sigma^*$, $3\sigma^*$) they play only a marginal role. The cor-

responding population analysis (not reported here) indicates a basically identical mechanism. This resemblance extends also to the S_N2 nucleophilic substitutions in aromatic compounds.

14.5.7 ELECTROPHILIC ATTACK $H^+ + H_2 \rightarrow H_2 + H^+$

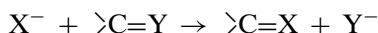
Let us see whether this mechanism is even more general and consider the *electrophilic* substitution in the model reaction $H^+ + H-H \rightarrow H-H + H^+$. This time the role of the donor is played by the hydrogen molecule, while that of the acceptor is taken over by the proton. The total number of electrons is only two. The DA structure corresponds to $(\chi)^2(n)^0(\chi^*)^0$. Other structures are defined in an analogous way to the previous case of the H_3 system: structure D^+A^- means $(\chi)^1(n)^1(\chi^*)^0$, structure $D^{+*}A^-$ obviously corresponds to $(\chi)^0(n)^1(\chi^*)^1$, structure D^*A to $(\chi)^1(n)^0(\chi^*)^1$, $D^{**}A$ to $(\chi)^0(n)^0(\chi^*)^2$ and $D^{+2}A^{-2}$ to $(\chi)^0(n)^2(\chi^*)^0$. As before, the ground-state Slater determinant may be expanded into the contributions of these structures. The results (the overlap neglected) are collected in Table 14.6.

Table 14.6. Expansion coefficients at the acceptor–donor structures for the reaction of proton with the hydrogen molecule at three different stages of the reaction: reactant (R), intermediate (I) and product (P) [S. Shaik, *J. Am. Chem. Soc.* 103 (1981) 3692. Adapted with permission from the American Chemical Society. Courtesy of the author.]

Structure	Coefficients		
	R	I	P
DA	1.000	0.729	0.250
D^+A^-	0	0.604	0.500
$D^{+*}A^-$	0	−0.104	−0.500
D^*A	0	−0.177	−0.354
$D^{**}A$	0	0.021	0.250
$D^{+2}A^{-2}$	0	0.250	0.500

It is worth stressing that we obtain the same reaction machinery as before. First, at stage R the DA structure prevails, next at intermediate stage I we have a mixture of the DA and D^+A^- structures, and we end up (stage P) with D^+A^- and $D^{+*}A^-$ (the energy levels for the donor are the same as the energy levels were previously for the acceptor, hence we have $D^{+*}A^-$, and not D^+A^{-*} as before). This picture would not change qualitatively if we considered electrophilic substitution of the ethylene or benzene.

14.5.8 NUCLEOPHILIC ATTACK ON THE POLARIZED CHEMICAL BOND IN THE VB PICTURE



What does the quasi-avoided crossing described above really mean? At the beginning we have the DA structure almost exclusively. The DA structure obviously

corresponds to a chemical bond in the acceptor and the lack of any bond between the donor and acceptor. In the D^+A^- structure which comes into play at the intermediate stage, we have two paired electrons: one on D^+ occupying orbital n , and the second on A^- occupying χ^* . *These electrons represent the pair that will be responsible for formation of the new bond, the D–A bond.* At the same time, the old bond in A is positively weakened, because one of the electrons in A occupies the antibonding χ^* orbital. Therefore, the quasi-avoided crossing between the diabatic hypersurfaces DA and D^+A^- represents the key region, in which breaking of the old bond in A and formation of new bond D–A are taking place.

The above theory is based on the acceptor/donor expansion functions (AD formalism). As has already been mentioned (p. 803), the third possibility (apart from AD and MO) is VB, in which the Slater determinants (playing the role of the expansion functions for Ψ_0) are built of the *atomic orbitals* of the interacting species (Chapter 10, p. 520). How does such a VB picture look? Let us consider a nucleophilic attack of the species X on the polarized double bond $\text{>C}=\text{Y}$, where Y represents an atom more electronegative than carbon (say, oxygen). Our goal is to expand the AD structures into the VB. The arguments of the kind already used for ethylene make it possible to limit ourselves exclusively to the frontier orbitals n , π and π^* (Fig. 14.18).

The bonding π orbital may be approximated as a linear combination of the $2p_z$ atomic orbitals of Y and C⁶⁶

$$\pi = a \cdot (2p_z)_C + b \cdot (2p_z)_Y, \quad (14.68)$$

where we assume (by convention) that the coefficients satisfy: $a, b > 0$. Note that the orbital π is *polarized* this time, and due to a higher electronegativity of Y we

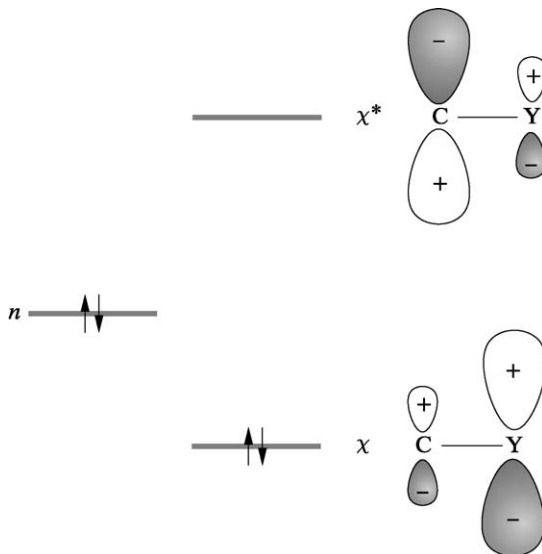


Fig. 14.18. Nucleophilic attack $X^- + \text{>C}=\text{Y} \rightarrow \text{>C}=\text{X} + \text{Y}^-$. The orbitals π and π^* are polarized (their polarizations are *opposite*). [S. Shaik, *J. Am. Chem. Soc.* 103 (1981) 3692. Adapted with permission from the American Chemical Society. Courtesy of the author.]

⁶⁶The z axis is perpendicular to the $\text{>C}=\text{Y}$ plane.

have $b > a$ with the normalization condition $a^2 + b^2 = 1$ (we neglect the overlap integrals between the atomic orbitals). In this situation the antibonding orbital π^* may be obtained from the orthogonality condition of the orbital π as:⁶⁷

$$\pi^* = b \cdot (2p_z)_C - a \cdot (2p_z)_Y. \quad (14.69)$$

The role of the donor orbital n will be played by $(2p_z)_X$. Note that π^* has the opposite polarization to that of π , i.e. the electron described by π^* prefers to be close to the less electronegative carbon atom, Fig. 14.18.

At the starting point the DA structure which corresponds to the double occupation of n and χ turned out to be the most important. In Chapter 8 on p. 371, a Slater determinant was analyzed that corresponded to double occupation of bonding orbital $\sigma 1s$ of the hydrogen molecule. In the present situation this corresponds to a double occupation of the π orbital of the acceptor. The Slater determinant was then expanded onto the VB structures (eq. (10.18), p. 521), and as it turns out, there are three of them. The first was the Heitler–London structure, which described a covalent bond: if one electron is close to the first nucleus then the other (with opposite spin) will be close to the second nucleus. Both electrons played exactly the same role with respect to the two nuclei. The second and third structures were of the ionic character, because both electrons were at the same nucleus (one or the other). The two ionic structures had equal coefficients and together with the Heitler–London structure, this led to treating both nuclei on an equal footing. If one of the nuclei were a bit different to the other (e.g., by increasing its charge, which would simulate its higher electronegativity), as is the case in a polarized bond ($a \neq b$), then the *Heitler–London function would continue to treat the nuclei in the same way*, but the polarity would be correctly restored by making the coefficients of the ionic structures different. The reason for this asymmetry is setting $b > a$.

This is why the chemical bond pattern corresponding to the VB picture may be expressed by the pictorial description shown in Fig. 14.19.a.

What happens at the intermediate stage, when the D^+A^- structure enters into play? In this structure one electron occupying n goes to χ^* . The Slater determinant

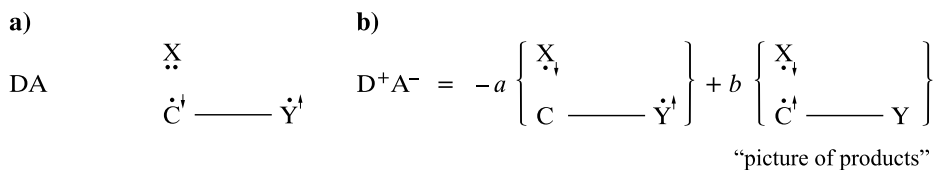


Fig. 14.19. Pictorial description of the DA and D^+A^- structures. For a large donor–acceptor distance the electronic ground state is described by the DA structure (a). Structure D^+A^- already becomes very important for the intermediate stage (I). This structure, belonging to the acceptor–donor picture, is shown (b) in the VB representation, where the opposite spins of the electrons remind us that we have the corresponding covalent structure.

⁶⁷Let us check:

$$\langle \pi | \pi^* \rangle = \langle a \cdot (2p_z)_C + b \cdot (2p_z)_Y | b \cdot (2p_z)_C - a \cdot (2p_z)_Y \rangle = ab + 0 + 0 - ba = 0.$$

that corresponds to this structure [one of its rows contains a spinorbital corresponding to orbital $\pi^* = b(2p_z)_C - a(2p_z)_Y$] may be expanded as a linear combination of the two Slater determinants, which instead of the spinorbital mentioned above have the corresponding atomic spinorbital $[(2p_z)_C \text{ or } (2p_z)_Y]$. The corresponding pictorial notation is shown in Fig. 14.19.b. Note that the weight of the second structure is higher. Therefore, we see what is going on in the VB picture. The DA structure corresponds to the “old” CY bond, while the D^+A^- structure becomes more and more important (when the reaction proceeds) and mainly represents the Heitler–London structure for the new CX covalent bond.

The avoided crossing is needed to cause such a change of the electronic structure as to break the old bond and form the new one. Taking the leading VB structures only, we may say that

the avoided crossing appears between two hypersurfaces, from which one corresponds to the old bond pattern (the first diabatic hypersurface) and the other to the new bond pattern (the second diabatic hypersurface).

We see from the VB results, why the variational method has chosen the D^+A^- structure among the six possible ones.

This configuration was chosen, because it corresponds exactly to the formation of the new bond: the two unpaired electrons with opposite spins localized on those atoms that are going to bind.

The mechanism given is general and applies wherever at least one of the reactants has a closed shell. When both the reacting molecules are of the open-shell type, there will be no avoided crossing and no reaction barrier: the reactants are already prepared for the reaction.

When we have a closed-shell system among the reactants, for the reaction to happen we have to reorganize the electronic structure. The reorganization may happen only *via* an avoided crossing and that means the appearance of a reaction barrier.

14.5.9 WHAT IS GOING ON IN THE CHEMIST'S FLASK?

Let us imagine the molecular dynamics on energy hypersurface calculated using a quantum-mechanical method (classical force fields are not appropriate since they offer non-breakable chemical bonds). The system is represented by a point that slides downhill (with an increasing velocity) and climbs uphill (with decreasing velocity). The system has a certain kinetic energy, because chemists often heat their flasks.

Let us assume that, first the system wanders through those regions of the hypersurface which are far from other electronic states in the energy scale. In such a situation, the adiabatic approximation (Chapter 6) is justified and the electronic

energy (corresponding to the hypersurface) represents potential energy for the motion of the nuclei. The system corresponds to a given chemical bond pattern (we may work out a structural formula). Bond lengths vibrate as do bond angles, torsional angles also change, even leading to new isomers (conformers), but a single bond remains single, double remains double, etc.

After a while the system climbs to a region of the configurational space in which another diabatic hypersurface (corresponding to another electronic state) lowers its energy to such an extent that the two hypersurfaces tend to intersect. In this region the adiabatic approximation fails, since we have *two* electronic states of comparable energies (both have to be taken into account), and the wave function cannot be taken as the product of an electronic function and a function describing the nuclear motion (as is required by the adiabatic approximation). As a result of mixing, electronic states crossing is avoided, and two *adiabatic* hypersurfaces (upper and lower) appear. Each is composed of two parts. One part corresponds to a molecule looking as if it had one bond pattern, while the other part pertains to a different bond pattern. The bond pattern on each of the adiabatic hypersurfaces changes and the Rubicon for this change is represented by the boundary, i.e. the region of the quasi-avoided crossing that separates the two diabatic parts of the adiabatic hypersurface. Therefore, when the system in its dynamics goes uphill and enters the boundary region, the corresponding bond pattern becomes fuzzy, and changes to another pattern after crossing the boundary. The reaction is completed.

What will happen next? The point representing the system in the configurational space continues to move and it may happen to arrive at another avoided-crossing region⁶⁸ and its energy is sufficient to overcome the corresponding barrier. This is the way multistep chemical reactions happen. It is important to realize that, in experiments, we have to do with an ensemble of such points rather than one. The points differ by their positions (configurations of the nuclei) and momenta. Only a fraction of them has sufficiently high kinetic energy to cross the reaction barrier. The rest wander through a superbasin (composed of numerous basins) of the initial region thus undergoing vibrations, rotations including internal rotations, etc. Of those which cross a barrier, only a fraction crosses the same barrier again (i.e. the barrier of the same reaction). Others, depending on the initial conditions (nuclear positions and momenta) may cross other barriers. The art of chemistry means that in such a complicated situation it is still possible to perform reactions with nearly 100% yield and obtain a pure chemical compound – the chemist's target.

14.5.10 ROLE OF SYMMETRY

A VB point of view is simple and beautiful, but sometimes the machinery gets stuck. For example, this may happen when the described mechanism has to be rejected, because it does not meet some symmetry requirements. Imagine that instead of a linear approach of H^- to H_2 , we consider a T-shape configuration. In

⁶⁸This new avoided crossing may turn out to be the old one. In such a case the system will cross the barrier in the opposite direction. Any chemical reaction is reversible (to different extents).

such a case the all-important D^+A^- structure becomes *useless* for us, because the resonance integral which is proportional to the overlap integral between the $1s$ orbital of H^- (HOMO of the donor) and χ^* (LUMO of the acceptor) is equal to zero for symmetry reasons. If the reaction were to proceed, we would have had to form molecular orbitals from the above orbitals and this is impossible.

Yet there is an emergency exit from this situation. Let us turn our attention to the D^+A^{-*} structure, which corresponds to a doubly occupied χ^* , but a singly occupied χ . This structure would lead to the avoided crossing, because the overlap integral of $1s H^-$ and χ H–H has a non-zero value. In this way,

a forbidden symmetry will simply cause the system to choose as the lead, another structure, such that it allows the formation of new bonds in *this situation*.

The above example shows that symmetry can play an important role in chemical reactions. The role of symmetry will be highlighted in what follows.

The cycloaddition reaction

Let us take the example of the cycloaddition of two ethylene molecules when they bind together forming the cyclobutane. The frontier orbitals of the ground-state ethylene molecule are: the doubly occupied π (HOMO) and the empty π^* (LUMO) molecular orbitals.

The right-hand side of Fig. 14.20.a shows that the reaction would go towards the products, if we prepared the reacting ethylene molecules in their triplet states. Such a triplet state has to be stabilized during the reaction, while the state corresponding to the old bond pattern should lose its importance. Is it reasonable to expect the triplet state to be of low energy in order to have the chance to be pulled sufficiently down the energy scale? Yes, it is, because the triplet state arises by exciting an electron from the HOMO (i.e. π) to the LUMO (i.e. π^*), and this energy cost is the lowest possible (in the orbital picture). Within the π -electron approximation the Slater determinant corresponding to the triplet state (and representing the corresponding molecular orbitals as linear combination of the carbon $2p_z$ atomic orbitals denoted simply as a and b) has the form

$$N \det (\pi(1)\alpha(1)\pi^*(2)\alpha(2)) \quad (14.70)$$

$$= N [\pi(1)\alpha(1)\pi^*(2)\alpha(2) - \pi(2)\alpha(2)\pi^*(1)\alpha(1)] \quad (14.71)$$

$$= N\alpha(1)\alpha(2) [(a(1) + b(1))(a(2) - b(2)) - (a(2) + b(2))(a(1) - b(1))] \quad (14.72)$$

$$= -2N\alpha(1)\alpha(2) [a(1)b(2) - a(2)b(1)]. \quad (14.73)$$

This means that when one electron is on the first carbon atom, the other is on the second carbon atom (no ionic structures!). The “parallel” electron spins of

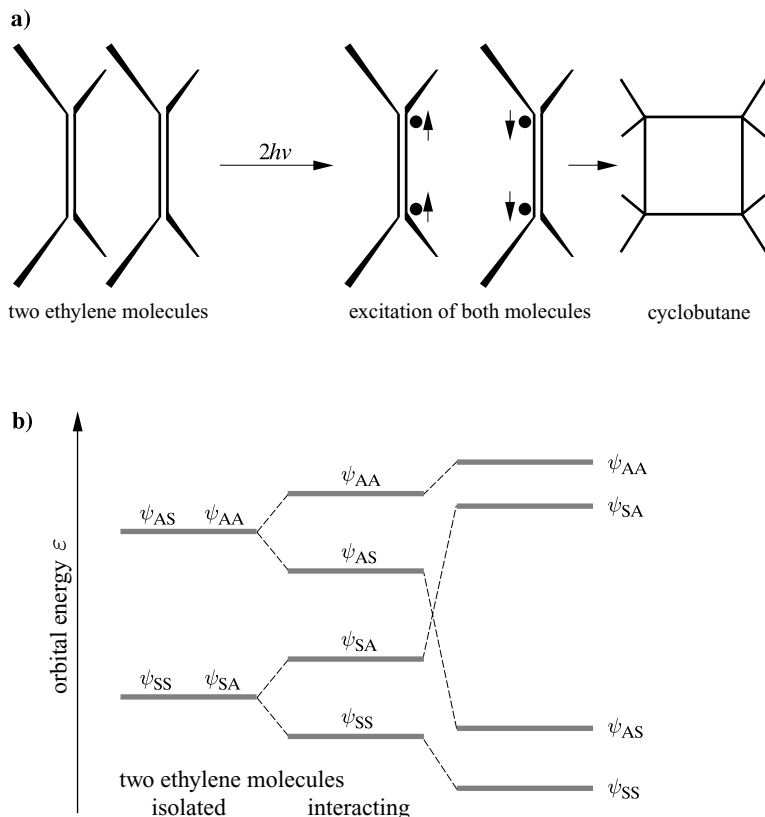
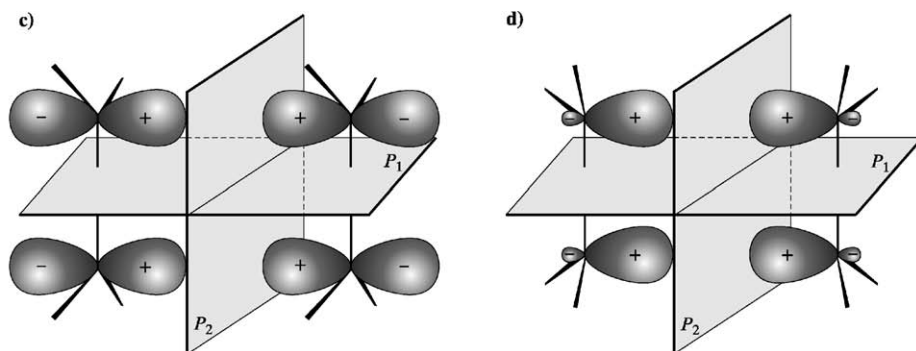


Fig. 14.20. Two equivalent schemes for the cycloaddition reaction of ethylene. Two ethylene molecules, after excitation to the triplet state, dimerize forming cyclobutane (a), because everything is prepared for electron pairing and formation of the new bonds (see text). We obtain the same from the Woodward–Hoffmann rules (Fig. (b), (c), (d)). According to these rules we assume that the ethylene molecules preserve two planes of symmetry: P_1 and P_2 during all stages of the reaction. We concentrate on four π electrons – the main actors in the drama. At the beginning the lowest-energy molecular orbital of the total system (b,c) is of the SS type (i.e. symmetric with respect to P_1 and P_2). The other three orbitals (not shown in Fig. (c)) are of higher energies that increases in the following order: SA, AS, AA. Hence, the four electrons occupy SS and SA, (b). Fig. (d) shows the situation after the reaction. The four electrons are no longer of the π type, we now call them the σ type, and they occupy the hybrid orbitals shown in the figure. Once more, the lowest energy (b) corresponds to the SS symmetry orbital (d). The three others (not shown in Fig. (d)) have higher energy, but their order is *different than before* (b): AS, SA, AA. The four electrons should occupy, therefore, the SS and AS type orbitals, whereas (according to the Woodward–Hoffmann rule) they still occupy SS and SA. This is energetically unfavourable and such a thermic reaction does not proceed. Yet, if before the reaction the ethylene molecules were excited to the triplet state $(\pi)^1(\pi^*)^1$, then at the end of the reaction they would correspond to the configuration: $(SS)^2(AS)^2$, of very low energy, and the photochemical reaction proceeds.

one molecule may be in the opposite direction to the similar electron spins of the second molecule. Everything is prepared for the cycloaddition, i.e. formation of the new chemical bonds.

Fig. 14.20. *Continued.*

Similar conclusions can be drawn from the Woodward–Hoffmann symmetry rules.

Woodward–Hoffmann symmetry rules

The rules pertain to such an approach of two molecules that all the time some symmetry elements of the nuclear framework are preserved (there is a symmetry group associated with the reaction, see Appendix C). Then,

- the molecular orbitals belong to the irreducible representations of the group,
- we assume that during the approach the orbital energies change, *but their electron occupancies do not*,
- the reaction is allowed when the sum of the (occupied) orbital energies lowers, otherwise it is forbidden.

Example 3. Two ethylene molecules – Diels–Alder reaction

The two ethylene molecules are oriented as shown in Fig. 14.20.c. Let us focus on the frontier (HOMO and LUMO) orbitals at long intermolecular distances. All are built of symmetry orbitals composed of four 2p carbon atomic orbitals (perpendicular to the planes corresponding to the individual molecules) and can be classified as symmetric (S) or antisymmetric (A) with respect to the symmetry planes P_1 and P_2 . Moreover, by recognizing the bonding or antibonding interactions, without performing any calculations, we can tell that the SS-symmetry orbital is of the lowest energy (because of the bonding character of the intra- as well as intermolecular interactions), then the SA-symmetry (the bonding intramolecular – the π orbitals and the antibonding intermolecular), next the AS-symmetry (the antibonding intramolecular and bonding intermolecular orbitals π^*), and the highest-energy orbital AA (the antibonding intra- and intermolecular). Since the number of electrons involved is four, they occupy the SS and SA orbitals.⁶⁹ This is what we have at the beginning of the reaction.

What do we have at the end of the reaction? At the end there are no π -electrons whatsoever, instead we have two new σ chemical bonds, each built from the two

⁶⁹What a nasty historical association.

sp^3 hybrids (Fig. 14.20.d) oriented towards the other ethylene molecule.⁷⁰ Therefore, we may form the symmetry orbitals once again, recognize their bonding and antibonding character and hence the order of their orbital energies without any calculations, just by inspection (Fig. 14.20.b). The lowest energy corresponds, of course, to SS (because the newly formed σ chemical bonds correspond to the bonding combination and the lateral overlap of the hybrids is also of the bonding character), *the next in energy however is the AS* (because of the bonding interactions in the newly formed σ bonds, while the lateral interaction is weakly antibonding), then follows the SA-symmetry orbital (antibonding interaction along the bonds that is only slightly compensated by the lateral bonding overlap of the hybrids), and finally, the highest-energy corresponds to the totally antibonding orbital of the AA-symmetry.

According to the Woodward–Hoffmann rules, the four π electrons, on which we focus, occupy the SS and SA orbitals from the beginning to the end of the reaction. This corresponds to low energy at the beginning of the reaction (R), but is very unfavourable at its end (P), because the unoccupied AS orbital is lower in the energy scale. And what if we were smart and excited the reactants by laser? This would allow double occupation of the AS orbital right at the beginning of the reaction and end up with a low energy configuration. To excite an electron per molecule, means to put one on orbital π^* , while the second electron stays on orbital π . Of two possible spin states (singlet and triplet) the triplet state is lower in energy (see Chapter 8, p. 391). This situation was described by eq. (14.73) and the result is that *when one electron sits on nucleus a, the other sits on b. These electrons have parallel spins – everything is prepared for the reaction.*

Therefore, the two ethylene molecules, when excited to the triplet state, open their closed-shells in such a way that favours cycloaddition.

14.5.11 BARRIER MEANS A COST OF OPENING THE CLOSED-SHELLS

Now we can answer more precisely the question of what happens when two molecules react. When the molecules are of the closed-shell character, first a change of their electronic structure has to take place. For that to happen, the kinetic energy of molecular collisions (the temperature plays important role) has to be sufficiently high in order to push and distort⁷¹ the nuclear framework, together with the electron cloud of each of the partners (kinetic energy contra valence repulsion described in Chapter 13), to such an extent that the new configuration already corresponds to that behind the reaction barrier. For example, in the case of an electrophilic or nucleophilic attack, these changes correspond to the transformation $D \rightarrow D^+$ and $A \rightarrow A^-$, while in the case of the cycloaddition to the excitation of the reacting molecules, to their triplet states. *These changes make the unpaired*

⁷⁰We have to do with a four-membered ring, therefore the sp^3 hybrids match the bond directions only roughly.

⁷¹Two molecules cannot occupy the same volume due to the Pauli exclusion principle, cf. p. 744.

electrons move to the proper reaction centres. As long as this state is not achieved, the changes within the molecules are small and, at most, a molecular complex forms, in which the partners preserve their integrity and their main properties. The profound changes follow from a quasi-avoided crossing of the DA diabatic hypersurface with an excited-state diabatic hypersurface, the excited state being to a large extent a “*picture of the product*”. Even the noble gases open their electronic shells when subject to extreme conditions. For example, xenon atoms under pressure of about 150 GPa⁷² change their electronic structure so much,⁷³ that their famous closed-shell electronic structure ceases to be the ground-state. The energy of some excited states lowers so much that the xenon atoms begin to exist in the *metallic state*.

Reaction barriers appear because the reactants have to open their valence shells and prepare themselves to form new bonds. This means their energy goes up until the “right” excited structure (i.e. the one which resembles the products) lowers its energy so much that the system slides down the new diabatic hypersurface to the product configuration.

The right structure means the electronic distribution in which, for each to-be-formed chemical bond, there is a set of two properly localized unpaired electrons. *The barrier height depends on the energetic gap between the starting structure and the excited state which is the “picture” of the products.* By proper distortion of the geometry (due to the valence repulsion with neighbours) we achieve a “pulling down” of the excited state mentioned, but the same distortion causes the ground state to go up. The larger the initial energy gap, the harder to make the two states interchange their order. The reasoning is supported by the observation that the barrier height for electrophilic or nucleophilic attacks is roughly proportional to the *difference between the donor ionization energy and the acceptor electronic affinity, while the barrier for cycloaddition increases with the excitation energies of the donor and acceptor to their lowest triplet states.* Such relations show the great interpretative power of the acceptor–donor formalism. We would not see this in the VB picture, because it would be difficult to correlate the VB structures based on the atomic orbitals with the ionization potentials or the electron affinities of the molecules involved. The best choice is to look at all three pictures (MO, AD and VB) simultaneously. This is what we have done.

⁷²M.I. Eremetz, E.A. Gregoryantz, V.V. Struzhkin, H. Mao, R.J. Hemley, N. Mulders, N.M. Zimmerman, *Phys. Rev. Letters* 85 (2000) 2797. The xenon was metallic in the temperature range 300 K–25 mK. The pioneers of these investigations were R. Reichlin, K.E. Brister, A.K. McMahan, M. Ross, S. Martin, Y.K. Vohra, A.L. Ruoff, *Phys. Rev. Letters* 62 (1989) 669.

⁷³Please recall the Pauli Blockade, p. 722. Space restrictions for an atom or molecule by the excluded volume of other atoms, i.e. mechanical pushing leads to changes in its electronic structure. These changes may be very large under high pressure.

14.6 BARRIER FOR THE ELECTRON-TRANSFER REACTION

In the AD theory, a chemical reaction of two closed-shell entities means opening their electronic shells (accompanied by an energy cost), and then forming the new bonds (accompanied by an energy gain). The electronic shell opening might have been achieved in two ways: either an electron transfer from the donor to the acceptor, or an excitation of each molecule to the triplet state and subsequent electron pairing between the molecules.

Now we will be interested in the barrier *height* when the first of these possibilities occurs.

14.6.1 DIABATIC AND ADIABATIC POTENTIAL

Example 4. *Electron transfer in $\text{H}_2^+ + \text{H}_2$*

Let us imagine two molecules, H_2^+ and H_2 , in a parallel configuration⁷⁴ at distance R from one another and having identical length 1.75 a.u. (Fig. 14.21.a). The value chosen is the arithmetic mean of the two equilibrium separations (2.1 a.u. for H_2^+ , 1.4 a.u. for H_2).

There are two geometry parameters to change (Fig. 14.21): the length q_1 of the left (or “first”) molecule and the length q_2 of the right (or “second”) molecule. Instead of these two variables we may consider the other two: their sum and their difference. Since our goal is to be as simple as possible, we will assume,⁷⁵ that $q_1 + q_2 = \text{const}$, and therefore the geometry of the total nuclear framework may be described by a single variable: $q = q_1 - q_2$, with $q \in (-\infty, \infty)$.

It is quite easy to imagine, what happens when q changes from 0 (i.e. from both bonds of equal length) to a somewhat larger value. Variable $q = q_1 - q_2 > 0$ means that $q_1 > q_2$, therefore when q increases, the energy of the system will decrease, because the H_2^+ molecule elongates, while the H_2 shortens, i.e. both approach their equilibrium geometries. If q increases further, it will soon reach the value $q = q_0 = 2.1 - 1.4 = 0.7$ a.u., the optimum value for both molecules. A further increase of q will mean, however, a kind of discomfort for each of the molecules and the energy will go up, for large q – very much up. This means that the potential energy $E(q)$ has a parabola-like shape.

And what will happen for $q < 0$? *It depends on where the extra electron resides.* If it is still on the second molecule (which means it is H_2), then $q < 0$ means an elongation of an already-too-long H_2 and a shortening of an already-too-short H_2^+ . The potential energy goes up and the total plot is similar to a parabola with the minimum at $q = q_0 > 0$. If, however, we assume that the extra electron resides all the time on the first of the molecules, then we will obtain the identical parabola-like curve as before, but with the minimum position at $q = -q_0 < 0$.

⁷⁴We freeze all the translations and rotations.

⁷⁵The assumption stands to reason, because a shortening of one molecule will be accompanied by an almost identical lengthening of the other, when they exchange an electron.

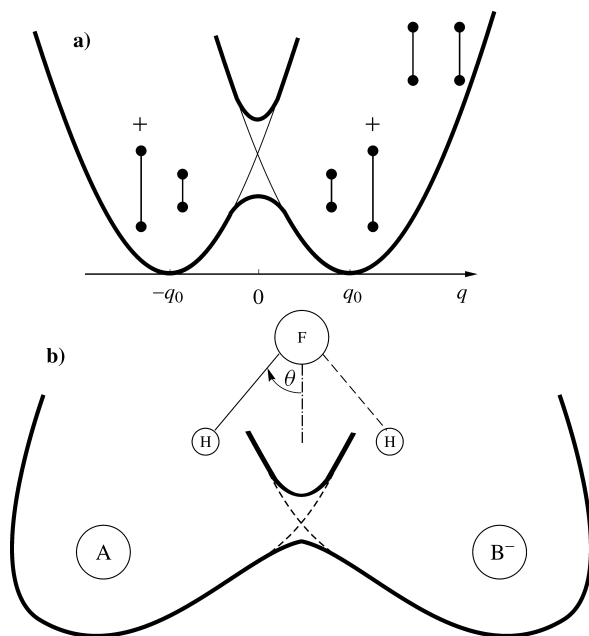


Fig. 14.21. An electron transfer is accompanied by a geometry change. (a) When H_2 molecule gives an electron to H_2^+ , both undergo some geometry changes. Variable q equals the difference of the bond lengths of both molecules. At $q = \pm q_0$ both molecules have their optimum bond lengths. (b) The HF pendulum oscillates between two sites, A and B, which accommodate an extra electron becoming either A^-B or AB^- . The curves similar to parabolas denote the energies of the diabatic states as functions of the pendulum angle θ . The thick solid line indicates the adiabatic curves.

DIABATIC AND ADIABATIC POTENTIALS:

Each of these curves with a single minimum represents the *diabatic* potential energy curve for the motion of the nuclei. If, when the donor-acceptor distance changes, the electron *keeps pace* with it and jumps on the acceptor, then increasing or decreasing q from 0 gives a similar result: we obtain a single electronic ground-state potential energy curve with *two* minima in positions $\pm q_0$. This is the *adiabatic* curve.

Whether the adiabatic or diabatic potential has to be applied is equivalent to asking *whether the electron will keep pace (adiabatic) or not (diabatic) with the motion of the nuclei*.⁷⁶ This is within the spirit of the adiabatic approximation, cf. Chapter 6, p. 253. Also, a diabatic curve corresponding to the same electronic

⁷⁶In the reaction $\text{H}_2^+ + \text{H}_2 \rightarrow \text{H}_2 + \text{H}_2^+$ the energy of the reactants is equal to the energy of the products, because the reactants and the products represent the same system. Is it therefore a kind of fiction? Is there any reaction at all taking place? From the point of view of a bookkeeper (thermodynamics) no reaction took place, but from the point of view of a molecular observer (kinetics) – such a reaction may take place. It is especially visible, when instead of one of the hydrogen atoms we use deuterium, then the reaction $\text{HD}^+ + \text{H}_2 \rightarrow \text{HD} + \text{H}_2^+$ becomes real even for the bookkeeper (mainly because of the difference in the zero-vibration energies of the reactants and products).

structure (the extra electron sitting on one of the molecules all the time) is an analogue of the diabatic hypersurface that preserved the same chemical bond pattern encountered before.

Example 5. The “HF pendulum”

Similar conclusions come from another ideal system, namely the hydrogen fluoride molecule treated as the pendulum of a grandfather clock (the hydrogen atom down, the clock axis going through the fluorine atom) moving over two molecules: A and B, one of them accommodates an extra electron (Fig. 14.21.b).

The electron is negatively charged, the hydrogen atom in the HF molecule carries a partial positive charge, and both objects attract each other. If the electron sits on the left-hand molecule and during the pendulum motion does not keep pace,⁷⁷ the potential energy has a single minimum for the angle $-\theta_0$ (the diabatic potential might be approximated by a parabola-like curve with the minimum at $-\theta_0$). An analogous curve with the minimum at θ_0 arises, when the electron resides on B all the time. When the electron keeps pace with any position of the pendulum, we have a single adiabatic potential energy curve with two minima: at $-\theta_0$ and θ_0 .

14.6.2 MARCUS THEORY

Rudolph Arthur Marcus (b. 1923), American chemist, professor at the University of Illinois in Urbana and at California Institute of Technology in Pasadena. In 1992 Marcus received the Nobel Prize “for his contribution to the theory of electron transfer reactions in chemical systems”.



The contemporary theory of the electron transfer reaction was proposed by Rudolph Marcus.⁷⁸ The theory is based to a large extent on the harmonic approximation for the diabatic potentials involved, i.e. the diabatic curves represent parabolas. One of the parabolas corresponds to the reactants $V_R(q)$, the other to the products $V_P(q)$ of the electron transfer reaction (Fig. 14.22).⁷⁹

Now, let us assume that both parabolas have the same curvature (force constant f).⁸⁰ The reactants correspond to the parabola with the minimum at q_R (without losing generality we adopt a convention that at $q_R = 0$ the energy is equal zero)

$$V_R(q) = \frac{1}{2}f(q - q_R)^2,$$

while the parabola with the minimum at q_P is shifted in the energy scale by ΔG^0

⁷⁷That is, does not jump over to the right-hand side molecule.

⁷⁸The reader may find a good description of the theory in a review article by P.F. Barbara, T.J. Meyer, M.A. Ratner, *J. Phys. Chem.* 100 (1996) 13148.

⁷⁹Let the mysterious q be a single variable for a while, whose deeper meaning will be given later. In order to make the story more concrete let us think about two reactant molecules (R) that transform into the product molecules (P): $A^- + B \rightarrow A + B^-$.

⁸⁰This widely used assumption is better fulfilled for large molecules when one electron more or less does not change much.

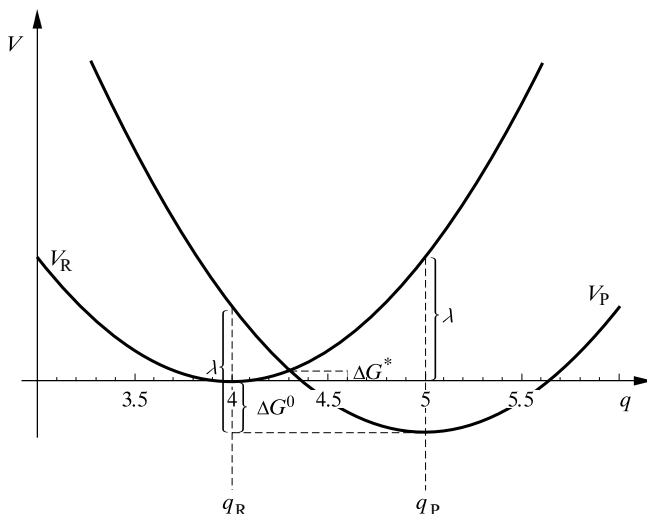


Fig. 14.22. The Marcus theory is based on two parabolic diabatic potentials $V_R(q)$ and $V_P(q)$ for the reactants and products, having minima at q_R and q_P , respectively. The quantity $\Delta G^0 \equiv V_P(q_P) - V_R(q_R)$ represents the energy difference between the products and the reactants, the reaction barrier $\Delta G^* \equiv V_R(q_c) - V_R(q_R) = V_R(q_c)$, where q_c corresponds to the intersection of the parabolas. The reorganization energy $\lambda \equiv V_R(q_P) - V_R(q_R) = V_R(q_P)$ represents the energy expense for making the geometry of the reactants identical with that of the products (and *vice versa*).

($\Delta G^0 < 0$ corresponds to an exothermic reaction⁸¹).

$$V_P(q) = \frac{1}{2}f(q - q_P)^2 + \Delta G^0.$$

So far we just treat the quantity ΔG^0 as a potential energy difference $V_P(q_P) - V_R(q_R)$ of the model system under consideration ($\text{H}_2^+ + \text{H}_2$ or the “pendulum” HF), even though the symbol suggests that this interpretation will be generalized in the future.

Such parabolas represent a simple situation.⁸² The parabolas’ intersection point q_c satisfies by definition $V_R(q_c) = V_P(q_c)$. This gives

$$q_c = \frac{\Delta G^0}{f} \frac{1}{q_P - q_R} + \frac{q_P + q_R}{2}.$$

Of course on the parabola diagram, the two minima are the most important, the intersection point q_c and the corresponding energy, which represents the reaction barrier reactants \rightarrow products.

MARCUS FORMULA:

The electron-transfer reaction barrier is calculated as

$$\Delta G^* = V_R(q_c) = \frac{1}{4\lambda}(\lambda + \Delta G^0)^2, \quad (14.74)$$

ET barrier

⁸¹That is, the energy of the reactants is higher than the energy of the products (as in Fig. 14.22).

⁸²If the curves did not represent parabolas, we might have serious difficulties. This is why we need harmonicity.

reorganization
energy

where the energy λ (*reorganization energy*) represents the energy difference between the energies of the products in the equilibrium configuration of the reactants $V_P(q_R)$ and the energy in the equilibrium configuration of the products $V_P(q_P)$:

$$\lambda = V_P(q_R) - V_P(q_P) = \frac{1}{2}f(q_R - q_P)^2 + \Delta G^0 - \Delta G^0 = \frac{1}{2}f(q_R - q_P)^2.$$

The reorganization energy is therefore always positive (energy expense).

REORGANIZATION ENERGY:

Reorganization energy is the energy cost needed for making products in the nuclear configuration of the reactants.

If we ask about the energy needed to transform the optimal geometry of the reactants into the optimal geometry of the products, we obtain the same number. Indeed, we immediately obtain $V_R(q_P) - V_R(q_R) = \frac{1}{2}f(q_R - q_P)^2$, which is the same as before. Such a result is a consequence of the harmonic approximation and the same force constant assumed for V_R and V_P , and shows that this is the energy cost needed to stretch a harmonic string from the equilibrium q_P position to the final q_R position (or *vice versa*). It is seen that the barrier for the thermic electron transfer reaction is higher if the geometry change is wider for the electron transfer [large $(q_R - q_P)^2$] and if the system is stiffer (large f).

From the Arrhenius theory the electron transfer reaction rate constant reads as

$$k_{\text{ET}} = A e^{-\frac{(\lambda + \Delta G^0)^2}{4\lambda k_B T}}. \quad (14.75)$$

How would the reaction rate change, if parabola $V_R(q)$ stays in place, while parabola $V_P(q)$ moves with respect to it? In experimental chemistry this corresponds to a *class* of the chemical reactions $A^- + B \rightarrow A + B^-$, with A (or B) from a homological series of compounds. The homology suggests that the

Svante August Arrhenius (1859–1927), Swedish physical chemist and astrophysicist, professor at the Stockholm University, originator of the electrolytic theory of ionic dissociation, measurements of the temperature of planets and of the solar corona, also of the theory deriving life on Earth from outer space. In 1903 he received the Nobel Prize in chemistry “for the services he has rendered to



the advancement of chemistry by his electrolytic theory of dissociation”.

parabolas are similar, because the mechanism is the same (the reactions proceed similarly), and the situations considered differ only by a lowering the second parabola with respect to the first. We may have four qualitatively different cases, eq. (14.74):

Case 1: If the lowering is zero, i.e. $\Delta G^0 = 0$, the reaction barrier is equal to $\lambda/4$ (Fig. 14.23.a).

Case 2: Let us consider an exothermic electron transfer reaction ($\Delta G^0 < 0$, $|\Delta G^0| < \lambda$). In this case the reaction barrier is lower, because of the subtraction in the exponent, and the reaction rate *increases* (Fig. 14.23.b). Therefore the $-\Delta G^0$ is the “driving force” in such reactions.

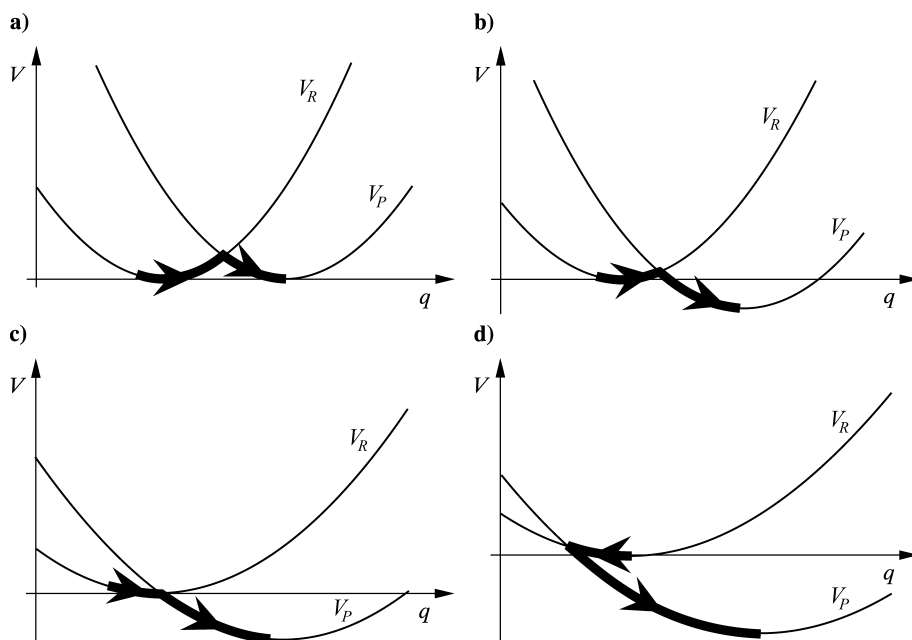


Fig. 14.23. Four qualitatively different cases in the Marcus theory. (a) $\Delta G^0 = 0$, hence $\Delta G^* = \frac{\lambda}{4}$. (b) $|\Delta G^0| < \lambda$ (c) $|\Delta G^0| = \lambda$ (d) inverse Marcus region $|\Delta G^0| > \lambda$.

Case 3: When the $|\Delta G^0|$ keeps increasing, at $|\Delta G^0| = \lambda$ the reorganization energy cancels the driving force, and the barrier vanishes to zero. Note that this represents the highest reaction rate possible (Fig. 14.23.c).

Case 4: Inverse Marcus region (Fig. 14.23.d). Let us imagine now that we keep increasing the driving force. We have a reaction for which $\Delta G^0 < 0$ and $|\Delta G^0| > \lambda$. Compared to the previous case, the *driving force has increased, whereas the reaction rate decreases*. This might look like a possible surprise for experimentalists. A case like this is called the *inverse Marcus region*, foreseen by Marcus in the sixties, using the two parabola model. People could not believe this prediction until experimental proof⁸³ in 1984.

inverse Marcus
region

New meaning of the variable q

Let us make a subtraction:

$$\begin{aligned} V_R(q) - V_P(q) &= f(q - q_R)^2/2 - f(q - q_P)^2/2 - \Delta G^0 \\ &= \frac{f}{2}[2q - q_R - q_P][q_P - q_R] - \Delta G^0 = Aq + B \end{aligned} \quad (14.76)$$

where A and B represent constants. This means that

⁸³J.R. Miller, L.T. Calcaterra, G.L. Closs, *J. Am. Chem. Soc.* 97 (1984) 3047.

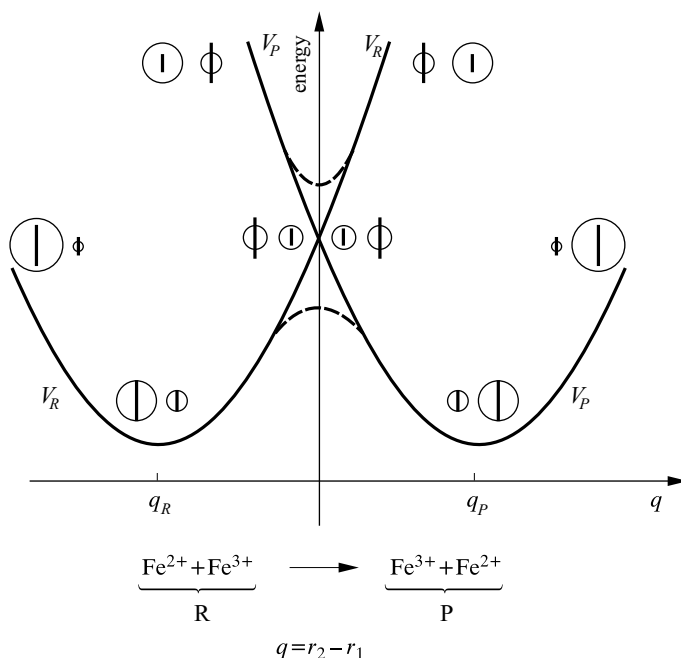


Fig. 14.24. The diabatic potential energy curves (V_R for the reactants and V_P for the products) pertaining to the electron transfer reaction $\text{Fe}^{2+} + \text{Fe}^{3+} \rightarrow \text{Fe}^{3+} + \text{Fe}^{2+}$ in aqueous solution. The curves depend on the variable $q = r_2 - r_1$ that describes the *solvent*, which is characterized by the radius r_1 of the cavity for the first (say, left) ion and by the radius r_2 of the cavity for the second ion. For the sake of simplicity we assume $r_1 + r_2 = \text{const}$ and equal to the sum of the ionic radii of Fe^{2+} and Fe^{3+} . For several points q the cavities were drawn as well as the vertical sections that symbolize the diameters of the left and right ions. In this situation, the plots V_R and V_P have to differ widely. The dashed lines represent the adiabatic curves (in the peripheral sections they coincide with the diabatic curves).

the diabatic potential energy difference depends *linearly* on coordinate q .

In other words for a given electron transfer reaction either q or $V_R(q) - V_P(q)$ represents the same information.

The above examples and derivations pertain to a one-dimensional model of electron transfer (a single variable q), while in reality (imagine a solution) the problem pertains to a huge number of variables. What happens here? Let us take the example of electron transfer between Fe^{2+} and Fe^{3+} ions in an aqueous solution $\text{Fe}^{2+} + \text{Fe}^{3+} \rightarrow \text{Fe}^{3+} + \text{Fe}^{2+}$ (Fig. 14.24)⁸⁴

The solvent behaviour is of key importance for the electron-transfer process.

⁸⁴In this example $\Delta G^0 = 0$, i.e. case 1 considered above.

The ions Fe^{2+} and Fe^{3+} are hydrated. For the reaction to proceed, the solvent has to *reorganize* itself next to both ions. The hydration shell of Fe^{2+} ion is of larger radius than the hydration shell of Fe^{3+} ion, because Fe^{3+} is smaller than Fe^{2+} and, in addition, creates a stronger electric field due to its higher charge (Fig. 14.24). Both factors add to a stronger association of the water molecules with the Fe^{3+} ion than with Fe^{2+} . In a crude approximation, the state of the solvent may be characterized by two quasi-rigid cavities, say: left and right (or, numbers 1 and 2) that could accommodate the ions. Let us assume the cavities have radii r_1 and r_2 , whereas the ionic radii are $r_{\text{Fe}^{2+}}$ and $r_{\text{Fe}^{3+}}$ with $r_{\text{Fe}^{2+}} > r_{\text{Fe}^{3+}}$. Let us assume, for the sake of simplicity, that $r_1 + r_2 = r_{\text{Fe}^{2+}} + r_{\text{Fe}^{3+}} = \text{const}$ and introduce a single variable $q = r_2 - r_1$ that in this situation characterizes the state of the solvent. Let us see what happens when q changes.

We first consider that the extra electron sits on the left ion all the time (reactant curve V_R) and the variable q is a negative number (with a high absolute value, i.e. $r_1 \gg r_2$). As seen from Fig. 14.24, the energy is very high, because the solvent squeezes the Fe^{3+} ion out (the second cavity is too small). It does not help that the Fe^{2+} ion has a lot of space in its cavity. Now we begin to move towards higher values of q . The first cavity begins to shrink, for a while without any resistance from the Fe^{2+} ion, the second cavity begins to lose its pressure thus making Fe^{3+} ion more and more happy. The energy decreases. Finally we reach the minimum of V_R , at $q = q_R$ and the radii of the cavities match the ions perfectly. Meanwhile variable q continues to increase. Now the solvent squeezes the Fe^{2+} ion out, while the cavity for Fe^{3+} becomes too large. The energy increases again, mainly because of the first effect. We arrive at $q = 0$. The cavities are of equal size, but do not match either of the ions. This time the Fe^{2+} ion experiences some discomfort, and after passing the point $q = 0$ the pain increases more and more, and the energy continues to increase. The whole story pertains to extra electron sitting on the left ion all the time (no jump, i.e. the reactant situation). A similar dramatic story can be told when the electron is sitting all the time on the right ion (products situation). In this case we obtain the V_P plot.

The V_R and V_P plots just described represent the diabatic potential energy curves for the motion of the nuclei, valid for the extra electron residing on the same ion all the time. Fig. 14.24 also shows the adiabatic curve (dashed line) when the extra electron has enough time to adjust to the motion of the approaching nuclei and the solvent, and jumps at the partner ion.

Taking a single parameter q to describe the electron transfer process in a solvent is certainly a crude simplification. Actually there are billions of variables in the game describing the degrees of freedom of the water molecules in the first and further hydration shells. One of the important steps towards successful description of the electron transfer reaction was the Marcus postulate,⁸⁵ that

⁸⁵Such collective variables are used very often in every-day life. Who cares about all the atomic positions when studying a ball rolling down an inclined plane? Instead, we use a single variable (the position of the centre of the ball), which gives us a perfect description of the system in a certain energy range.

despite the multidimensionality of the problem, eq. (14.76) is *still valid*, i.e. $V_R - V_P$ is a *single* variable describing the position of system on the electron-transfer reaction path (it is therefore a collective coordinate that describes the positions of the solvent molecules).

No doubt the potential energy value is important, but how often can this value be reached by the system, is equally important. This is connected to the *width* of the low-energy basin associated with the *entropy*⁸⁶ and to the *free energy*. In statistical thermodynamics we introduce the idea of the *potential of the mean force*, related to the free energy. Imagine a system in which we have two motions on different time scales: fast (e.g., of small solvent molecules) and slow (e.g., which change the shape of a macromolecule). To focus on the slow motion, we average the energy over the fast motions (the Boltzmann factor will be needed, which will introduce a temperature dependence on the resulting energy). In this way, from the potential energy we obtain the mean force potential depending only on the slow variables, sometimes called the free energy (which is a function of geometry of the macromolecule), cf. p. 293.

mean force
potential

The second Marcus assumption is that the ordinate axis should be treated as the *mean force potential*, or the free energy rather than just potential energy.

It is very rare in theoretical chemistry⁸⁷ that a many-dimensional problem can be transformed to a single variable problem. This is why the Marcus idea described above of a collective coordinate, provokes the reaction: “no way”. However, as it turned out later, this simple postulate lead to a solution that grasps the essential features of electron transfer.

What do the Marcus parabolas mean?

The example just considered of the electron transfer reaction: $\text{Fe}^{2+} + \text{Fe}^{3+} \rightarrow \text{Fe}^{3+} + \text{Fe}^{2+}$ reveals that in this case the reaction barrier is controlled by the solvent, i.e. by billions of coordinates. As shown by Marcus, this plethora can be effectively replaced by a single collective variable. Only after this approximation, may we draw the diabatic parabola-like curves. The intersection point of the two

⁸⁶A wide potential energy well can accommodate a lot of closely lying vibrational levels and therefore the number of possible states of the system in a given energy range may be huge (large entropy). Please recall the particle-in-a-box problem: the longer the box the closer the energy levels.

⁸⁷The free energy is defined as $F(T) = -kT \frac{\partial}{\partial T} \ln Z$, where $Z = \sum_i \exp(-\frac{E_i}{kT})$ represents the partition function, E_i stands for the i -th energy level. In the classical approach this energy level corresponds to the potential energy $V(x)$, where x represents a point in configurational space, and the sum corresponds to an integral over the total configurational space $Z = \int dx \exp(-\frac{V}{kT})$. Note that the free energy is a function of temperature only, not of the spatial coordinates x . If however, the integration were only carried out over part of the variables, say, only the fast variables, then Z , and therefore also F , would become a function of the slow variables and of temperature (mean force potential). Despite the incomplete integration, we sometimes use the name “free energy” for this mean force potential by saying that “the free energy is a function of coordinates...”.

diabatic curves can easily be found only after assuming their parabolic character. And yet any collective variable means motion along a line in an extremely complex configurational space (solvent molecules plus reactants). Moving along this line means that, according to Marcus, we encounter the intersection of the ground and excited electronic states. As shown in Chapter 6, such a crossing occurs at the conical intersection. Is it therefore that during the electron transfer reaction, the system goes through the conical intersection point? How to put together such notions as reaction barrier, reaction path, entrance and exit channels, not to speak of acceptor–donor theory? Fig. 14.25.a shows the paraboloid model of the diabatic DA and D^+A^- surfaces, while Fig. 14.25.b shows them in a more realistic way.

- The *diabatic hypersurfaces*, one corresponds to DA (i.e. the extra electron is on the donor all the time) and the second to D^+A^- (i.e. the extra electron resides on the acceptor), undergo the conical intersection. For conical intersection to happen at least three atoms are required. Imagine a simple model, with a diatomic acceptor A and an atom D as donor. Atom D has a dilemma: either to transfer the electron to the first or the second atom of A. This dilemma means conical intersection. Like the coordinate system shown in Fig. 14.25, the variables ξ_1 and ξ_2 described in Chapter 6 were chosen (they lead to splitting of the adiabatic hypersurfaces), which measure the deviation of the donor D with respect to the corner of the equilateral triangle of side equal to the length of the diatomic molecule A. The conical intersection point, i.e. (0, 0) corresponds to the equilateral triangle configuration. The figure also shows the upper and lower cones touching at (0, 0).
- The conical intersection led to two *adiabatic* hypersurfaces: lower (electronic ground state) and upper (electronic excited state). Each of the adiabatic hypersurfaces shown in Fig. 14.25.b consists of the “reactant half” (the diabatic state of the reactants, DA) and the “product half” (the diabatic state of the products, D^+A^-). The border between them reveals the intersection of the two diabatic states and represents the line of change of the electronic structure reactants/products. Crossing the line means the chemical reaction happens.
- The “avoided crossing” occurs everywhere along the border except at the conical intersection. It is improbable that the reactive trajectory passes through the conical intersection, because it usually corresponds to higher energy. It will usually pass at a distance from the conical intersection and this resembles an avoided crossing. This is why we speak of the avoided crossing in a polyatomic molecule, whereas the concept pertains to diatomics only.
- Passing the border is easiest at *two* points. These are the two saddle points (barriers I and II). A thermic electron transfer reaction goes through one of them, the corresponding IRCs are denoted by dotted lines. In each case we obtain different products. Both saddle points differ in that D, when attacking A has the choice of joining either of the two ends of A, usually forming *two different* products. We therefore usually have *two* barriers. In the example given (H_3) they are identical, but in general they may differ. When the barrier heights are equal because of symmetry, it does not matter which is overcome. When they are dif-

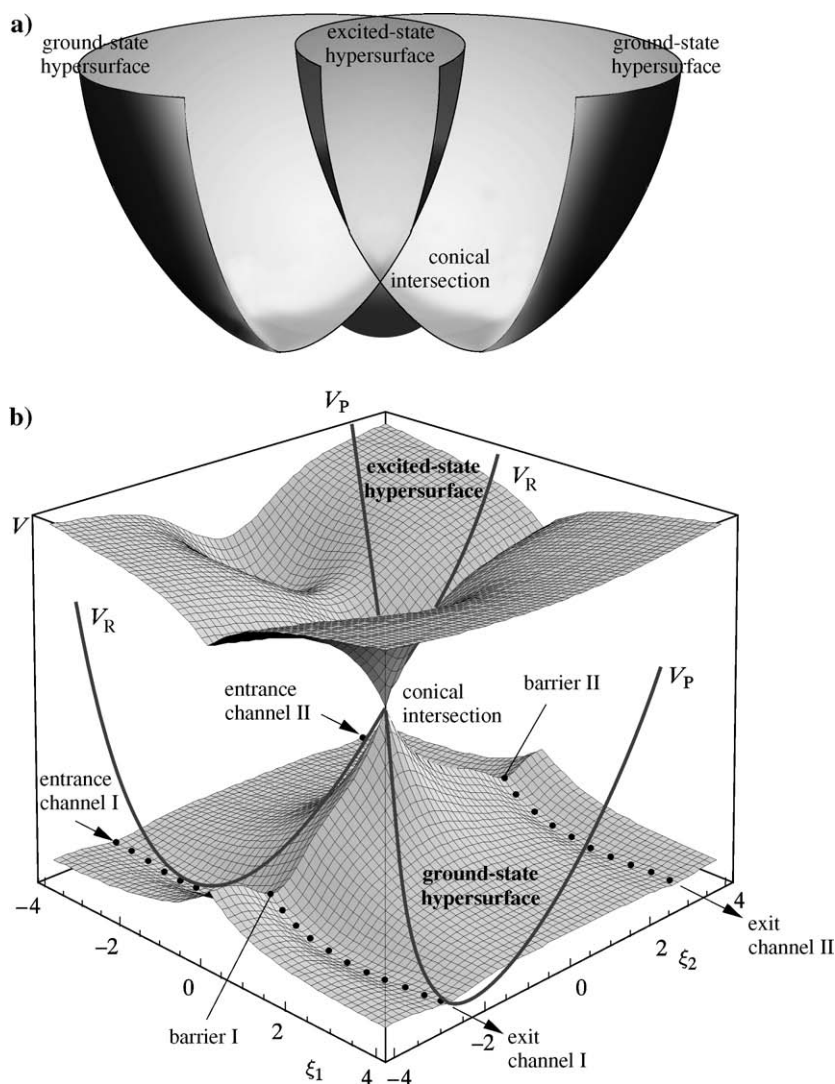


Fig. 14.25. Electron transfer in the reaction $DA \rightarrow D^+A^-$ as well as the relation of the Marcus parabolas to the concepts of the conical intersection, diabatic and adiabatic states, entrance and exit channels and the reaction barrier. Fig. (a) shows two diabatic (and adiabatic) surfaces of the electronic energy as functions of the ξ_1 and ξ_2 variables that describe the deviation from the conical intersection point (cf. p. 262). Both diabatic surfaces are shown schematically in the form of the two parabolooids: one for the reactants (DA), the second for products (D^+A^-). The region of the conical intersection is also indicated. Fig. (b) also shows the conical intersection, but the surfaces are presented more realistically. The upper and lower parts of Fig. (b) touch at the conical intersection point. On the lower part of the surface we can see two reaction channels each with its reaction barrier (see the text), on the upper part (b) an energy valley is shown that symbolizes a bound state that is separated from the conical intersection by a reaction barrier.

ferent, one of them dominates (usually the lower barrier⁸⁸). The channels shown in the figure are not curved, because we use a coordinate system different from that used in the collinear reaction.

- The Marcus parabolas represent a special section (along the collective variable) of the hypersurfaces passing through the conical intersection (parabolas V_R and V_P in Fig. 14.25.b). Each parabola represents a diabatic state, therefore a part of each reactant parabola is on the lower hypersurface, while the other one on the upper hypersurface. We see that the parabolas are only an approximation to the hypersurface profile. The reaction is of a thermic character, and as a consequence, the parabolas should not pass through the conical intersection, because it corresponds to high energy, instead it passes through one of the saddle points.
- The “product half” of the excited state hypersurface runs up to the “reactant half” of the ground state hypersurface and *vice versa*. This means that photoexcitation (following the Franck–Condon rule this corresponds to a vertical excitation) means a profound change: the system looks as if it has already reacted (*photoreaction*).

photoreaction

Quantum mechanical modification

In Marcus formula (14.74) we assume that in order to make the electron transfer effective, we have to supply at least the energy equal to the barrier height. The formula does not obviously take into account the quantum nature of the transfer. The system may overcome the barrier not only by having energy higher than the barrier, but also by tunnelling, when its energy is lower than the barrier height (cf. p. 153). Besides, the reactant and product energies are quantized (vibrational-rotational levels⁸⁹). The reactants may be excited to one of such levels. The reactant vibrational levels will have different abilities to tunnel.

According to Chapter 2 only a time-dependent perturbation is able to change the system's energy. Such a perturbation may serve the electric field of the electromagnetic wave. When the perturbation is periodic, with the angular frequency ω matching the energy difference of initial state k and one of the states of higher energy (n), then the transition probability between these states is equal to: $P_k^n(t) = \frac{2\pi t}{\hbar} |v_{kn}|^2 \delta(E_n^{(0)} - E_k^{(0)} - \hbar\omega)$ (the Fermi golden rule, eq. (2.23), p. 85 is valid for relatively short times t), where $v_{kn} = \langle k|v|n\rangle$, with $v(\mathbf{r})$ representing the perturbation amplitude,⁹⁰ $V(\mathbf{r}, t) = v(\mathbf{r})e^{i\omega t}$. The Dirac delta function δ is a quantum-mechanical way of saying that the total energy has to be conserved. In phototransfer of the electron, state “ k ” represents the quantum mechanical state of the reactants, and “ n ” – a product state, each of diabatic character.⁹¹ In practice the adiabatic approximation is used, in which the reactant and product wave

⁸⁸There may be some surprises. Barrier height is not all that matters. Sometimes it may happen that what decides is access to the barrier region, in the sense of its width (this is where the entropy and free energy matter).

⁸⁹For large molecules, we may forget the rotational spectrum, since, because of the large moment of inertia, the rotational states form a quasi-continuum (“no quantization”).

⁹⁰ \mathbf{r} stands for those variables on which the wave functions depend.

⁹¹They will be denoted by the subscripts R and P.

functions are products of the electronic wave functions (which depend on the electronic coordinates \mathbf{r} and, parametrically, on the nuclear configuration \mathbf{R}) and the vibrational functions $f(\mathbf{R})$ describing the motion of the nuclei: $\psi_{k,R}(\mathbf{r}; \mathbf{R})f_{v_1,R}(\mathbf{R})$ and $\psi_{n,P}(\mathbf{r}; \mathbf{R})f_{v_2,P}(\mathbf{R})$. The indices v_1 and v_2 in functions f denote the vibrational quantum numbers.

Then, the transition probability depends on the integral (Chapter 2)

$$v_{kn} = \langle \psi_{k,R}(\mathbf{r}; \mathbf{R})f_{v_1,R}(\mathbf{R}) | v(\mathbf{r}) | \psi_{n,P}(\mathbf{r}; \mathbf{R})f_{v_2,P}(\mathbf{R}) \rangle.$$

Let us rewrite it, making the integration over the nuclear and electronic coordinates explicit (where dV_{nuc} and $d\tau_e$ mean that the integrations is over the nuclear and electronic coordinates, respectively)

$$v_{kn} = \int dV_{\text{nuc}} f_{v_1,R}^*(\mathbf{R})f_{v_2,P}(\mathbf{R}) \int d\tau_e \psi_{k,R}^*(\mathbf{r}; \mathbf{R})v(\mathbf{r})\psi_{n,P}(\mathbf{r}; \mathbf{R}).$$

Now, let us use the Franck–Condon approximation that the optical perturbation makes the electrons move instantaneously while the nuclei do not keep pace with the electrons and stay in the same positions (we assume therefore equilibrium positions of the nuclei \mathbf{R}_0 in the reactants):

$$v_{kn} \approx \int dV_{\text{nuc}} f_{v_1,R}^*(\mathbf{R})f_{v_2,P}(\mathbf{R}) \int d\tau_e \psi_{k,R}^*(\mathbf{r}; \mathbf{R}_0)v(\mathbf{r})\psi_{n,P}(\mathbf{r}; \mathbf{R}_0).$$

The last integral therefore represents a constant and therefore

$$v_{kn} = V_{\text{RP}}S_{\text{osc}}(v_1, v_2),$$

where

$$\begin{aligned} V_{\text{RP}} &= \int d\tau_e \psi_{k,R}^*(\mathbf{r}; \mathbf{R}_0)v(\mathbf{r})\psi_{n,P}(\mathbf{r}; \mathbf{R}_0), \\ S_{\text{osc}}(v_1, v_2) &= \int dV_{\text{nuc}} f_{v_1,R}^*(\mathbf{R})f_{v_2,P}(\mathbf{R}). \end{aligned} \quad (14.77)$$

The last integral is called the *Franck–Condon factor*.

Franck–Condon
factor

FRANCK–CONDON FACTOR:

A Franck–Condon factor is the overlap integral of the vibrational wave functions: one pertaining to the reactants with dV_{nuc} vibrational quantum number v_1 and the second, pertaining to the products with vibrational quantum number v_2 .

The calculation of V_{RP} is not an easy matter, we prefer often therefore an empirical approach by modelling the integral as⁹²

$$V_{\text{RP}} = V_0 \exp[-\beta(R - R_0)],$$

where R_0 stands for the van der Waals distance of the donor and acceptor, R represents their distance, $\beta > 0$ represents a constant and V_0 means V_{RP} for the van der Waals distance.⁹³

A large Franck–Condon factor means that by exciting the reactants to the vibrational state v_1 there is a particularly high probability for the electron transfer (by tunnelling) with the products in vibrational state v_2 .

Reorganization energy

In the Marcus formula, reorganization energy plays an important role. This energy is the main reason for the electron-transfer reaction barrier.

The reorganization pertains to the neighbourhood of the transferred electron,⁹⁴ i.e. to the solvent molecules, but also to the donors and acceptors themselves.⁹⁵ This is why the reorganization energy, in the first approximation, consists of the internal reorganization energy (λ_i) that pertains to the donor and acceptor molecules, and of the solvent reorganization energy (λ_0):

$$\lambda = \lambda_i + \lambda_0.$$

Internal reorganization energy. For the electron to have the chance of jumping from molecule A^- to molecule⁹⁶ B, it has to have the neighbourhood reorganized in a special way. The changes should make the extra electron's life hard on A^- (together with solvation shells) and seduce it by the alluring shape of molecule B and its solvation shells. To do this, work has to be done. First, this is an energy cost for the proper deformation of A^- to the geometry of molecule A, i.e. already without the extra electron (the electron obviously does not like this – this is how it is forced out). Next, molecule B is deformed to the geometry of B^- (this is what

⁹²Sometimes the dependence is different. For example, in *Twisted Intramolecular Charge Transfer* (TICT), after the electron is transferred between the donor and acceptor moieties (a large V_{RP}) the molecule undergoes an internal rotation of the moieties, which causes an important decreasing of the V_{RP} [K. Rotkiewicz, K.H. Grellmann, Z.R. Grabowski, *Chem. Phys. Letters* 19 (1973) 315].

⁹³As a matter of fact, such formulae only contain a simple message: V_{RP} decreases very fast when the donor and acceptor distance increases.

⁹⁴The neighbourhood is adjusted perfectly to the extra electron (to be transferred) in the reactant situation, and very unfavourable for its future position in the products. Thus the neighbourhood has to be reorganized to be adjusted for the electron transfer products.

⁹⁵It does not matter for an electron what in particular prevents it from jumping.

⁹⁶“Minus” denotes the site of the extra electron. It does not necessarily mean that A^- represents an anion.

makes B attractive to the extra electron – everything is prepared for it in B). These two energy effects correspond to λ_i .

Calculation of λ_i is simple:

$$\lambda_i = E(\text{A}^-\text{B}; \text{geom AB}^-) - E(\text{A}^-\text{B}; \text{geom A}^-\text{B})$$

where $E(\text{A}^-\text{B}; \text{geom AB}^-)$ denotes the energy of A^-B calculated for the equilibrium geometry of another species, namely AB^- , while $E(\text{A}^-\text{B}; \text{geom A}^-\text{B})$ stands for the energy of A^-B at its optimum geometry.

Usually the geometry changes in AB^- and A^-B attain several percent of the bond lengths or the bond angles. The change is therefore relatively small and we may represent it by a superposition of the normal mode vectors⁹⁷ L_k , $k = 1, 2, \dots, 3N$, described in Chapter 7. We may use the normal modes of the molecule A^-B (when we are interested in electron transfer from A^- to B) or of the molecule AB^- (back transfer). What for? Because some normal modes are more effective than others in facilitating electron transfer. The normal mode analysis would show⁹⁸ that

the most effective normal mode of the reactants deforms them in such a way as to resemble the products. This vibration reorganizes the neighbourhood in the desired direction (for electron transfer to occur), and therefore effectively lowers the reaction barrier.

Solvent reorganization energy. Spectroscopic investigations are unable to distinguish between the internal or solvent reorganization, because Nature does not distinguish between the solvent and the rest of the neighbourhood. An approximation to the solvent reorganization energy may be calculated by assuming a continuous solvent model. Assuming that the mutual configuration of the donor and acceptor (separated by distance R) allows for enclosing them in non-overlapping spheres of radii a_1 and a_2 , the following formula was derived by Marcus:

$$\lambda_0 = (\Delta e)^2 \left\{ \frac{1}{2a_1} + \frac{1}{2a_2} - \frac{1}{R} \right\} \left\{ \frac{1}{\epsilon_\infty} - \frac{1}{\epsilon_0} \right\},$$

where ϵ_∞ and ϵ_0 denote the dielectric screening constants measured at infinite and zero electromagnetic field frequency, respectively, and Δe is equal to the effective electric charge transferred between the donor and acceptor. The dielectric screening constant is related to the polarization of the medium. The value ϵ_0 is

⁹⁷Yet the normal modes are linear combinations of the Cartesian displacements.

⁹⁸It usually turns out that there are several such vibrations. They will help electron transfer from A^- to B. The reason is quite obvious, e.g., the empirical formula for V_{RP} implies that a vibration that makes the AB distance smaller will increase the transfer probability. This can be seen in what is known as resonance Raman spectroscopy close to a charge transfer optical transition. In such spectroscopy, we have the opportunity to observe particular vibronic transitions. The intensity of the vibrational transitions (usually from $v = 0$ to $v = 1$) of those normal modes which facilitate electron transfer will be highest.

larger than ϵ_∞ , because, at a constant electric field, the electrons as well as the nuclei (mainly an effect of the reorientation of the molecules) keep pace to adjust to the electric field. At high frequency only the electrons keep pace, hence $\epsilon_\infty < \epsilon_0$. The last parenthesis takes care of the difference, i.e. of the reorientation of the molecules in space (cf. Chapter 12).

Summary

- A chemical reaction represents a molecular catastrophe, in which the electronic structure, as well as the nuclear framework of the system changes qualitatively. Most often a chemical reaction corresponds to the breaking of an old and creation of a new bond.
- Simplest chemical reactions correspond to overcoming single reaction barrier on the way from reactants to products through saddle point along the intrinsic reaction coordinate (IRC). The IRC corresponds to the steepest descent trajectory (in the mass-weighted coordinates) from the saddle point to configurations of reactants and products.
- Such a process may be described as the system passing from the entrance channel (reactants) to the exit channel (products) on the electronic energy map as a function of the nuclear coordinates. For a collinear reaction $A + BC \rightarrow AB + C$ the map shows a characteristic reaction “drain-pipe”. Passing along the “drain-pipe” bottom usually requires overcoming a reaction barrier, its height being a fraction of the energy of breaking the “old” chemical bond.
- The reaction barrier reactants \rightarrow products, is as a rule, of different height to the corresponding barrier for the reverse reaction.
- We have shown how to obtain an accurate solution for three atom reaction. After introducing the democratic hyperspherical coordinates it is possible to solve the Schrödinger equation (within the Ritz approach). We obtain the rate constant for the state-to-state elementary chemical reaction.

A chemical reaction may be described by the reaction path Hamiltonian in order to focus on the intrinsic reaction coordinate (IRC) measuring the motion along the “drain-pipe” bottom (reaction path) and the normal mode coordinates orthogonal to the IRC.

- During the reaction, energy may be exchanged between the vibrational normal modes, as well as between the vibrational modes and the motion along the IRC.
- Two atoms or molecules may react in many different ways (reaction channels). Even if under some conditions they do not react (e.g., the noble gases), the reason for this is that their kinetic energy is too low with respect to the corresponding reaction barrier, and the opening of their electronic closed shells is prohibitively expensive on the energy scale. If the kinetic energy increases, more and more reaction channels open up, because it is possible for higher and higher energy barriers to be overcome.
- A reaction barrier is a consequence of the “quasi-avoided crossing” of the corresponding diabatic hypersurfaces, as a result we obtain two adiabatic hypersurfaces (“lower” or electronic ground state, and “upper” or electronic excited state). Each of the adiabatic hypersurfaces consists of two diabatic parts stitched along the border passing through the conical intersection point. On both sides of the conical intersection there are usually two saddle points along the border line leading in general to two different reaction products (Fig. 14.25).
- The two intersecting diabatic hypersurfaces (at the reactant configuration) represent (a) the electronic ground state DA (b) and *that electronic excited state that resembles the electronic charge distribution of the products*, usually D^+A^- .

- The barrier appears therefore as the cost of opening the closed shell in such a way as to prepare the reactants for the formation of new bond(s).
- In Marcus electron transfer theory, the barrier also arises as a consequence of the intersection of the two diabatic potential energy curves. The barrier height depends mainly on the (solvent and reactant) reorganization energy.

Main concepts, new terms

- | | |
|---|---|
| critical points (p. 767) | curvature coupling (p. 785 and 791) |
| femtosecond spectroscopy (p. 768) | exo- and endothermic reactions (p. 787) |
| saddle point (p. 768) | donating mode (p. 792) |
| steepest descent path (SDP) (p. 769) | spectator bond (p. 795) |
| reactive and non-reactive trajectories (p. 770) | molecular electrostatic potential (p. 798) |
| skew coordinate system (p. 770) | steric effect (p. 799) |
| reaction “drain-pipe” (p. 772) | acceptor–donor (AD) reaction theory (p. 803) |
| entrance and exit channels (p. 772) | MO and AD pictures (p. 805) |
| early and late reaction barriers (p. 773) | reaction stages (p. 806) |
| bobsleigh effect (p. 774) | role of states DA , D^+A^- , D^+A^{-*} (p. 811) |
| democratic coordinates (p. 776) | HOMO-LUMO crossing (p. 815) |
| cross section (p. 779) | nucleophilic attack (p. 816) |
| reaction rate (p. 779) | electrophilic attack (p. 818) |
| Berry phase (p. 780) | cycloaddition reaction (p. 823) |
| mass-weighted coordinates (p. 781) | Woodward–Hoffmann rules (p. 825) |
| intrinsic reaction coordinate (IRC) (p. 781) | Diels–Alder reaction (p. 825) |
| “trajectory-in-molasses” (p. 782) | diabatic and adiabatic potentials (p. 828) |
| reaction path Hamiltonian (p. 783) | inverse Marcus region (p. 833) |
| natural coordinates (p. 784) | collective coordinate (p. 836) |
| vibrationally adiabatic approximation (p. 785) | mean force potential (p. 836) |
| vibrationally adiabatic potential (p. 786) | Franck–Condon factors (p. 840) |
| Coriolis coupling (p. 785 and 791) | reorganization energy (p. 841) |

From the research front

Chemical reactions represent a very difficult problem for quantum chemistry, because:

- There are a lot of possible reaction channels. Imagine the number of all combinations of atoms in a monomolecular dissociation reaction, also in their various electronic states. We have to select first which reaction to choose and a good clue may be the lowest possible reaction barrier.
- A huge change in the electronic structure is usually quite demanding for standard quantum mechanical methods.
- Given a chosen single reaction channel we confront the problem of calculating the potential energy hypersurface. Let us recall (Chapters 6 and 7) the number of quantum mechanical calculations to perform this is of the order of 10^{3N-6} . For as small number of nuclei as $N = 4$ we already have a million computation tasks to perform.
- Despite unprecedented progress in the computational technique, the cutting edge possibilities are limited in *ab initio* calculations to two diatomic molecules.

On the other hand, a chemist always has some additional information on which chemical reactions are expected to occur. Very often the most important changes happen in a limited set of atoms, e.g., in functional groups, their reactivity being quite well understood. Freezing the positions of those atoms which are reaction spectators only, allows us to limit the number of degrees of freedom to consider.

Ad futurum...

Chemical reactions with the reactants precisely oriented in space will be more and more important in chemical experiments of the future. Here it will be helpful to favour some reactions by supramolecular recognition, docking in reaction cavities or reactions on prepared surfaces. For theoreticians, such control of orientation will mean the reduction of certain degrees of freedom. This, together with eliminating or simulating the spectator bonds, may reduce the task to manageable size. State-to-state calculations and experiments that will describe an effective chemical reaction that starts from a given quantum mechanical state of the reactants and ends up with another well defined quantum mechanical state of the products will become more and more important. Even now, we may design with great precision practically any sequence of laser pulses (a superposition of the electromagnetic waves, each of a given duration, amplitude, frequency and phase). For a chemist, this means that we are able to change the shape of the hypersurfaces (ground and excited states) in a controllable way, because every nuclear configuration corresponds to a dipole moment that interacts with the electric field (cf. Chapter 12). The hypersurfaces may shake and undulate in such a way as to make the point representing the system move to the product region. In addition, there are possible excitations and the products may be obtained *via* excited hypersurfaces. As a result we may have selected bonds broken, and others created in a selective and highly efficient way. This technique demands important developments in the field of chemical reaction theory and experiment, because currently we are far from such a goal.

Note that the most important achievements in the chemical reaction theory pertained to concepts (von Neumann, Wigner, Teller, Woodward, Hoffmann, Fukui, Evans, Polanyi, Shaik) rather than computations. The potential energy hypersurfaces are so complicated that it took the scientists fifty years to elucidate their main machinery. Chemistry means first of all chemical reactions, and most chemical reactions still represent *terra incognita*. This will change considerably in the years to come. In the longer term this will be the main area of quantum chemistry.

Additional literature

R.D. Levine, R.B. Bernstein, "Molecular Reaction Dynamics and Chemical Reactivity", Oxford University Press, 1987.

An accurate approach to the reactions of small molecules.

H. Eyring, J. Walter, G.F. Kimball, "Quantum chemistry", John Wiley, New York, 1967.

A good old textbook, written by the outstanding specialists in the field. To my knowledge no later textbook has done it in more detail.

R.B. Woodward, R. Hoffmann, "The Conservation of Orbital Symmetry", Academic Press, New York, 1970.

A summary of the important discoveries made by these authors (Woodward-Hoffmann symmetry rules).

S.S. Shaik "What Happens to Molecules as They React? Valence Bond Approach to Reactivity", *Journal of the American Chemical Society* 103 (1981) 3692.

An excellent paper that introduces many important concepts in a simple way.

Questions

- The intrinsic reaction coordinate means:
 - a trajectory of an atom when the reaction proceeds;
 - the steepest descent path in the Cartesian space of the nuclear coordinates;
 - the steepest descent path from a saddle point in the Cartesian space of the mass-weighted nuclear coordinates;
 - a straight line in the Cartesian space of $3N - 6$ coordinates that connects the minima of the two basins.
- In the vibrationally adiabatic approximation (reaction path Hamiltonian method) with all the normal modes in their ground states:
 - the potential energy does not depend on the normal mode frequencies;
 - the zero-vibrations depend on the reaction path coordinate s ;
 - the normal modes may exchange energy;
 - the oscillators may exchange energy with the reaction path degree of freedom.
- An endothermic reaction proceeds spontaneously ($T > 0$), because:
 - the "drain-pipe" bottom potential energy plus the energies of the normal modes is lower in the entrance than in the exit channel;
 - the oscillators are anharmonic;
 - the "drain-pipe" bottom potential energy in the entrance channel is lower than that in the exit channel;
 - the exit channel is wider than the entrance channel.
- Donating mode:
 - couples with the reaction path in the entrance channel;
 - increases the reaction barrier;
 - corresponds to high Coriolis couplings with other modes;
 - corresponds to the lowest zero-vibration energy in the entrance channel.
- In the acceptor–donor picture at the intermediate reaction stage (I) the following structures prevail:
 - DA; b) D^+A^- and $D^{2+}A^{2-}$; c) D^+A^- and D^+A^{-*} ; d) DA and D^+A^- .
- In the acceptor–donor picture at the product reaction stage (P) the following structures prevail:
 - DA; b) D^+A^- , $D^{2+}A^{2-}$ and D^+A^{-*} ; c) D^+A^{-*} ; d) DA and D^+A^- .
- The ground-state adiabatic hypersurface in the neighbourhood of the conical intersection for three atoms:
 - does not touch the excited-state adiabatic hypersurface;
 - is a plane;
 - consists of two diabatic parts of different electronic structures;
 - does not touch a diabatic hypersurface.
- In Marcus electron transfer theory:
 - the reaction barrier is always equal to $\frac{1}{4}$ of the reorganization energy;

- b) the larger the absolute value of the energy difference between products and reactants, the faster the reaction;
 - c) the activation energy is equal to the reorganization energy;
 - d) if the reactant energy is equal to the product energy, then the reaction barrier is equal to $\frac{1}{4}$ of the reorganization energy.
9. In Marcus theory of electron transfer:
- a) we assume the same force constant for the reactants and products;
 - b) the reorganization energy in the reaction $\text{Fe}^{2+} + \text{Fe}^{3+} \rightarrow \text{Fe}^{3+} + \text{Fe}^{2+}$ in solution is equal to zero;
 - c) to have electron transfer we have to have the inverse Marcus region;
 - d) the solvent reorganization energy is equal to zero.
10. The reaction barrier:
- a) has the same height from the reactant side and from the product side;
 - b) appears, because the hypersurface of an excited state that resembles the products intersects with the ground-state hypersurface for reactants;
 - c) means that the reactants have to have kinetic energy higher than its height;
 - d) results from the tunnelling effect.

Answers

1c, 2b, 3d, 4a, 5d, 6b, 7c, 8d, 9a, 10b